Design and Development of Nano-Sized Formulations for Oral Delivery of Insulin and C-Peptide

THESIS

SUBMITTED TO

ACADEMY OF SCIENTIFIC & INNOVATIVE RESEARCH

FOR THE AWARD OF THE DEGREE OF

Doctor of Philosophy

In

BIOLOGICAL SCIENCES

By

Raval Kavit Harsiddharay

Enrollment No. 10BB14J04009

Under the guidance of

Dr. Manish K. Chourasia

Principal Scientist

PHARMACEUTICS & PHARMACOKINETICS DIVISION

CSIR-CENTRAL DRUG RESEARCH INSTITUTE

LUCKNOW- 226031, INDIA

2020

Dedicated to Lord Shiva,
Mummy, Pappa and Suuu;
The Inevitable Constants in My Life

CERTIFICATE

This is to certify that the work incorporated in this Ph.D. thesis entitled ***"Design and Development of Nano-Sized Formulations for Oral Delivery of Insulin and C-peptide"*** submitted by Mr. Raval Kavit Harsiddharay to Academy of Scientific and Innovative Research (AcSIR) in fulfillment of the requirements for the award of the Degree of Doctor of Philosophy, embodies original research work under my supervision. I further certify that this work has not been submitted to any other University or Institution in part or full for the award of any degree or diploma. Research material obtained from other sources has been duly acknowledged in the thesis. Any text, illustration, table etc., used in the thesis from other sources, have been duly cited and acknowledged.

It is also certified that this work done by the student, under my supervision, is plagiarism free.

Raval Kavit Harsiddharay

Dr. Manish K. Chourasia
Principal Scientist,
Pharmaceutics & Pharmacokinetics Division,
CSIR – Central Drug Research Institute,
Lucknow – 226 031

ACKNOWLEDGEMENT

I am grateful and indebted to my revered supervisor ***Dr. Manish K chourasia,*** *whose vision, ideas, patience and support were instrumental in me accomplishing this project. His diligent efforts and professional competency, contributed towards my growth, 'both academically as well as personally'. His conscientious suggestions, creative ideas, critical evaluation and homely atmosphere in which he made me work, were some of the qualities that will be cherished as a quintessential example of his brilliant guidance. The traits which I have acquired from him will hold me in good stead throughout my life in any field and it has been a real privilege to have worked under him.*

I am sincerely thankful to ***Dr. Amit Misra,*** *chairperson, Pharmaceutics & Pharmacokinetics Division, CSIR-CDRI, for invoking in me a sense of fascination towards pharmaceutics, in whatever little interactions we had throughout my tenure. I am obliged and thankful to* ***Dr. A. K. Dwivedi, Dr. P. R. Mishra, Dr. Rabi Shankar Bhatta and Dr. Wahajuddin*** *for allowing unhindered access to their lab facilities.*

I am extremely thankful to ***Dr. Jiaur R. Gayen*** *(Pharmaceutics & Pharmacokinetics Division) for actively taking up this project and mentoring me in In vivo studies, so that this research work could be conducted in appropriate animal models.*

I welcome contributions by ***Dr. Yuvraj singh, Dr. Pankaj Singh, Dr. Anand gupta, and Mani Sharma*** *without whom this work would probably not have attained fruition. I am extremely thankful to* ***Mr. A.L. Vishwakarma and Mrs. Madhu*** *for teaching me trivial details of flow cytometry and* ***Dr. Tofan Kumar Rout*** *of SAIF Division for helping me with MALDI-TOF analysis and CD spectroscopy.*

A special token of thanks to my seniors ***Dr. Vivek K. Pawar, Dr. Yuvraj singh, Dr. Pankaj Singh, Dr. Jaya Gopal Meher, Dr. Komal Sharma, and Dr. K.K. Durga Rao Viswanadham,*** *who were very welcoming initially and then mentored my progress throughout. I thank all the supporting staff of Pharmaceutics & Pharmacokinetics Division for their kind co-operation.*

Everyone says lab is a boring place, but my experience was to the contrary. I really do feel that my lab partners Dr. ***yuvraj,*** *Dr.* ***Jay,*** *Dr.* ***Pankaj, Dr. Vivek, Dr. Sanket, Animesh, Ravi, Mani, Sakshi, Suruchi, Amrendra, Abhiram, Pawan, and Rafaqat Rana*** *made it a fun place to work at, tolerating my ego and carrying me along in a jovial manner. The time we spent together was special and will always bring back good memories.*

Words cannot express my love and gratitude for my ***mother, father, wife and siblings*** *who have constantly been there for me. The financial assistance in form of junior/senior research fellowship by CSIR is also acknowledged. The facilities provided by CSIR-CDRI have been world class and for that I am deeply grateful to the founding fathers and the long line of illustrious directors who have headed this great institution. Thanks to all.*

PCS-004, CSIR-CDRI, Lucknow ***Raval Kavit Harsiddharay***

Table of Contents

ABBREVIATIONS

%	Percentage
µg	Micro gram
AUC	Area under the curve
CAP	Cellulose acetate phthalate
CD	Circular dichroism
CLNE	Poly-l-lysine coated linseed oil nano-emulsion blank
CLNE	Poly-l-lysine coated nanoemulsion bearing insulin and c-peptide
Cmax	Maximum plasma concentration
DM	Diabetes mellitus
DMEM	Dulbecco's modified eagle's medium
DMSO	Dimethyl sulphoxide
FBS	Fetal bovine serum
FTIR	Fourier transform infra-red
g	Gram
GIT	Gastro-intestinal tract
HPLC	High performance liquid chromatography
INS-CAP@TNPs	Insulin bearing CAP coated TNPs
INS-CLNE	Poly-l-lysine coated linseed oil nano-emulsion bearing insulin and c-peptide
INS-ULNE	Uncoated linseed oil nano-emulsion bearing insulin and c-peptide
IU	International unit
kDa	Kilo dalton
LNE	Linseed oil nano-emulsion
MALDI	Matrix-assisted laser desorption/ionization
mg	Milli gram
Mv	Milli volt
MWCO	Molecular weight cut off
NE	Nanoemulsion
NE	Nano-emulsion
ng	Nano gram
NMR	Nuclear magnetic resonance

NPs	Nanoparticles
OPA	Ortho phosphoric acid
PBS	Phosphate buffer saline
PDI	Polydispersivity index
PDI	Polydispersity index
PEG	Polyethylene glycol
PEO	Poly ethylene oxide
PLA	Poly Lactic Acid
PLA-NH_2	Amine terminated Poly Lactic Acid
PLGA	Poly(lactic-co-glycolic acid
PLL	Poly-l-lysine
PPG	Polypropylene glycol
PPO	Poly propylene oxide
RP-HPLC	Reverse phase - high performance liquid chromatography
rpm	Rotation per minute
RPMI	Roswell Park Memorial Institute medium
SD	Standard deviation
SEM	Standard error of means
SGF	Simulated gastric fluid
SIF	Simulated intestinal fluid
$T_{1/2}$	Half-life
T1DM	Type I diabetes mellitus
T2DM	Type II diabetes mellitus
TDW	Triple distilled water
TEER	Trans-epithelial electrical resistance
TEM	Transmission electron microscopy
Tmax	Time until Cmax is reached
TNPs	Thermo-responsive size sifting PLA-NH_2 nanoparticles
TPGS	Tocopheryl Polyethylene Glycol Succinate
ULNE	Uncoated linseed oil nano-emulsion blank
USD	U.S. Dollar

LIST OF TABLES

LIST OF FIGURES

CHAPTER 1

Introduction

&

Outline of the work

1. INTRODUCTION

1.1 Statistical epidemiology and economic burden of Diabetes Mellitus

Diabetes will be the seventh foremost reason of death in 2030 due to an exponential increase in affected peoples from 347 million adults in 2015 to 400 million adults by 2030 as per WHO database. The global economic burden caused by diabetes is rising massively due to very complicate management of the disease. The estimated global healthcare expenditure behind diabetes treatment without including indirect cost such as lost work time, has arrived to 548 billion U.S. dollar (USD) in 2013 which is expected to increase to 627 billion USD in 2035 [1]. These account approximately 12% of the world's total health expenditure with on an average 1330 USD to be spent on each diabetic person as an anticipated per capita health expenditure [2]. There remains a great discrepancy in health expenses for diabetes among developed and developing countries from 198.0 billion USD to 1.3 million USD, respectively. The highest total expenditure, 57.2% of global expenditure, will be spend by United States of America whilst India, the country with the largest number of people affected with diabetes will spend an estimated 2.8 billion USD which is less than 1% of the world's total expenditure. According to the trend it is estimated that Asia will contribute more than 60% of the world's diabetic population. The high prevalence of diabetes in Asians compared to other European countries recently posed an interesting mysterious question in minds of Asian scientists to search for. The investigation postulate multiple factors to be responsible such as strong ethnic and genetic inclination towards diabetes, a lower thresholds for epigenetic risk factors, changing lifestyle and food intake due to socio-economic growth, industrialization and urbanization resulting in diabetes at early stage in children and adults both accompanied by lower body mass index and large waist circumference as compared to western population [3]. Consequently, complications of diabetes are becoming more common and raising economic burden in developing Asian countries with poor strata of society. This situation subjugates the national endeavours towards early and reliable diagnosis, efficacious treatment and preventive measures against diabetes.

1.2 An introduction to Diabetes Mellitus

Diabetes mellitus (DM) is basically a complex metabolic disorder characterized by hyperglycaemic state which demands constant medical care with multifactorial risk

reducing approaches beyond just maintaining glycaemic rheostat [4]. Diminished production and/or response to insulin leads to hyperglycaemic state which originates a group of metabolic disorders known as diabetes mellitus. Type 1 diabetes mellitus (T1DM), also known as juvenile diabetes or early onset diabetes due to its existence in early stage of life, shares 10% of total diabetes mellitus patients. The culprit phenomena behind T1DM is auto-immune response mediated through T cells and leucocyte infiltration, which results in propagative destruction of β cells of Langerhans ultimately heading towards hypoinsulinemia driven hyperglycaemia. Type 2 diabetes mellitus (T2DM) is the most common type of DM and dominates in terms of its existence in 90% of the affected population. The patients with T2DM generally have age above 45 years and mostly above 65 years. It originates as a life style disorder associated with obesity and physical inactivity which is due to dampened response of peripheral cells to secret insulin termed as insulin resistance [5].

The most important and anticipated long term upshot of diabetes treatment is the maintenance of blood glucose level within euglycaemic range. Bumpy blood glucose level with ups and downs for longer period, if left untreated may lead to various micro and macro vascular complications associated with diabetes such as retinopathy, nephropathy and neuropathy with additionally higher risk to infections. Contrariwise, overtreatment with insulin or oral hypoglycaemic agents may result in hypoglycaemic episodes with seizures, unconsciousness or even death, consequently. The basic approach for T1DM treatment includes insulin replacement through administration of exogenously produced recombinant insulin to achieve imitation of natural levels of insulin secretion throughout the day [6]. For this, injections of long acting insulin to maintain basal insulin level supplemented with bolus injections of fast acting insulin at meals to provide post prandial temporary hike of insulin are being prescribed by physicians to mimic routine fluctuations of insulin in T1DM patients [7]. While in patients with early stage of T2DM, primary treatment is directed to delay the disease progression by suggesting regular exercise and meals [8]. Oral hypoglycaemic agents are also used to improve insulin production and performance. Finally in a well grown state of T2DM treatment urges insulin in combination to oral hypoglycaemic agents as inborn insulin production reduces [9, 10].

1.3 Insulin delivery: A finale treatment

As a first line treatment at an early stage of type II diabetes mellitus, preventive approaches such as exercise, meditation, low calorie food intake, weigh loss etc., are generally being suggested with oral hypoglycaemic agents. Most commonly, the oral hypoglycaemic agents such as sulfonylureas (glipizide, glimepiride, and glyburide), biguinides (metformin), α glucosidase inhibitors (acarbose, miglitol, voglibose), thizolidinediones (roziglitazones, pioglitazones), and dipeptidyl peptidase IV inhibitors (sitagliptin, vildagliptin, teneligliptin) are being prescribed as monotherapy as well as combination therapy [11]. However, the progressive nature of diabetes drives the insulin level to the least and hence at certain stage external insulin has to be administered to maintain the glycaemic rheostat. Therefore, it can be concluded that insulin delivery is the ultimate treatment irrespective of the type of diabetes [12].

Despite of its discovery in early 20th century (1921), insulin could not become omnipresent therapeutic agent in diabetes treatment and remained at suboptimal utility with limited priority in patients with Type I diabetes, especially due to its requisite invasive administration and short biological half-life [13]. The chief limitation of insulin therapy is poor patient compliance associated with multiple painful subcutaneous injections [14]. The root stems in our very own gastrointestinal tract's physiology which is adverse to proteins and peptides like insulin and glucagon like peptide -1, when administered orally. Very harsh and acidic environment with the presence of protease enzymes at upper part of GIT damage the proteins and peptides such as insulin and make them therapeutically ineffective. Moreover, due to hydrophilic nature proteins and peptides like insulin possess lower permeability through lipophilic intestinal milieu. Collectively, the aforementioned factors significantly reduce the bioavailability of proteins and peptides after oral administration. Therefore, various nanotechnology assisted approaches have been applied for delivery of insulin by alternative routes such as buccal, nasal, transdermal, pulmonary and oral but still their prolonged existence in clinics and pharmaceutical market is yet to be achieved [15].

1.3.1 Open vs. close loop delivery

If we try to focus on the whole picture of physiological phenomena, the loop can be found wherein there is constant balance between blood glucose elevation and release of insulin from the beta cells [16]. The insulin delivery through conventional subcutaneous route supply the payload in "open loop" manner. Simply, an open-loop insulin delivery system

consists a scheduled administration of insulin at specific constant rate to preserve euglycaemia in the fasting or calorie challenged states. But it is true that during caloric challenge (meals) the 'basal' rate would not be able to manage the glycaemic hike to normal range [17]. The open loop does not contain blood glucose sensor[17] so that there is no link between real time blood glucose level and insulin releasing device to complete the loop [18], providing glucose independent insulin release as set by algorithmic waveform extracted from previous understanding of subject's blood glucose response to different meals and insulin treatments at different dosages [17, 19]. With the help of massively advanced technology of continuous glucose monitoring system the 'closed loop' insulin delivery became possible which can deliver insulin according to real time glucose level. The close loop circuit consists three components: a continuous glucose sensor, an insulin pump and a control algorithm to run the loop in a self-regulative automated manner [20]. Due to its likeliness to normal pancreatic function the subcutaneous closed loop delivery of insulin is being considered as "artificial pancreas' and has generated a hope to manage glycaemia in target range with reduced frequency of hypo and hyper glycaemic episodes in diabetics. Recently, one noteworthy phase II clinical trial carried out in 20 adults and 32 adolescents with type 1 diabetes mellitus revealed that a wearable, automated, bihormonal (insulin and glucagon), 'bionic' pancreas improved mean glycaemic level within normoglycaemic range with very rare lower glucose level period (4.8% of time ; <70 mg/dl) with low frequency (only once in 1.6 days) compared to subcutaneously implanted insulin pump [21]. Despite of difficulties to achieve closed loop delivery of insulin and tight glycaemic control the fascinating drug delivery aspects of nanotechnology has gained much attention of scientists to serve the global health issue – diabetes mellitus type II.

1.4 Nano technological advancements in diabetes mellitus

From last three decades, nanotechnology has showered immense advancement for better diagnosis [22] and treatment in various disease conditions such as cancer [23-25], diabetes [26, 27], cardiovascular disorders [28, 29] and infectious diseases etc. The extraordinary physical, chemical and biological features of nano-sized materials make them most attractive and suitable for various biomedical applications [30-33]. Nano-sized materials have done a great job in evolving the field of molecular diagnostics with point of care to provide personalized medicines [22]. A very substantial exploitation of potential benefits from nanotechnology have been done in delivering small as well as large macromolecular

(i.e. DNA, RNA, peptides and proteins) bioactives, in a therapeutically viable form for various medical applications [34]. A countless nanoparticulate systems with varying architectures and unique features have been developed for many bio-medical applications including polymeric nanoparticles, inorganic nanoparticles, metallic nanoparticles, magnetic nanoparticles, quantum dots, nanocrystals, nano-fibres, dendrimers, liposomes, lipoploymerosomes, nano-structured self-assembling peptides, nano emulsions, stimuli-responsive smart nanoparticles and nanofabricated devices [35-47] .

1.5 Outline of the research envisaged

Conventionally, proteins and peptides are being administered by commonly not much-liked invasive routes i.e. intravenous, intra-muscular, and sub-cutaneous. Despite of universal need for better alternative routes, the formulation as well as medical experts are unable to achieve this elusive goal, till date. Therefore, in the quest to solve this problem of the century, efforts have been made and outcomes are reported. Though oral route is the most preferred and patient friendly, oral delivery of labile proteins and peptides remains challenging due to hostile physiology of gastro-intestinal tract such as harsh acidic pH, proteolytic enzymes and absorption barriers [48]. Therefore, essential endeavours are needed to formulate an alternative pulmonary, nasal or oral drug delivery system that can protect the labile macromolecule from all the physiological barriers and deliver it at desired site in therapeutically viable form.

1.5.1 Thermo-responsive size shifting polymeric nanoparticles as a platform for oral delivery of insulin

Objective: To develop thermo-responsive polymeric nano-particulate drug delivery system for oral delivery of proteins and peptides.

Hypothesis: To minimize the problems associated with delivery of biologics, a novel approach has been undertaken to provide labile proteins and peptides by the most preferred route i.e. oral. Generally, the nano-materials are formulated by methods like salting out or nano-precipitation, emulsification-solvent evaporation, emulsification-solvent diffusion, emulsion polymerization, interfacial poly-condensation, solvent displacement and interfacial deposition, phase separation coacervation, double emulsification – solvent evaporation etc [49, 50]. However, these aforementioned methods of preparation includes different forces such as mechanical energy whilst stirring, impact under pressure during homogenization and ultrasound wave led acoustic cavitation throughout ultra-sonication

that help in generating nano-scale size. Moreover, various organic solvents are also used to get the polymer dissolved which can be precipitated afterwards to form hard nanoparticles. When analysed at the molecular scale, it is found that these energy and organic solvents are inadvertently affecting the structural integrity, conformational stability and biological activity of labile proteins and peptides making them partially or fully inactive. Thus, one of the great challenges in the formulation development of proteins and peptide is to keep them intact and viable during process of nanoparticle preparation. Hence, a unique approach of organic solvent free platform has been developed to load the labile macromolecules with positive or negative charge in the nano-particulate system.

The core-shell nanoparticles with charged core of polymeric material enclosed in thermo-sensitive shell has been architected to incorporate hydrophilic proteins. To avoid the exposure of energy and organic solvent, method of preparation is divided in two sub parts. In the first part, polymeric nanoparticles were prepared by nano-precipitation method and afterwards, the passive loading of labile protein molecules was done by solvent free incubation method. In the first step for making nanoparticles, the negatively charged polymer like poly (lactic-co-glycolic acid) (PLGA) with carboxyl group at terminal and positively charged poly lactic acid (PLA-NH_2) with amine group at terminal end have been utilised which can incorporate positively charged proteins (such as interleukin 10, erythropoietin) and negatively charged proteins (such as insulin), respectively, by electrostatic interaction. The employment of hydrophobic polymers like PLGA and PLA have following reasons:

- biodegradable and biocompatible nature
- provides controlled release of hydrophilic protein molecules due to potential electrostatic binding force

Various pluronics (PF 127, PF 68 and P 123) were tried to impart a thermo-sensitive shell. These pluronics possess thermo responsive swelling behaviour depending on PEO residues in various grades. Basically, they are tri-co-block polymer cum surfactants made up of hydrophilic poly ethylene oxide (PEO) and hydrophobic poly propylene oxide (PPO) blocks arranged in PEO-PPO-PEO manner. Their thermal property depends on content of PEO and hence, PF 127 and PF 68 containing 70% and 80% PEO blocks, respectively, were selected for trial [51]. Additionally, Pluronic P 123 having poly (ethylene glycol)-

poly (proplylene glycol)- poly (ethylene glycol) was also taken in consideration due to the presence of hydrophilic blocks. While preparation of NPs by nano-precipitation method, pluronics were used as surfactant which make shell on the polymeric core made up of PLGA or PLA.

The shell made up of pluronic has distinct property of loosening their assembly of block molecules at lower temperature (4°C) and condensing at high temperature (37°C). Advantage of this phenomena was taken for efficient yet solvent free loading of protein molecules. During incubation of NPs in protein solution at 4°C, the loosened state of shell allows the charged protein molecules to bind to the oppositely charged hydrophobic core by electrostatic interaction. Then, at 37°C temperature in body it provides controlled release of protein molecules due to entrapment in tightly shrunk shell. The schematic diagram of thermo-responsive NPs is shown in figure 1.1.

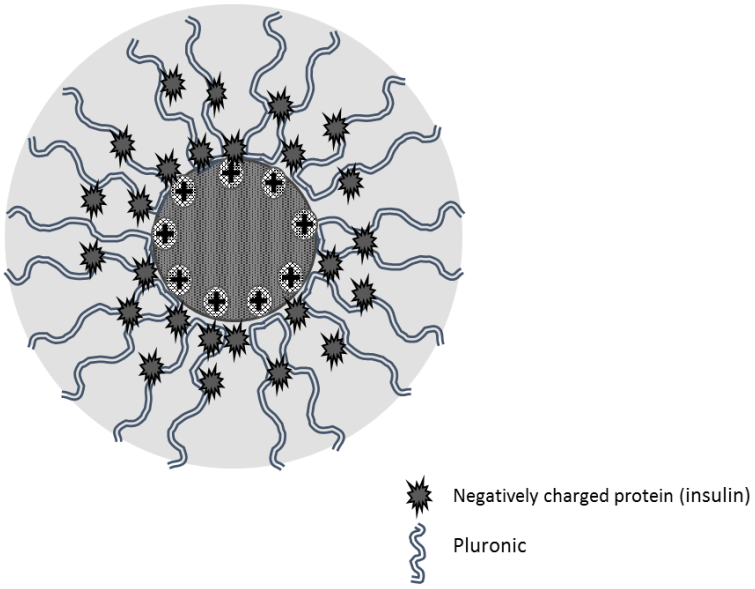

Figure 1.1 Schematic illustration of positively charged PLA-NH_2 thermo-responsive NPs bearing negatively charged protein insulin.

Despite of being first recombinant protein with early discovery in 1921, insulin delivery yet requires invasive and painful subcutaneous injections presenting a great discomfort to patients of diabetes [13]. Insulin suffers from certain difficulties such as short biological half-life, degradation by protease in GIT and poor absorption due to higher molecular weight (5808 daltons) and hydrophilic nature. In patients with diabetes mellitus type I,

insulin needs to be injected at high frequency to maintain blood glucose in euglycaemic range. To imitate natural levels of insulin, injection of long acting insulin to maintain basal insulin level supplemented with bolus injections of fast acting insulin at meals are being prescribed by the physicians [7]. In well-developed stage of diabetes mellitus type II also, the insulin therapy is needed in addition to oral hypoglycaemic agents to maintain tight glycaemic control [9]. To maintain tight glycaemic control is the only long-term outcome of diabetes treatment and hence, oral nanoparticulate formulation that can provide insulin in its biologically active form in controlled manner would be highly recommended to meet the unmet medical need. Keeping above mentioned facts in mind insulin was selected as model protein for the thermo-responsive nanoparticles. Insulin possesses slightly negative charge at physiological pH (7.4) and hence NPs with hydrophobic core of positively charged PLA-NH_2 were selected for its delivery. Then, NPs were coated by an enteric coating material cellulose acetate phthalate to protect them from upper part of GIT.

1.5.2 Poly-l-lysine coated oral nano-emulsion for combined delivery of insulin and c-peptide

Objective: Design and development of Poly-l-lysine coated oral nano-emulsion bearing insulin and c-peptide for comprehensive management of diabetes.

Hypothesis: Mere control of blood glucose level by insulin administration is not sufficient in patient with diabetic complications. Complications with vascularization (micro and macro) are major cause for morbidity and mortality in both type I and II diabetes [52]. Generally, the detrimental effects of hyperglycemia are classified into macro-vascular complications (coronary artery disease, peripheral arterial disease, and stroke) and micro-vascular complications (diabetic nephropathy, neuropathy, and retinopathy). Yet now there is no such drug available in the market that can manage the earlier mentioned complications. Recent studies have reported physiological role and beneficial properties of c-peptide which was earlier considered as by product of insulin biosynthesis [53, 54]. According to the meta-analysis, external recombinant insulin therapy lacks c-peptide maintenance in body and hence it's beneficial physiological effects which play pivotal role in managing the diabetic complications. [55, 56] C-peptide acts through G-protein coupled receptors to activate calcium channel and increases Na^+-K^+-ATPase activity, which is usually found decreased in the patients with advanced micro-vascular complications (nephropathy and retinopathy) of diabetes [57]. Moreover, c-peptide enhances endothelial

nitric oxide synthase activities. Study done by Wahren, Ekberg [58] et al, reports that c-peptide administration in type I diabetic patients who lacks natural c-peptide resulted in augmented blood flow in skeletal muscle and skin, diminished glomerular hyper-filtration, reduced urinary albumin excretion, and improved nerve function without any such effects in healthy subjects. Several clinical studies have been done by Johansson et al. evaluating short term replacement of c-peptide in type I diabetes patients. They inspected low dose c -peptide infusion for renal function and whole body glucose uptake in comparison to sodium chloride infusion and found that c-peptide increased whole body glucose utilization by 25 percent while decreased glomerular hyper-filtration by 6 percent [59]. In a follow up study, they demonstrated that one month administration of c-peptide decreased HbA1C level in type I diabetics by 9 to 16 percent versus control suggesting improved glycaemic control. They also reported 55 percent decrease in albuminuria after 4 weeks indicating its potential to ameliorate diabetic nephropathy [60]. A randomized double-blind placebo controlled study by Ekberg et al, found that three month administration of c-peptide, in type I diabetic patients with neuropathy, improved sensory nerve conduction and vibration perception illustrating its indication in diabetic neuropathy [61]. Diabetics are vulnerable to heart disorders and usually have diastolic dysfunction and myocardial perfusion abnormalities. A randomized double-blind crossover study was done by Hansen et al. in which they compared the effect of c-peptide infusion with saline infusion for myocardial dysfunction in type I diabetics. They found that during c-peptide administration the diastolic velocities and myocardial blood flow of the diabetics was increased to the levels observed in the healthy controls showing myocardial benefits [62]. Therefore, combined delivery of insulin and c-peptide has been envisaged with a view to provide tight glycaemic control without any diabetic complications.

Adroit nano-formulations have been reported to deliver the protein insulin and c-peptide by oral route. Various nano sized formulations such as polymeric nanoparticles [63, 64], liposomes [65], solid lipid nanoparticles [66] etc., have been extensively investigated and found suitable for oral delivery of proteins and peptides, however, none of them have attained commercial success till date. Nano-emulsions provide promising avenue for oral delivery of protein and peptide [67]. In the present investigation we have worked on formulation of oral w/o/w nano-emulsion to shelter hydrophilic insulin and c-peptide in internal aqueous droplets housed inside linseed oil droplet - dispersed in external aqueous phase. The hydrophobic boundary created by linseed oil will provide controlled release to

hydrophilic insulin and c-peptide housed in the aqueous core. Herein, instead of using inert oils, biologically active oils were selected. Oils having either anti-diabetic effect and/or helpful to reduce diabetic complication were screened from the array of naturally occurring resources. After this primary screening four oils such as olive oil, sesame oil, palm oil and linseed oil were found suitable due to their distinct properties. According to excipient compatibility linseed oil came up as preferred oil. Moreover, alpha linolenic acid, a major constituent of linseed oil, increases the GLUT4 membrane receptor present on skeletal muscles and thereby augments insulin sensitivity leading to better glucose uptake in skeletal muscle which in turn reduces the blood glucose level [68]. Poly-arginine has been exploited as coating material for oral insulin delivery via oleic acid nano-emulsion [69]. To protect the labile insulin and c-peptide from hostile acidic condition oil globules were coated with positively charged poly-l-lysine [70] in addition to the surfactant layer of pluronic F 127 at the interface. The schematic diagram of proposed formulation is shown in figure 1.2.

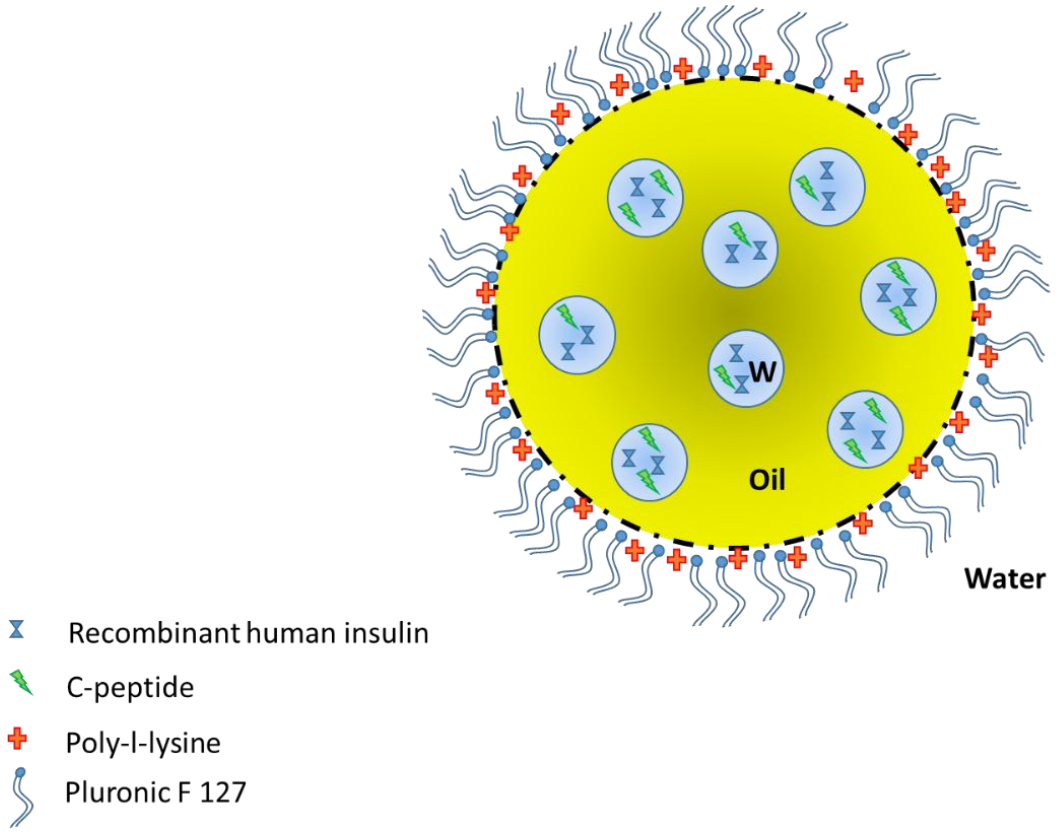

Figure 1.2 Schematic diagram of poly-l-lysine coated w/o/w nano-emulsion.

It is expected that the architected poly-l-lysine coated nano-emulsion will protect and release proteins in a controlled manner at intestinal membrane due to adhesive property of poly-l-lysine to cell membrane [71].

1.6 Plan of work

1.6.1 Extensive literature review: To search out outstanding strategies for accomplishing elusive goal of orally deliverable insulin, myriad of literature was thoroughly reviewed.

1.6.2 Pre-formulation studies

Procurement and authentication of drugs (insulin, c-peptide) and excipients

- Identification of insulin
  - Physical characteristics
  - Melting point assessment
  - Spectroscopic analysis**:** Mass, NMR, FTIR, CD
- Solubility studies
- Analytical method development (RP-HPLC)
- Stability studies of stock solutions
- Drug – Excipient Interaction through FTIR

1.6.3 Formulation development and optimization

1.6.3.1 Thermo-responsive size shifting polymeric nanoparticles as a platform for oral delivery of insulin

- Preparation of thermo-responsive NPs by nano-precipitation method
- Solvent free loading of insulin
- Cellulose acetate phthalate (CAP) coating on NPs

1.6.3.2 Optimization of formulation

- Selection of suitable pluronic
- Selection of suitable polymer core for insulin (PLGA vs. PLA-NH2)

1.6.3.3 *In vitro* evaluation

- Physicochemical characterization: size, zeta potential, PDI
- Investigation and Enhancement of entrapment efficiency
- *In Vitro* release study
- Transmission Electron Microscopy (TEM)

- Stability study
- Protein confirmation and stability study
- *In vitro* cell uptake study
- Trans Epithelial Electrical Resistance (TEER)
- *In vitro* bio-activity

1.6.3.4 *In Vivo* evaluation

- Induction of diabetes
- Assessment of Hypoglycemic activity, Plasma insulin level and Pharmacokinetic profile (oral bio-availability)

1.6.4 Poly-l-lysine coated oral Nano-emulsion for combined delivery of insulin and c-peptide

1.6.4.1 Preparation of Nano-emulsion (w/o/w) by double emulsification method

1.6.4.2 Selection of the formulation components

- Selection of oil
- Selection of surfactant and co-surfactant

1.6.4.3 Optimization process

- **Optimization of nano-emulsion components**
  - Optimization of surfactant: co-surfactant ratio
  - Optimization of oil: surfactant mixture ratio
  - Optimization of aqueous surfactant
- **Optimization of process variables**
  - Effect of sonication time

1.6.4.4 Characterization and *In Vitro* evaluation

- Visual inspection
- Physicochemical characterization (mean globule size, PDI and zeta potential)
- Entrapment efficiency
- *In vitro* drug release study
- Transmission Electron Microscopy (TEM)
- Protein confirmation and stability study
- *In vitro* cell uptake study
- Trans Epithelial Electrical Resistance (TEER)
- *In vitro* bio-activity of insulin
- Stability study

1.6.4.5 *In Vivo* evaluation

- Induction of diabetes (STZ induced diabetes mellitus type II)
- *In vivo* efficacy (blood glucose lowering effect)
- Estimation of plasma insulin and c-peptide level
- Pharmacokinetic profile and valuation of oral bio-availability

1.6.5 Statistical Analysis

1.6.6 Summary and conclusion

1.7 REFERENCES

1. *IDF Diabetes Atlas* 2013 November 2013; Sixth Edition:[Available from: http://www.statista.com/statistics/241820/estimated-global-healthcare-expenditures-to-treat-diabetes/.
2. Zhang, P., et al., *Global healthcare expenditure on diabetes for 2010 and 2030.* Diabetes Research and Clinical Practice, 2010. **87**(3): p. 293-301.
3. Ramachandran, A., et al., *Trends in prevalence of diabetes in Asian countries.* World Journal of Diabetes, 2012. **3**(6): p. 110-117.
4. *Standards of medical care in diabetes--2014.* Diabetes Care, 2014. **37 Suppl 1**: p. S14-80.
5. Lebovitz, H.E., *Insulin resistance: definition and consequences.* Exp Clin Endocrinol Diabetes, 2001. **109 Suppl 2**: p. S135-48.
6. Berenson, D.F., et al., *Insulin analogs for the treatment of diabetes mellitus: therapeutic applications of protein engineering.* Annals of the New York Academy of Sciences, 2011. **1243**(1): p. E40-E54.
7. *Continuous Glucose Monitoring and Intensive Treatment of Type 1 Diabetes.* New England Journal of Medicine, 2008. **359**(14): p. 1464-1476.
8. Sigal, R.J., et al., *Physical activity/exercise and type 2 diabetes: a consensus statement from the American Diabetes Association.* Diabetes Care, 2006. **29**(6): p. 1433-8.
9. Hermann, L.S., *Combination therapy with insulin and metformin.* Endocr Pract, 1998. **4**(6): p. 404-12.
10. Hemmingsen, B., et al., *Comparison of metformin and insulin versus insulin alone for type 2 diabetes: systematic review of randomised clinical trials with meta-analyses and trial sequential analyses.* BMJ, 2012. **344**: p. e1771.
11. Inzucchi, S.E., *Oral antihyperglycemic therapy for type 2 diabetes: scientific review.* Jama, 2002. **287**(3): p. 360-372.
12. Shah, R.B., et al., *Insulin delivery methods: Past, present and future.* International journal of pharmaceutical investigation, 2016. **6**(1): p. 1-9.
13. Sabetsky, V. and J. Ekblom, *Insulin: a new era for an old hormone.* Pharmacol Res, 2010. **61**(1): p. 1-4.
14. Owens, D.R., *New horizons [mdash] alternative routes for insulin therapy.* Nat Rev Drug Discov, 2002. **1**(7): p. 529-540.
15. Reis, C.P. and C. Damge, *Nanotechnology as a promising strategy for alternative routes of insulin delivery.* Methods Enzymol, 2012. **508**: p. 271-94.
16. Farmer, T.G., Jr., T.F. Edgar, and N.A. Peppas, *The future of open- and closed-loop insulin delivery systems.* The Journal of pharmacy and pharmacology, 2008. **60**(1): p. 1-13.
17. Botz, C.K., E.B. Marliss, and A.M. Albisser, *Blood glucose regulation using closed- and open-loop insulin delivery systems.* Diabetologia, 1979. **17**(1): p. 45-49.
18. Hovorka, R., *Continuous glucose monitoring and closed-loop systems.* Diabet Med, 2006. **23**(1): p. 1-12.
19. Pickup, J.C., *Management of diabetes mellitus: is the pump mightier than the pen?* Nat Rev Endocrinol, 2012. **8**(7): p. 425-433.
20. Hovorka, R., *Closed-loop insulin delivery: from bench to clinical practice.* Nat Rev Endocrinol, 2011. **7**(7): p. 385-395.
21. Russell, S.J., et al., *Outpatient Glycemic Control with a Bionic Pancreas in Type 1 Diabetes.* New England Journal of Medicine, 2014. **371**(4): p. 313-325.
22. Jain, K.K., *Nanotechnology in clinical laboratory diagnostics.* Clin Chim Acta, 2005. **358**(1-2): p. 37-54.
23. Ferrari, M., *Cancer nanotechnology: opportunities and challenges.* Nat Rev Cancer, 2005. **5**(3): p. 161-171.

24. Misra, R., S. Acharya, and S.K. Sahoo, *Cancer nanotechnology: application of nanotechnology in cancer therapy.* Drug Discovery Today, 2010. **15**(19–20): p. 842-850.
25. Goldstein, B.J., et al., *Effect of initial combination therapy with sitagliptin, a dipeptidyl peptidase-4 inhibitor, and metformin on glycemic control in patients with type 2 diabetes.* Diabetes Care, 2007. **30**(8): p. 1979-87.
26. Veiseh, O., et al., *Managing diabetes with nanomedicine: challenges and opportunities.* Nat Rev Drug Discov, 2015. **14**(1): p. 45-57.
27. DiSanto, R.M., V. Subramanian, and Z. Gu, *Recent advances in nanotechnology for diabetes treatment.* Wiley Interdisciplinary Reviews: Nanomedicine and Nanobiotechnology, 2015: p. n/a-n/a.
28. Godin, B., et al., *Emerging applications of nanomedicine for the diagnosis and treatment of cardiovascular diseases.* Trends in Pharmacological Sciences, 2010. **31**(5): p. 199-205.
29. Wickline, S.A., et al., *Applications of Nanotechnology to Atherosclerosis, Thrombosis, and Vascular Biology.* Arteriosclerosis, Thrombosis, and Vascular Biology, 2006. **26**(3): p. 435-441.
30. LaVan, D.A., D.M. Lynn, and R. Langer, *Moving smaller in drug discovery and delivery.* Nat Rev Drug Discov, 2002. **1**(1): p. 77-84.
31. Snee, P.T., et al., *A Ratiometric CdSe/ZnS Nanocrystal pH Sensor.* Journal of the American Chemical Society, 2006. **128**(41): p. 13320-13321.
32. Farokhzad, O.C. and R. Langer, *Impact of nanotechnology on drug delivery.* ACS Nano, 2009. **3**(1): p. 16-20.
33. Medintz, I.L., et al., *Quantum dot bioconjugates for imaging, labelling and sensing.* Nat Mater, 2005. **4**(6): p. 435-446.
34. McNeil, S.E., *Unique benefits of nanotechnology to drug delivery and diagnostics.* Methods Mol Biol, 2011. **697**: p. 3-8.
35. Elsabahy, M. and K.L. Wooley, *Design of polymeric nanoparticles for biomedical delivery applications.* Chem Soc Rev, 2012. **41**(7): p. 2545-61.
36. Tan, M., et al., *Inorganic Nanoparticles for Biomedical Applications*, in *NanoScience in Biomedicine*, D. Shi, Editor. 2009, Springer Berlin Heidelberg. p. 272-289.
37. Gao, J., H. Gu, and B. Xu, *Multifunctional Magnetic Nanoparticles: Design, Synthesis, and Biomedical Applications.* Accounts of Chemical Research, 2009. **42**(8): p. 1097-1107.
38. Kogan, M.J., et al., *Peptides and metallic nanoparticles for biomedical applications.* Nanomedicine, 2007. **2**(3): p. 287-306.
39. Klostranec, J.M. and W.C.W. Chan, *Quantum Dots in Biological and Biomedical Research: Recent Progress and Present Challenges.* Advanced Materials, 2006. **18**(15): p. 1953-1964.
40. Wu, X., et al., *Immunofluorescent labeling of cancer marker Her2 and other cellular targets with semiconductor quantum dots.* Nat Biotech, 2003. **21**(1): p. 41-46.
41. Pawar, V.K., et al., *Engineered nanocrystal technology: In-vivo fate, targeting and applications in drug delivery.* Journal of Controlled Release, 2014. **183**(0): p. 51-66.
42. Bao, Y. and K.M. Krishnan, *Preparation of functionalized and gold-coated cobalt nanocrystals for biomedical applications.* Journal of Magnetism and Magnetic Materials, 2005. **293**(1): p. 15-19.
43. Liang, D., B.S. Hsiao, and B. Chu, *Functional electrospun nanofibrous scaffolds for biomedical applications.* Advanced Drug Delivery Reviews, 2007. **59**(14): p. 1392-1412.
44. Roy, A., O.L. Franco, and S.M. Mandal, *Biomedical exploitation of self assembled peptide based nanostructures.* Curr Protein Pept Sci, 2013. **14**(7): p. 580-7.
45. Svenson, S. and D.A. Tomalia, *Dendrimers in biomedical applications—reflections on the field.* Advanced Drug Delivery Reviews, 2005. **57**(15): p. 2106-2129.
46. Alarcon, C.d.l.H., S. Pennadam, and C. Alexander, *Stimuli responsive polymers for biomedical applications.* Chemical Society Reviews, 2005. **34**(3): p. 276-285.

47. Kumar, C.S., J. Hormes, and C. Leuschner, *Nanofabrication towards biomedical applications: Techniques, tools, applications, and impact*. 2006: John Wiley & Sons.
48. Pawar, V.K., et al., *Targeting of gastrointestinal tract for amended delivery of protein/peptide therapeutics: strategies and industrial perspectives.* J Control Release, 2014. **196**: p. 168-83.
49. Rao, J.P. and K.E. Geckeler, *Polymer nanoparticles: Preparation techniques and size-control parameters.* Progress in Polymer Science, 2011. **36**(7): p. 887-913.
50. Pinto Reis, C., et al., *Nanoencapsulation I. Methods for preparation of drug-loaded polymeric nanoparticles.* Nanomedicine: Nanotechnology, Biology and Medicine, 2006. **2**(1): p. 8-21.
51. Seymour, M., *Coal-aqueous mixtures having a particular coal particle size distribution*. 1986, Google Patents.
52. Fowler, M.J., *Microvascular and Macrovascular Complications of Diabetes.* Clinical Diabetes, 2008. **26**(2): p. 77-82.
53. Yosten, G.L.C., et al., *Physiological effects and therapeutic potential of proinsulin C-peptide.* American Journal of Physiology - Endocrinology And Metabolism, 2014. **307**(11): p. E955-E968.
54. Hills, C.E. and N.J. Brunskill, *Cellular and physiological effects of C-peptide.* Clin Sci (Lond), 2009. **116**(7): p. 565-74.
55. Janghorbani, M., M. Dehghani, and M. Salehi-Marzijarani, *Systematic Review and Meta-analysis of Insulin Therapy and Risk of Cancer.* Hormones and Cancer, 2012. **3**(4): p. 137-146.
56. Erpeldinger, S., et al., *Efficacy and safety of insulin in type 2 diabetes: meta-analysis of randomised controlled trials.* BMC Endocrine Disorders, 2016. **16**(1): p. 39.
57. Marques, R.G., M.J. Fontaine, and J. Rogers, *C-peptide: much more than a byproduct of insulin biosynthesis.* Pancreas, 2004. **29**(3): p. 231-8.
58. Wahren, J., et al., *Role of C-peptide in human physiology.* Am J Physiol Endocrinol Metab, 2000. **278**(5): p. E759-68.
59. Johansson, B.L., S. Sjoberg, and J. Wahren, *The influence of human C-peptide on renal function and glucose utilization in type 1 (insulin-dependent) diabetic patients.* Diabetologia, 1992. **35**(2): p. 121-8.
60. Johansson, B.L., et al., *Influence of combined C-peptide and insulin administration on renal function and metabolic control in diabetes type 1.* J Clin Endocrinol Metab, 1993. **77**(4): p. 976-81.
61. Ekberg, K., et al., *Amelioration of sensory nerve dysfunction by C-Peptide in patients with type 1 diabetes.* Diabetes, 2003. **52**(2): p. 536-41.
62. Hansen, A., et al., *C-Peptide Exerts Beneficial Effects on Myocardial Blood Flow and Function in Patients With Type 1 Diabetes.* Diabetes, 2002. **51**(10): p. 3077-3082.
63. des Rieux, A., et al., *Nanoparticles as potential oral delivery systems of proteins and vaccines: A mechanistic approach.* Journal of Controlled Release, 2006. **116**(1): p. 1-27.
64. Ensign, L.M., R. Cone, and J. Hanes, *Oral drug delivery with polymeric nanoparticles: The gastrointestinal mucus barriers.* Advanced Drug Delivery Reviews, 2012. **64**(6): p. 557-570.
65. Swaminathan, J. and C. Ehrhardt, *Liposomal delivery of proteins and peptides.* Expert Opin Drug Deliv, 2012. **9**(12): p. 1489-503.
66. Fan, T., et al., *Design and evaluation of solid lipid nanoparticles modified with peptide ligand for oral delivery of protein drugs.* Eur J Pharm Biopharm, 2014. **88**(2): p. 518-28.
67. Venkata Ramana Rao, S. and J. Shao, *Self-nanoemulsifying drug delivery systems (SNEDDS) for oral delivery of protein drugs: I. Formulation development.* International Journal of Pharmaceutics, 2008. **362**(1–2): p. 2-9.

68. Kato, M., et al., *Effect of Alpha-Linolenic Acid on Blood Glucose, Insulin and GLUT4 Protein Content of Type 2 Diabetic Mice.* JOURNAL OF HEALTH SCIENCE, 2000. **46**(6): p. 489-492.
69. Niu, Z., et al., *Rational design of polyarginine nanocapsules intended to help peptides overcoming intestinal barriers.* Journal of Controlled Release.
70. Nitta, S.K. and K. Numata, *Biopolymer-Based Nanoparticles for Drug/Gene Delivery and Tissue Engineering.* International Journal of Molecular Sciences, 2013. **14**(1): p. 1629-1654.
71. Nojehdehian, H., et al., *Preparation and surface characterization of poly-L-lysine-coated PLGA microsphere scaffolds containing retinoic acid for nerve tissue engineering: in vitro study.* Colloids Surf B Biointerfaces, 2009. **73**(1): p. 23-9.

CHAPTER 2

Pre-formulation studies

2.1 Brief insight into drugs and major excipients used in the study

2.1.1 Insulin

- **Structure:** Physiologically, it is synthesized from its precursor proinsulin, an 86 amino acid single chain peptide which upon cleavage produces equimolar amount of insulin and c peptide. Herein, insulin is composed of total 51 amino acid subdivided into two chains linked by two disulphide bonds; 21 amino acid residue chain A and 30 amino acid residue chain B as shown in figure 2.1(a). Human insulin exists as monomer (6kDa), dimer (12kDa), and hexamer (36kDa) forms in equilibrium as shown in figure 2.1(b). However, the monomer structure of insulin is solely responsible for binding with insulin receptor and generating the pharmacological actions [1].

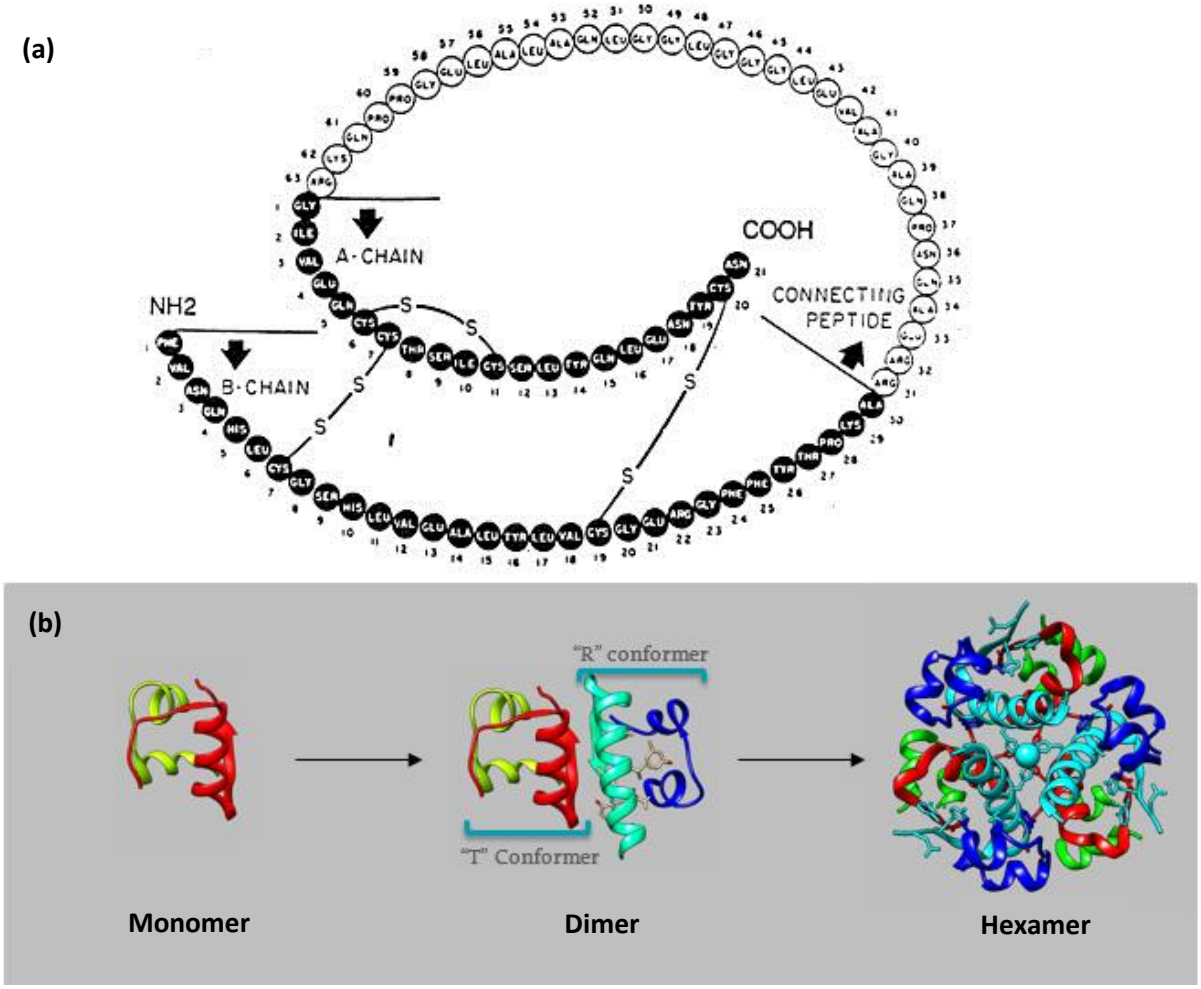

Figure 2.1 Structures of porcine insulin (a) schematic structure with peptide chains [2] (b) 3D structure of insulin monomer, dimer and hexamer [3, 4]

- **Source:** Before the employment of recombinant DNA technology, insulin was majorly obtained from animal source for example, bovine insulin from cow, ox and beef etc., and porcine insulin from pigs. Despite the structural differences as compared to human insulin in terms of amino acids (bovine - 3; porcine - 1), the physiological functions are almost analogous. Due to immunogenic potential and local or systemic hypersensitivity reactions, insulin obtained from animal sources is not in clinical use these days. The niche has been filled by recombinant human insulin which rarely produces immunogenic response due to structural analogy with endogenously produced insulin and high purity [5].
- **Immunogenicity:** Immunogenicity was mainly associated with the past versions of insulin which were usually sub-purified and having traces of proinsulin, c-peptide and other peptides as contaminants. It is well-notified that patients treated with this kind of insulin were having high titres of IgG-insulin antibodies which inactivates insulin by making a complex and in turn further increases the immune mediated insulin resistance [6]. Usually, patients with previous exposure to insulin have more chances of showing immunogenic hypersensitivity when retreated with insulin [7].

  Despite prominent use of recombinant human insulin now a days, rarely a hypersensitivity (immediate, local or systemic IgE mediated respone) to insulin has been observed [8]. Another clinical complication of insulin originates at the site of injection in terms of lipodystrophy due to routine multiple shots[9]. Lipodystrophy, an abnormality in adipose tissue, includes two conditions lipoatrophy (local fat loss recognized by cutaneous depression and substantial atrophy of subcutaneous fat) and lipohypertrophy (tumour like lump or swelling of subcutaneous fatty tissues nearby the insulin injection site) [10]. It is reported that more than 50 percentage of diabetic patients treated with insulin are having lipohypertrophy [11, 12]. Moreover, it also varies the absorption of insulin and leads to meagre glycaemic control with unpredicted hypoglycaemic episodes [13]. The rotation of site for injection and relatively low dose of insulin remains the ultimate treatment for management of lipohypertrophy.
- **Insulin preparations:** Various insulin preparations, their brand names, commercial preparations available, dosage regimen, duration of action and specific remarks regarding structure or usage is presented in the table 2.1.

Table 2.1 Various insulin preparations available in the market

Category/Name of Insulin	Brand Name (manufacturer)	Preparation	Dosage regimen	Duration of action (hours)	Specific Remarks (in comparison to Human insulin)
Rapid-Acting					
Insulin Lispro	Humalog (Lilly)	Vial, cartridge, disposable pen	Injected before and immediately after meal	3-5	interchange of B28 (proline) and B29 (lysine) amino acid sequence of insulin [14]
Insulin Aspart	Novolog (Novo Nordisk)	Vial, cartridge, disposable pen	Before or at meal time, twice a day	3-5	Replacement of proline with aspartic acid at B 28 position [15]
Insulin Glulisine	Apidra (Sanofi-Aventis)	Vial, disposable pen	15 minutes before or 20 minutes after starting a meal [16]	4	Two replacements -at B3 asparagine replaced by lysine -at B29 lysine replaced by glutamic acid [17]
Inhaled (Technosphere) insulin	Afreeza	Inhaler	Powdered insulin delivered	~ 3	pulmonary absorption is very rapid, and its elimination time is shorter than SC [18]
Short-Acting					
Regular Human	Humulin R (Lilly) Novolin R (Novo Nordisk)	Vial	Injected 30 min before meal	5-8	Forms hexamers, which gradually dissociates into absorbable insulin dimers and monomers[19]
Intermediate-Acting					
NPH Human	Humulin N (Lilly) Novolin N (Novo Nordisk)	Vial, disposable pen Vial	Dosed at bed-time	<14	Complexed with protamine for prolong action [20]
Long-Acting					
Insulin Detemir	Levemir (Novo Nordisk)	Vial, disposable pen	Once or twice daily	20-24	a long-acting insulin analogue in which the B30 amino acid is omitted followed by addition of myristic

					acid (C14) at the B29 lysine [21]
Insulin Glargine	Lantus (Sanofi-Aventis) Basaglar (Lilly) Toujeo (Sanofi-Aventis)	Vial, cartridge, disposable pen disposable pen disposable pen	Once daily at any time of day or twice daily at higher doses	24	- C-terminus of B chain has extra two arginines which alters the isoelectric point from a pH 5.4 to pH 6.7[22] - Asparagine is substituted by glycine at A21, protecting it from deamidation and dimerization
Insulin Degludec	Tresiba (Novo Nordisk)	Disposable pen	once a day at any time [23]	42	Subtraction of B30 amino acid is done and B29 amino acid is linked to a C16 di-acid through glutamic acid spacer to make it ultra-long-acting [24]
Insulin Mixtures					
NPH/Regular (70%/30%)	Humulin 70/30 (Lilly) Novolin 70/30 (Novo Nordisk)	Vial, disposable pen Vial	Twice daily before breakfast and dinner	18-24	Mixture of prolong acting NPH insulin and rapid-acting regular insulin, which act as a maintenance dose and loading dose respectively[25]
Protamine/Lispro (50%/50%)	Humalog Mix 50/50 (Lilly)	Vial, disposable pen	Twice daily before breakfast and dinner	14-24	Speedy onset of blood glucose-lowering action (due to Lispro) followed by maintenance provided by protamine [26]
Protamine/Lispro (75%25%)	Humalog Mix 75/25 (Lilly)	Vial, disposable pen	Twice daily before breakfast and dinner	14-24	For customized glucose lowering activity [27] percentage is varied with respect to its 50/50 analogue [17]
Protamine/Aspart (70/30)	Novolog Mix 70/30 (Novo Nordisk)	Vial, disposable pen	Twice daily before breakfast and dinner	18-24	Absorbed more rapidly from SC route. 70% of its crystalline form has prolong absorption profile[28]

- **Strength:** The generally used concentration of insulin ranges from 40 to 500 units/ml according to its type and the targeted population i.e. country. Commonly found strengths are 100U/ml, 200U/ml and 500U/ml [29]. The different concentrations offers a space to fine tune the required dose for patient's condition and help physicians in recommending proper regimen for patients.
- **Physico-chemical properties:**
    a. **Molecular weight:** 5808.1 Daltons
    b. **Chemical formula:** $C_{257}H_{383}N_{65}O_{77}S_6$
    c. **Melting point:** 81°C
    d. **Isoelectric point:** 5.5
    e. **State:** solid crystalline powder
    f. **Colour:** white to off white
- **Mechanism of action and Pharmacodynamics**

Insulin shows numerous effects at cellular level. It provokes uptake of glucose by skeletal muscle cells, peripherally and hence, decreases the blood glucose level. It facilitates diffusion of glucose into fat and muscle cells via modulation of GLUT 4 translocation which is afterwards stored in to glycogen and fat as fuel storage. Moreover, it also dampens the glucose production from liver by rendering gluconeogenesis and glycogenolysis [30]. The modified insulin preparations exhibit different pharmacodynamics as well as pharmacokinetic parameters such as onset time and onset of hypoglycaemic action, maximum (peak) action and length of action (quick, short, intermediate and long action) [31]. However, a dose reliant effects are also noted with regular insulin and NPH (isophane) intermediate acting insulin, wherein, higher doses may delay the onset but increase the duration [32].

- **Pharmacokinetics**

a) Absorption

After SC injection, the absorption of insulin into the bloodstream is the key phenomena which governs its activity. The monomers and dimers of insulin get absorbed straight into the blood capillaries due to their small size but the hexamer form is not absorbed into the blood capillaries. However, with the help of lymphatic system insulin hexamers are being able to absorb up to somewhat level [33, 34]. Despite having comparatively low absorption, hexameric form of insulin offers advantage of better storage stability. Therefore, for better

stability during storage, excipients are added which can increase the equilibrium constant (K_{HD}) so that equilibrium between oligomers will be shifted towards hexmeric form of insulin as shown in figure 2.2 [35, 36]. The main factors that affect absorption of insulin from subcutaneous tissue are a) type of insulin, b) site of injection and c) flow of blood at site of injection [37].

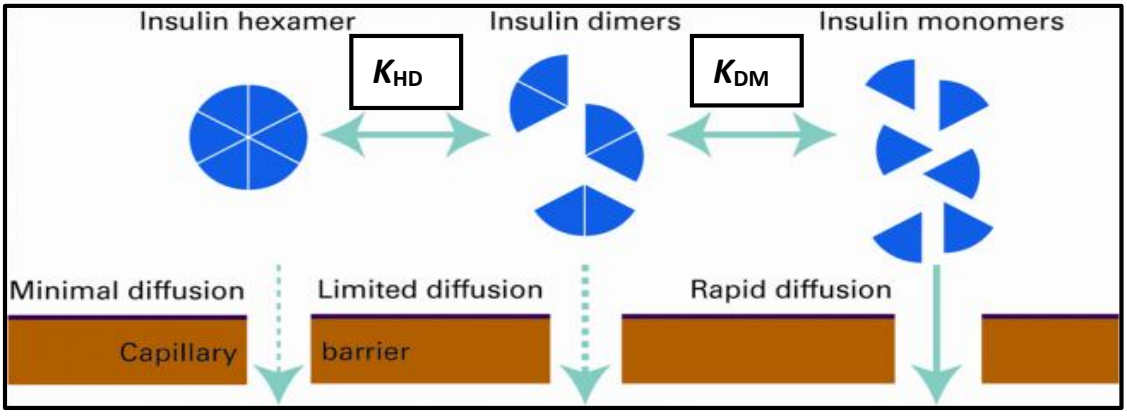

Figure 2.2 Absorption pattern of different oligomers of insulin with equilibrium constants K_{HD} (between hexamer and dimer form) and K_{DM} (between dimer and monomer form) [38]

b) Metabolism and Elimination

Basically, the insulin is being degraded by insulin degrading enzyme and the prime sites for insulin clearance are liver and kidney. Almost 50 to 60 percentage of insulin, released into the portal vein from pancreas, is being eliminated by liver and remaining 40 to 30 percentage insulin is being eliminated by kidney in normal physiological condition. However, the situation alters in the diabetic patients receiving insulin externally via SC injections, kidney accounts for the majority of degradation (around 60%) and liver accounts for relatively lesser level (approximately 35%) of degradation, due to unavailability of directly secreted insulin into the hepato-portal vein [39]. The pivotal role of kidney in insulin clearance leads to the critical concerns in the diabetic patients with chronic kidney diseases and renal failure [40]. A compromised functioning of kidney leads to the decremented clearance and prolonged effect of insulin, setting alarm for gradual reduction of insulin administration but with increased risk of hypoglycemia [41]. However, for clinically significant decline in administered dose of insulin, there has to be a significant deterioration of renal function.

2.1.2 Excipient Profile

2.1.2.1 PLGA

PLGA is a well-known and extensively exploited polymer for the delivery of drugs or therapeutic payload due to its biocompatibility and biodegradability [42]. It is co-polymer made up of Poly lactic acid (PLA) and Poly glycolic acid (PGA), which consist iterative moieties of lactic acid and glycolic acid, respectively [43]. The synthesis of PLGA is driven by copolymerization through two different ways resulting in PLGA with different molecular weights. For synthesizing low molecular weight (<10 KDa) PLGA poly-condensation of its monomers lactic acid and glycolic acid in solution phase at temperature above 120°C with water removal process is preferred. However, this process is not capable of synthesizing high molecular weight PLGA due to inability of producing high degree of dehydration. Therefore, synthesis of PLGA with high MW subjugates ring opening directed polymerization of diesters of lactic acid and glycolic acid in the presence of catalysts such as powdered zinc, zinc chloride, antimony trifluoride, and organometallic catalysts i.e. triethyl aluminum and stannous octoate [44] as shown in Figure 2.3. Based on percentage of its formative units PLGA is coined accordingly; for instance PLGA 50:50 stands for PLGA made up of 50% lactic acid and 50% glycolic acid units. Similarly, PLGA 75:25 is implied for PLGA having 75% lactic acid and 25% glycolic acid units. However, it should be noted that change in percentage of monomers, either lactic acid or glycolic acid, result in PLGA with different characteristics. Lactic acid (2-hydroxypropanoic acid) possess one more methyl group as compared to glycolic acid (2-hydroxyethanoic acid) and hence it is more hydrophobic. Therefore, PLGA with more percentage of lactic acid than glycolic acid (PLGA 75:25) stands to be more hydrophobic and vice versa. The in vivo fate of PLGA follows a safe route converting it into its components lactic acid and glycolic acid which enter in tri carboxylic acid cycle and ultimately throw out the carbon dioxide and water as the end product. This phenomenon showcase PLGA as biodegradable as well as biocompatible polymer [45, 46]. As being USFDA approved and generally recognized as safe (GRAS) polymer, PLGA owns a long list of clinically sanctioned applications in various biomedical fields for example, biodegradable sutures, as fixating devices in bone surgery and orthopedics, in tissue engineering, as drug delivery carriers for controlled and targeted release of drug, as implant material, etc [47]. Moreover, PLGA is especially well

exploited for delivery of protein and peptide making it a suitable polymer as an platform for development of nano sized carriers for oral delivery of insulin and c-peptide [48-50].

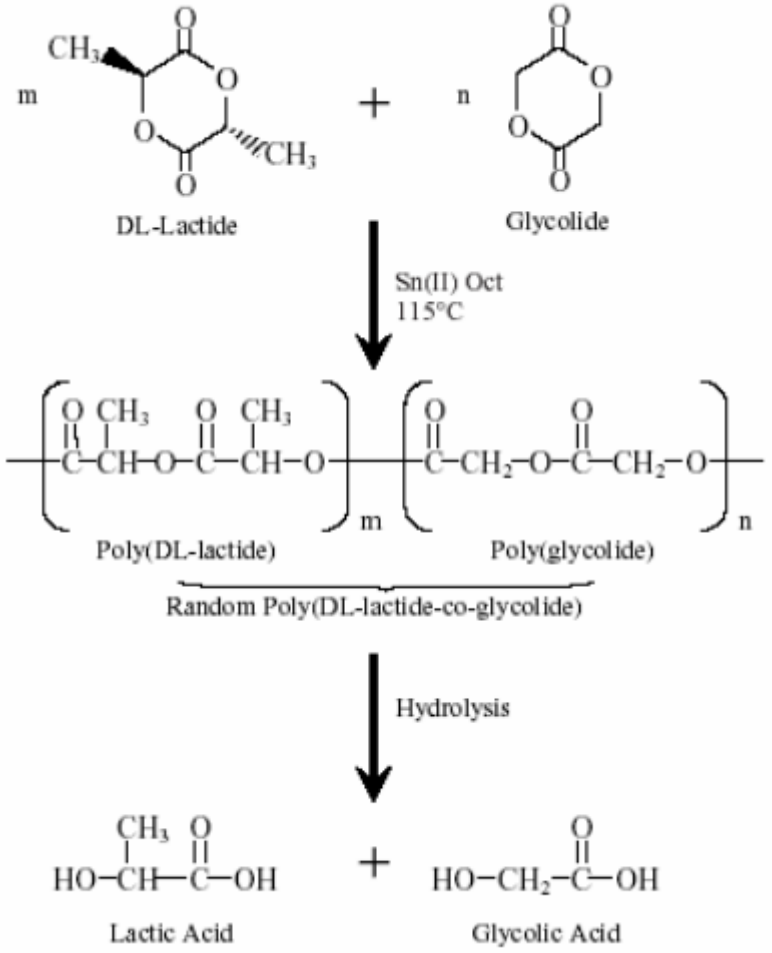

Figure 2.3 Synthesis and metabolic hydrolysis of PLGA [51]

2.1.2.2 Poly Lactic Acid (PLA)

In 1932 Carothers at DuPont discovered low molecular weight PLA by a raw poly-condensation wherein lactic acid was heated under vacuum [52]. Similar to the PLGA, to produce high MW PLA, synthesis via ring-opening polymerization process has to be selected. PLA is widely deployed for various applications such as dissolvable sutures and anchors, bone fracture support while surgery and matrix material for drug delivery systems. PLA is biodegradable and biocompatible similar to the PLGA but more hydrophobic in nature which can provide better controlled release of entrapped hydrophilic payload such as proteins and peptides. PLA and PLGA both offers carboxylic acid (anionic) as well as

amine (cationic) terminal which provides additional benefits for architecture of electrostatic interaction based drug delivery systems bearing charged molecules, proteins and peptides [53, 54].

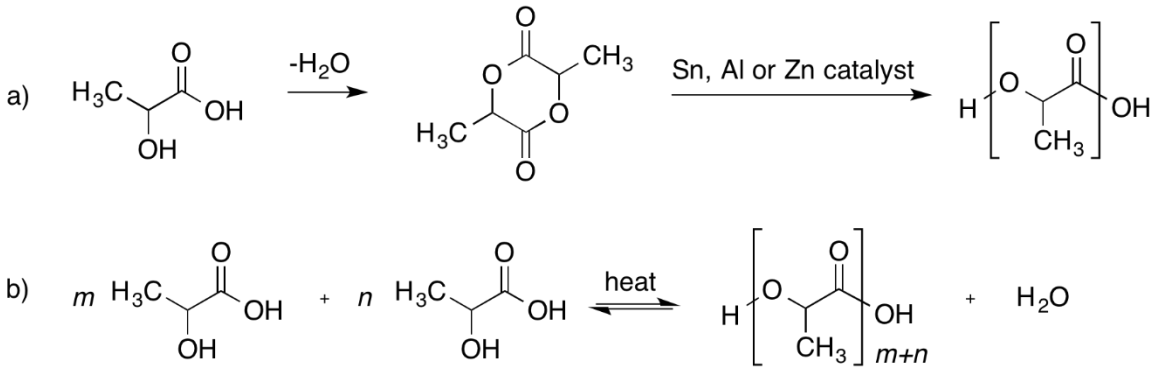

Figure 2.4 Synthesis of PLA by a) Ring-opening polymerization of lactide and b) poly-condensation method [55]

2.1.2.3 Pluronics

Pluronics or Poloxamers are group of tri-block co-polymers of Polyoxyethylene (PEO) and Polyoxypropylene (PPO), wherein two PEO are connected to one PPO molecule in a flanked way as shown in figure 2.5. Pluronic F127 is nonionic and water soluble amphiphilic surfactant widely used for solubilizing poorly soluble molecules, for stabilizing drug delivery systems and for developing self-assembled miceller systems [56]. Its molecular weight is approximately 12,500 Daltons. Interestingly, Pluronics exhibit temperature dependent micellization as well as swelling or gelling properties depending on the percentage content of PEO block [57]. Pluronic F127 is reported to show temperature governed reversible gelling phenomena above 20% w/v concentration. Similarly, Pluronic F68 and Pluronic P123 are also reported for their temperature regulated gelling behavior.

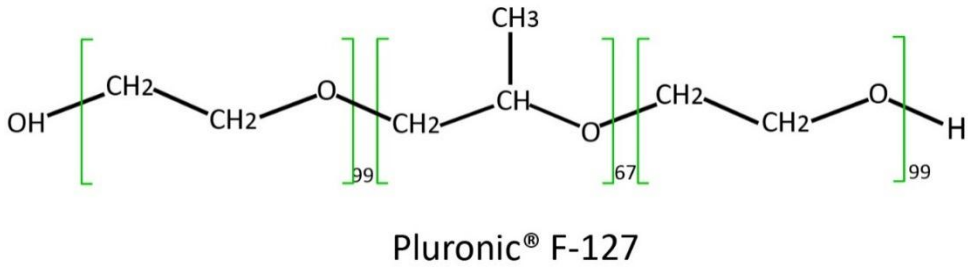

Figure 2.5 Structure of Pluronic F127 [58]

2.1.2.4 Tocopheryl Polyethylene Glycol Succinate (TPGS)

FDA approved TPGS as a water-soluble imitative of vitamin E (tocopherol) and vehicle which has a molecular weight of 1000 Daltons (figure 2.6). TPGS is inventive with amphiphilic nature and used as an emulsifier, surfactant, and stabilizer, dispersant, gallant, or micelle/self-construction material for poorly dispersible ingredients [59]. It act as a benign additive and commonly used in many drug delivery vectors. Recently, researchers have found its inhibitory activity against P-glycoprotein which makes it an important ingredient for overcoming multiple drug resistance in tumor patients [60, 61].

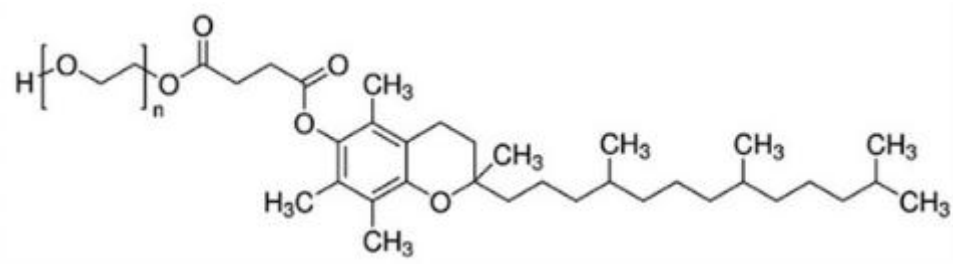

Figure 2.6 Structure of Tocopheryl Polyethylene Glycol Succinate

2.1.3 Analytical methods for estimation of Human recombinant insulin

Myriad of literature is available illustrating qualitative and quantitative estimation of human recombinant insulin in pharmaceutical preparations, drug delivery carriers and biological fluids such as plasma or serum. Spectroscopic as well as chromatographic methods are available for quantitative estimation of insulin in analytical samples. However, estimation of insulin in biological samples is somewhat difficult as the extraction/separation of insulin from matrix proteins of biological samples requires heavy efforts despite using advanced extraction processes such as Liquid-Liquid Extraction or Solid phase extraction method.

2.2 Materials and methods

Materials

Human recombinant insulin (regular), Amine group terminated Poly -l-lactide (PLA- NH_2), Poly lactide co-glycolide (PLGA) 50:50, Pluronic F127, Pluronic F68, Pluronic F123, dialysis membrane (MWCO 100KDa), Human recombinant insulin ELISA kit (RAB0327), and DNase/RNase free distilled water were procured from Sigma Aldrich , St. Louis, MO, USA. Membrane filters were purchased from Sartorius, Darmstadt, Germany.

Animals

The Male Sprague Dawley rats, 6 – 8 weeks old and weighing 180 – 200 grams, were acquired and handled as per the standard guidelines approved by IAEC, National Animal Laboratory Center, CSIR – Central Drug Research Institute, Lucknow, India. Blank plasma/serum (means without drug herein, without externally delivered insulin) was separated from the collected blood samples according to standard procedure and stored at -20 °C until used.

2.2.1 Identification of insulin

2.2.1.1 Physical characteristics

Human recombinant insulin was evaluated for its physical aspects including solid state and colour. These physical properties were compared with pharmacopoeial specifications.

2.2.1.2 Melting point

5 mg lyophilized powder was taken and melting point of insulin was measured by using capillary fusion method. Prior to estimation, melting point apparatus was calibrated using calibration standards as shown in table 2.2. Obtained result was compared with the reference values.

Table 2.2 Calibration standards used for melting point apparatus

Calibration Standards	Melting point (°C)
diphenylamine	54 ± 1
m-dinitrobenzene	90 ± 1
benzoic acid	122.5 ± 1
3,5-dinitrobenzoic acid	205 ± 2

2.2.1.3 Mass spectroscopy

Mass spectra of insulin was recorded on MALDI mass spectrophotometer with time-of-flight (TOF) analyser (Applied Biosystems 4700 Proteomics Analyzer with TOF/TOF™ Optics). Molecular ion peak, parent ion peak and any possible disintegration of insulin was observed carefully from obtained spectra.

2.2.1.4 Nuclear magnetic resonance (NMR) spectroscopy

^{1}H NMR spectrum of insulin was recorded on a Bruker DRX-400 NMR spectrophotometer after dissolving 5 mg lyophilized human recombinant insulin sample in D_2O.

2.2.2 Fourier Transform Infrared (FTIR) spectroscopy

The FTIR spectra shows respective peaks of the functional groups present in the compound. Any change in the chemical structure over the storage or its incompatibility/interaction with other chemical moiety can be easily spotted. Therefore, it can be used to assess any possible interaction between drug and excipients. Potassium bromide pellet method was used for sample preparation. The samples were analysed using Perkin Elmer Attenuated Total Reflectance (ATR) -FTIR spectrometer. Perfectly dried sample (5 mg) was placed under detection probe and scanned at 4 mm/s at a resolution of $1cm^{-1}$ over a region of 400-$4000cm^{-1}$ and observed characteristic peaks were compared with spectrum of reference standard as well as the literature.

2.2.3 Circular dichroism (CD) spectroscopy

CD spectroscopic analysis was carried out to assess the conformational changes in secondary structure of insulin using Jasco J-1500 CD spectrophotometer.

2.2.4 Solubility studies

The saturation solubility of insulin was determined in triple distilled MilliQ water having neutral pH, 0.1 N acetic acid solution pH 2.3, Phosphate buffer saline pH 7.0, 125mM NaHCO3 solution pH 8.3 and ethanol by shake flask method [62]. As insulin is a protein molecule and almost insoluble at isoelectric point which is 5.4 and very little soluble at neutral pH 7.0. Excess of insulin powder (10 mg) was added to 2 ml of respective solvent and placed on electric bench top orbital shaker (Thermo Fischer, India) at 25±2 °C for 24 hours. Afterwards, solution was filtered through sterile membrane filter with pore size 0.22µ and filtrate was analyzed by RP-HPLC method after suitable dilutions.

2.2.5 Analytical method development

A HPLC based analytical assay was established for quantification of insulin in developed formulations.

2.2.5.1 RP-HPLC method for insulin quantification

A single unit HPLC instrument LC-2010 (shimadzu®, japan), with autosampler unit, SPD-M10UV-PDA detector and a quaternary gradient pump was used. A validated RP-HPLC method was used with subtle fine tuning [63, 64]. Briefly, Lichrospher® 100 RP-18e, C18 HPLC column; (4.6 X 250 mm, 5 μm) was used for chromatographic separation of insulin at ambient temperature. 0.2 M sodium sulphate anhydrous attuned to pH 2.3 with OPA and acetonitrile in 70:30 v/v ratio, filtered (0.45μm Millipore membrane filter) under negative pressure and degassed by sonication was used as the mobile phase. The flow rate was maintained at 1.0 mL/min and detection was carried out at 214 nm. The injection volume was 20 μL. Chromatographic conditions set during chromatographic evaluation of insulin are summarized in table 2.3.

Table 2.3 Critical HPLC conditions used for detection of insulin

S.No.	Condition	Specifications
1	Column	Lichrospher® 100 RP-18e; C18 (4.6 X 250 mm,5 μm)
2	Mobile phase	0.2 M sodium sulphate : acetonitrile (70:30, v/v; pH 2.3)
3	Pressure	Up to 350 kgf/cm^2
4	Temperature	4±2 °C
5	Flow	Isocratic
6	Flow rate	1.0 mL/min
7	Injection volume	20 μL
8	Detector	Uv-Visible (UV), Photo Diode Array (PDA)
9	Wavelength	214 nm

2.2.5.2 Calibration curve of insulin

For making a calibration curve, first of all stock solution of insulin (100 μg/ml) in mobile phase was prepared. Herein, 1 mg lyophilized powder of insulin was dissolved in 1 ml of dilute acetic acid solution and further diluted to 10 ml by mobile phase to avoid the solvent peak in HPLC. After preparing the working standard stock solution of insulin (100 μg/ml),

dilutions were made to get the solutions of; 50, 100, 250, 500, 1000, 2000, 3000, 4000, and 5000 ng/ml. All the samples were run in triplicate under the specific chromatographic conditions mentioned in table 2.3. Peak area was calculated and graph of peak area vs. concentration was plotted.

2.2.6 Stability Studies

Stability of working stock solutions of insulin was investigated for period of 60 days. After 60 days, analytical aliquots from stored stock solutions were made and analysed by RP-HPLC method mentioned earlier. Recorded peak areas were compared with peak area obtained after analysis of aliquots made from newly prepared stock solution. Samples having less than 5% difference in concentration as compared to control (new stock solution) were considered stable. Moreover, chemical stability of insulin in analytical samples as well as biological matrices was assayed at low and high concentrations (n=6) for samples stored at different conditions for specific time intervals. For autosampler stability, long term stability and bench top stability samples were maintained for 10 hours at 4 °C, 30 days at -80 °C, and 6 hours at 25 ± 2 °C, respectively. For freeze thaw stability samples were frozen at -80 °C and then thawed at room temperature. This cycle was repeated thrice.

2.2.7 Drug – Excipient Interaction

Any sort of chemical interaction between API (herein, insulin and c-peptide) and excipients were traced by FTIR spectroscopy. FTIR spectrums of insulin, c-peptide and each excipient used in the formulations were obtained and compared with the FTIR spectrum of their physical mixtures. For CAP coated size shifting PLA nanoparticles, the FTIR spectra obtained from physical mixture of PLA (amine terminated), pluronic F127, insulin and cellulose acetate phthalate was compared with each of their respective FTIR spectra. Similarly, for linseed oil nano-emulsion bearing insulin and c-peptide, FTIR spectra of physical mixture of all the components of formulation was compared with FTIR spectra of each component. Any disappearance or emergence of specific characteristic peak (corresponding to specific functional group) was carefully traced and reported.

2.3 Results and Discussion

2.3.1 Identification of insulin

2.3.1.1 Physical characteristics

Physical characteristics of procured human recombinant insulin were identical to that of pharmacopoeial specifications i.e. it was lyophilized crystalline white coloured powder.

2.3.1.2 Melting point

According to the melting point apparatus calibrated with respect to calibration standards mentioned in the method part (table 2.2), the melting point of insulin was observed at 81 ± 1 °C which was identical to the reported values in pharmacopoeias and other literatures.

2.3.1.3 Mass spectroscopy

Molecular mass of human recombinant insulin was confirmed by MALDI-TOF tandem mass spectrophotometer. Most intense peak was obtained at 5809.1 m/z confirming its molecular mass of 5808.1 Daltons which is clearly visible in the mass spectra shown in figure 2.7.

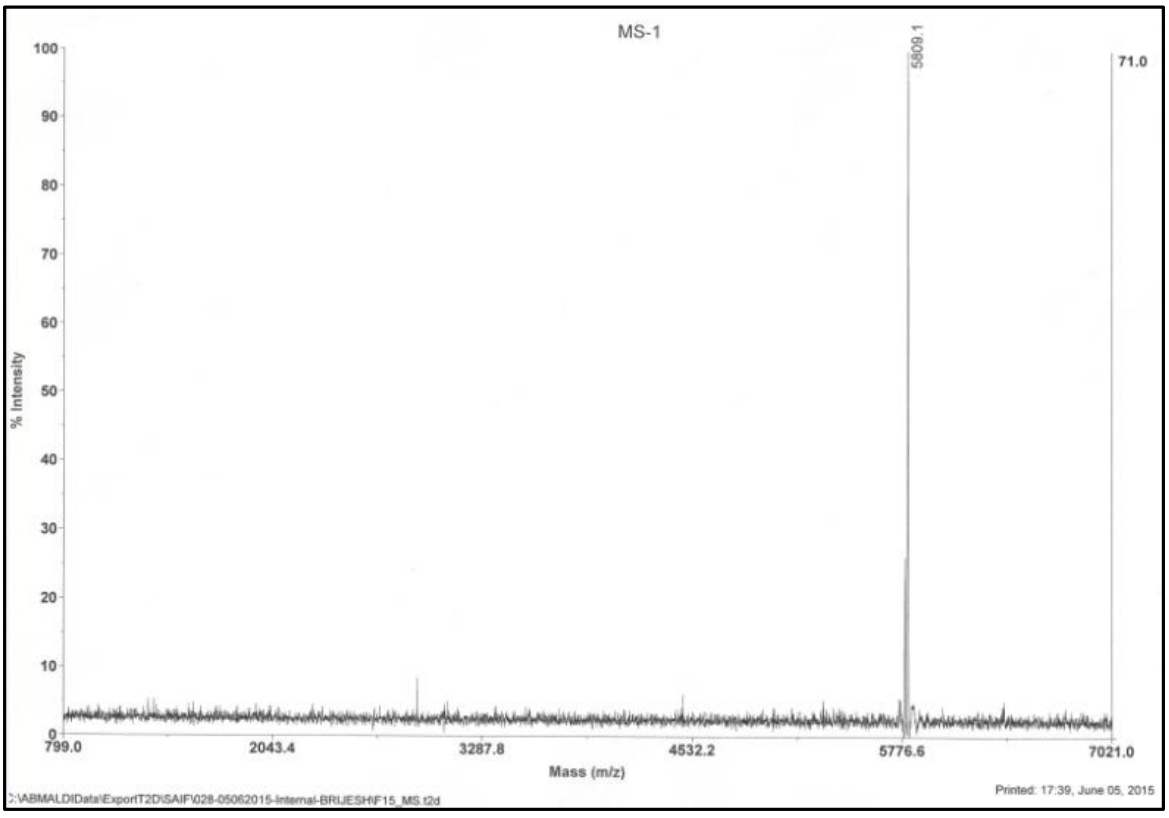

Figure 2.7 MALDI-TOF Mass spectra of human recombinant Insulin

2.3.1.4 Nuclear magnetic resonance (NMR) spectroscopy

^{1}H NMR spectrum of insulin obtained at 500 MHz is shown in figure 2.8 which is identical to native insulin in the literature [65, 66].

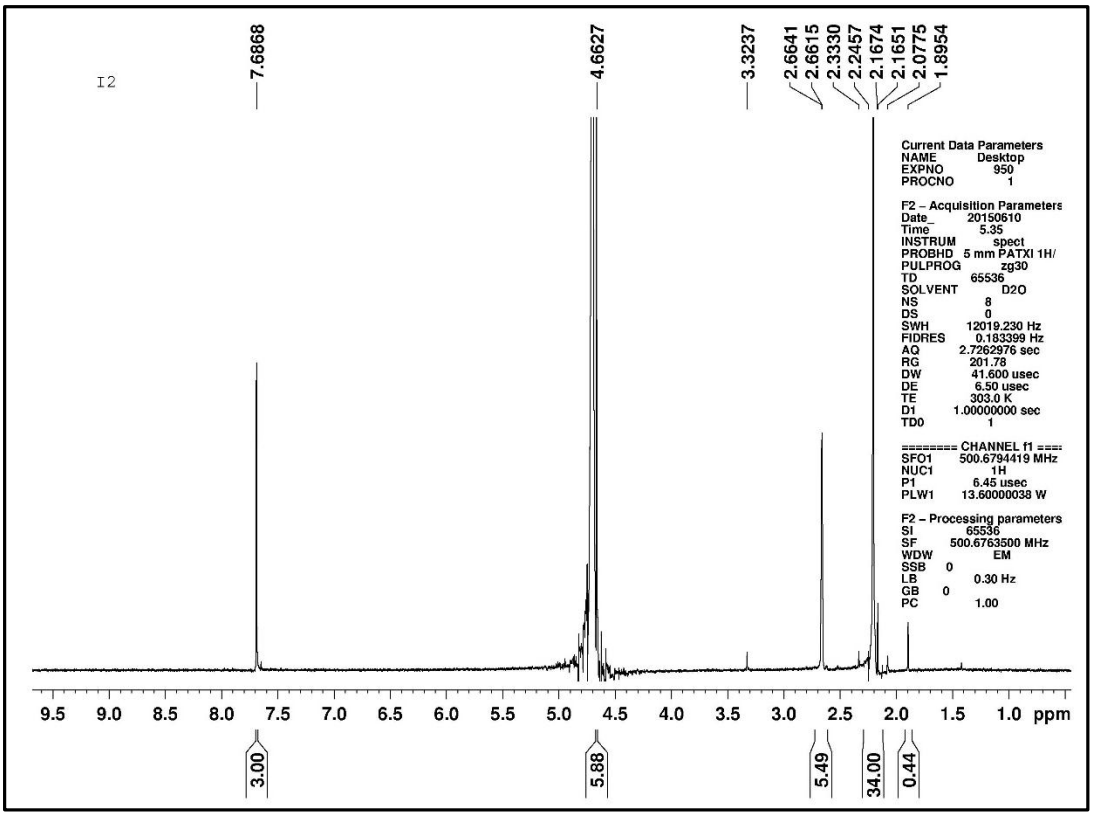

Figure 2.8 ^{1}H NMR spectrum of human recombinant insulin

2.3.2 Fourier Transform Infrared (FTIR) spectroscopy

FTIR spectrum of human recombinant insulin as shown in figure 2.9 was compared with the spectrum in literature and official pharmacopoeias. All the experimentally observed peaks were correlated with data in the literature and responsible functional groups for each peak are enlisted in the table 2.4 [67-69].

Table 2.4 Peaks observed in FTIR spectra of insulin and its inference

S.No.	Peak - Wavenumber (cm^{-1})		Functional group responsible for peak
	Experimental	Literature	
1	1525, 1640	1502, 1645	C=O stretching
2	3394	3400	H-N-H
3	1073	1098	C-N
4	1215	1267	C-O
5	3020	3300	N-H

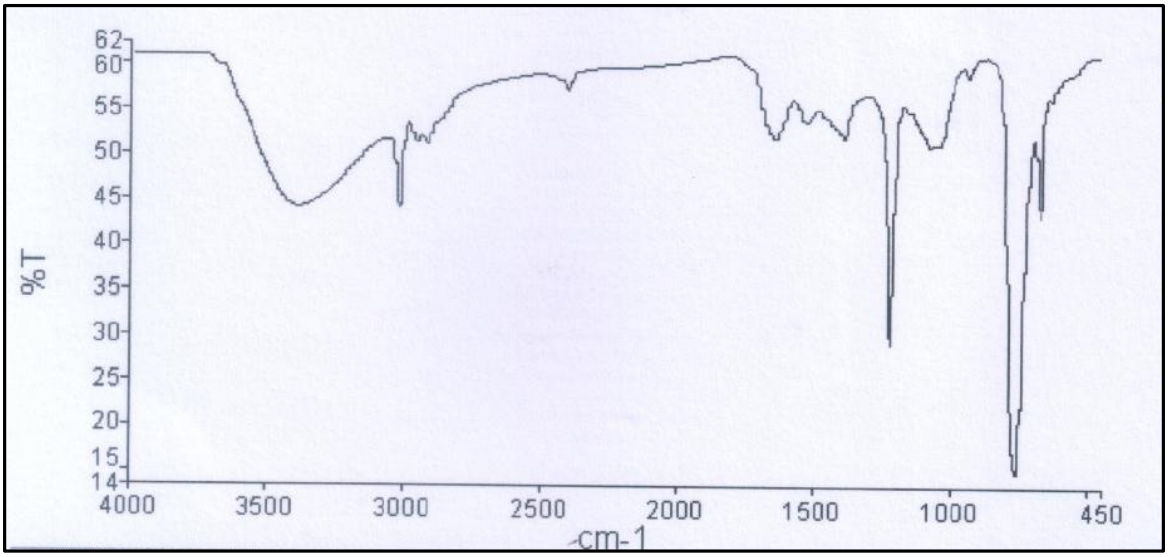

Figure 2.9 FTIR spectrum of human recombinant insulin

2.3.3 Circular dichroism (CD) spectroscopy

The confirmation stability of secondary structure of insulin was checked with CD spectrometry. The CD spectra showed characteristic peaks of alpha helix (negative band at 208 nm) as well as beta sheet structure (negative band at 223 nm) identical to standard insulin as shown in figure 2.10.

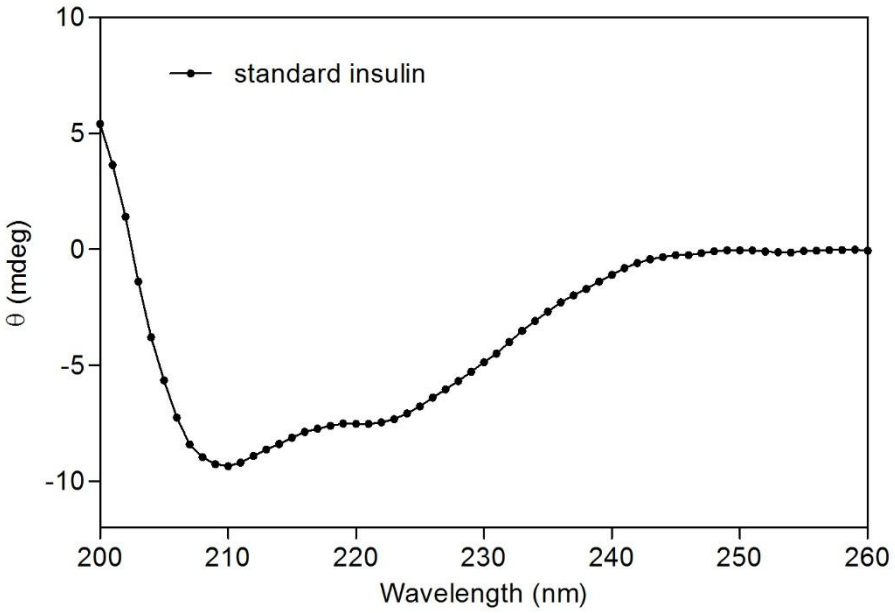

Figure 2.10 Circular dichroism spectra of human recombinant insulin

2.3.4 Solubility studies

The saturation solubility of insulin in triple distilled MilliQ water having neutral pH, 0.1 N acetic acid solution pH 2.3, Phosphate buffer saline pH 7.0, 125mM NaHCO3 solution pH 8.3 and ethanol is presented in table 2.5.

Table 2.5 Insulin solubility profile

S. No.	Solvent	Solubility status
1	Triple distilled water	**Insoluble**
2	0.1 N acetic acid solution pH 2.3	**Freely soluble**
3	Phosphate buffer saline pH 7.0	**Very slightly soluble**
4	125mM NaHCO3 solution pH 8.3	**Freely soluble**
5	Ethanol	**Insoluble**

2.3.5 Analytical RP-HPLC method development

The RP-HPLC method was partially validated for linearity and specificity according to the ICH Q2 guidelines.

2.3.5.1 Preparation of calibration curve

Analytical calibration curve of insulin was made as mentioned in the method part. The graph of peak area vs. insulin concentration is plotted in figure 2.11.

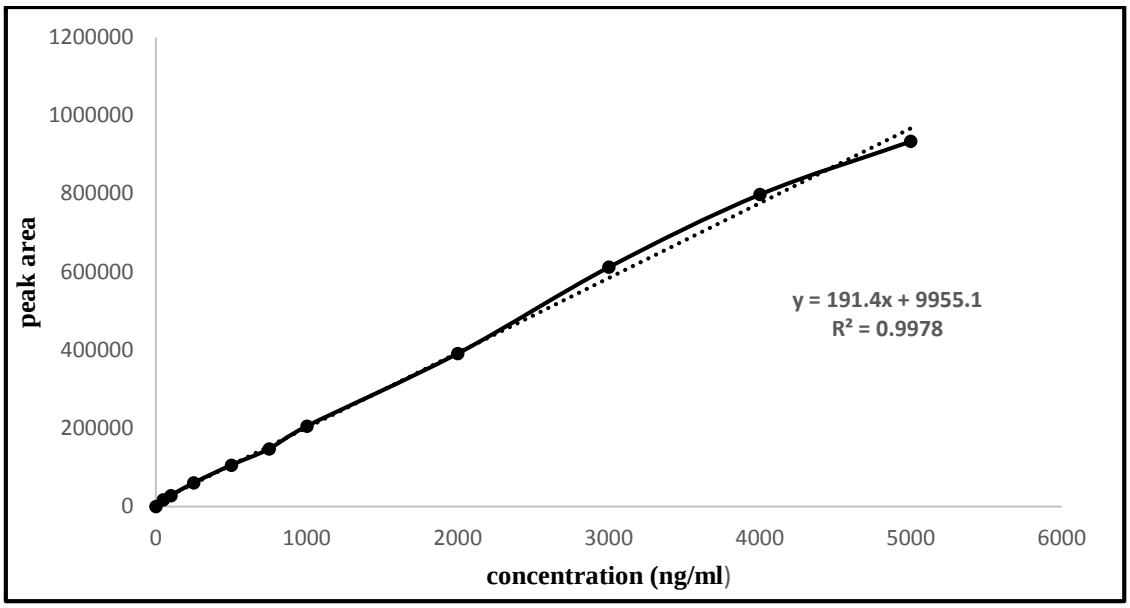

Figure 2.11 Analytical calibration curve of insulin

2.3.5.2 Linearity and range

Regression analysis was executed for estimating linearity of calibration curve described by equation: **y=191.4x+9955.1.** The correlation coefficient **(R^2)** was found to be **0.9978** which demonstrated high degree of correlation. The linearity was found in the range of **50 - 5000 ng/ml**.

2.3.5.3 Specificity

A separate, well-shaped peak with high resolution was obtained for insulin at 5.2 minutes retention time without any interference by blank solutions or solvents. Figure 2.12 represents a chromatogram of insulin illustrating high specificity of the analytical method.

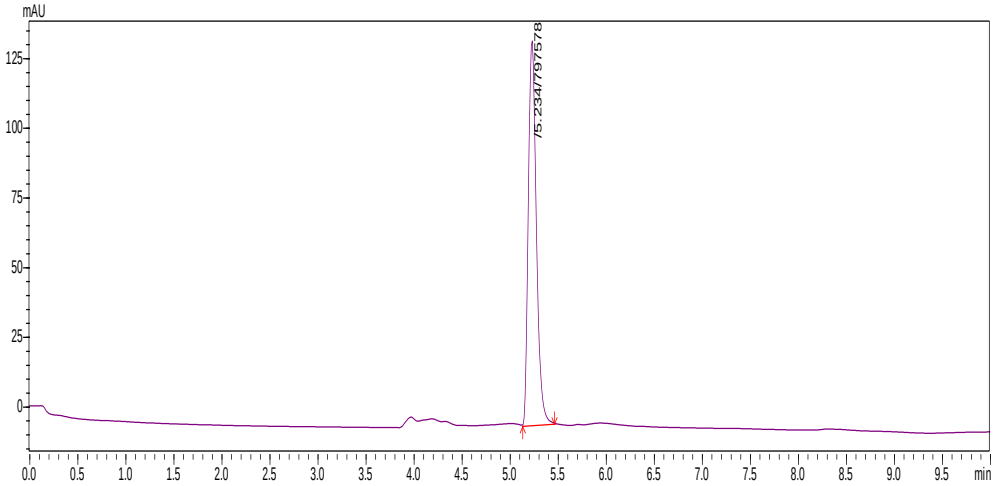

Fig. 2.12 HPLC chromatogram of insulin

2.3.6 Stability studies

Stability investigations were made to assure chemical stability of insulin in stock solutions and analytical samples during the storage and execution of study. From Table 2.6 it is can be concluded that all the stock solutions were stable for 60 days. Observations obtained are presented in the table 2.6. Variations were in the limit of acceptance.

Table 2.6 Stability of insulin stock solutions

Storage condition	Concentration (ng/ml)	Variation (% deviation)
Autosampler stability (4 °C, 10 hours)	100	2.7
	1000	1.8
Bench top stability (25 ± 2 °C, 6 hours)	100	2.5
	1000	1.2
Freeze thaw stability (-80 °C, 3 cycles)	100	0.8
	1000	1.3
Long term stability (-80 °C, 30 days)	100	4.6
	1000	3.2

2.3.7 Drug-excipient interaction by FTIR

The characteristic peaks of the functional groups present in the chemical compound are enlisted in the tabular form showing experimental peak value and peak reported in the standard literature along with inference to the corresponding molecular vibration of the specific functional group. From figure 2.13 to figure 2.21 are respectively showing the FTIR spectra of insulin, PLA-NH2, PLGA, pluronic F127, cellulose acetate phthalate (CAP), TPGS, linseed oil and physical mixture 1 and physical mixture 2. Similarly the table 2.7 to 2.15 are indicating the characteristic peak details as mentioned formerly. Herein, physical mixture 1 consisted of equal amount of components used to formulate CAP coated size sifting PLA-NH2 nanoparticles of insulin. Similarly, physical mixture 2 consisted equal amount of linseed oil, TPGS, pluronic F127 and insulin. After keen observation it was noted that there was no disappearance as well as emergence of most of the characteristic peaks indicating absence of drug-excipient interactions.

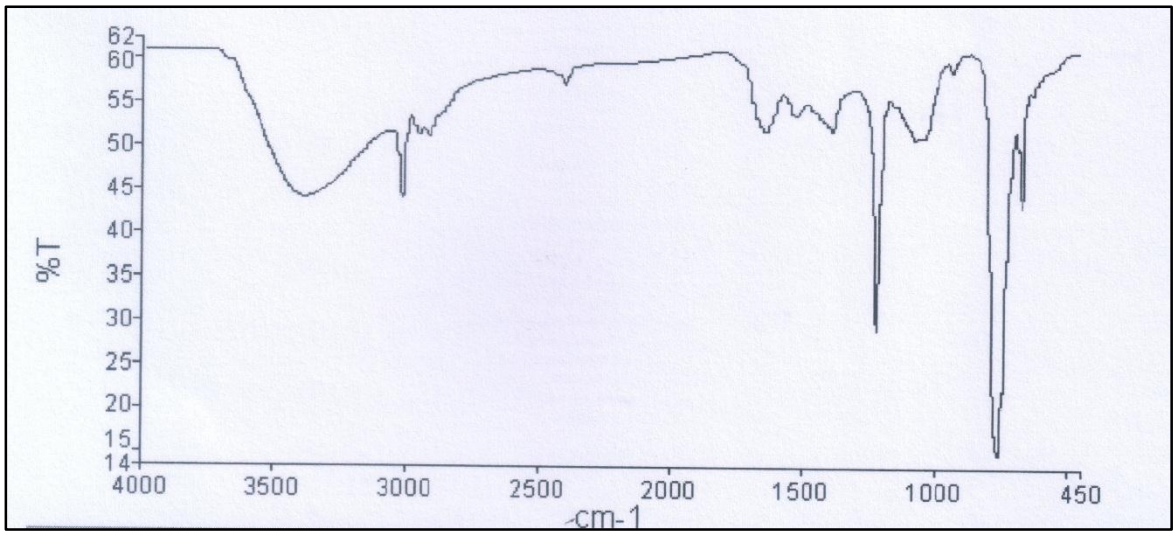

Figure 2.13 FTIR spectrum of insulin

Table 2.7 Experimental and reported characteristic peaks of insulin [67-69]

S.No.	Peak (cm^{-1})		Inference/ Responsible functional group
	Experimental	Literature	
1	1525 1640	1502 1645	C=O stretching
2	3394	3400	H-N-H
3	1073	1098	C-N
4	1215	1267	C-O
5	3020	3300	N-H

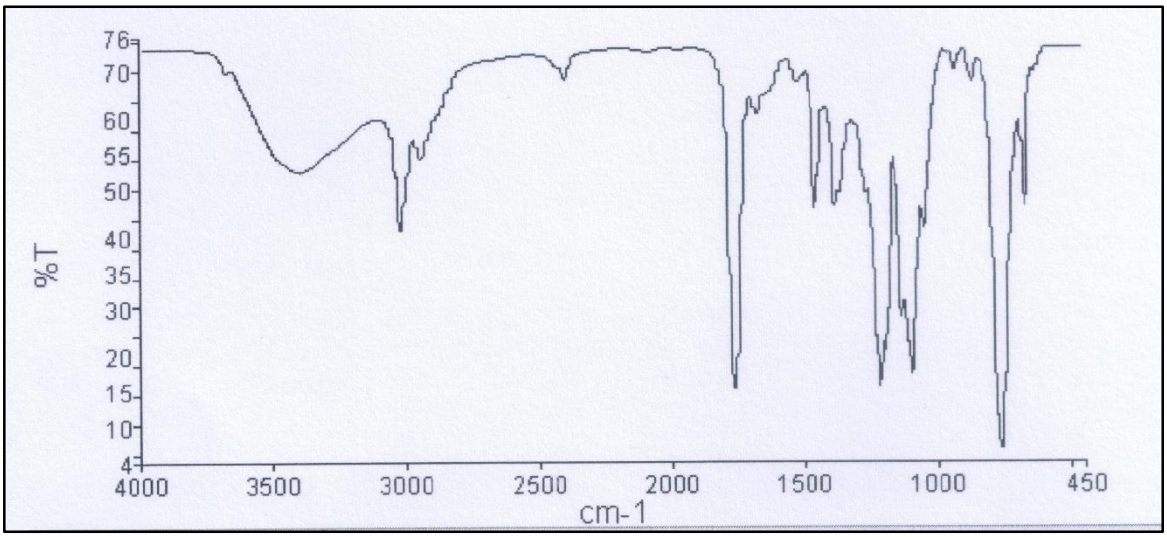

Figure 2.14 FTIR spectrum of amine terminated poly lactic acid (PLA-NH_2)

Table 2.8 Experimental and reported characteristic peaks of PLA-NH_2 [70, 71]

S.No.	Peak (cm^{-1})		Inference/ Responsible functional group
	Experimental	Literature	
1	1678	1680	C=O stretching
2	3404	3600	O-H Stretching
3	1189	1180	C=O, C-O-C stretching

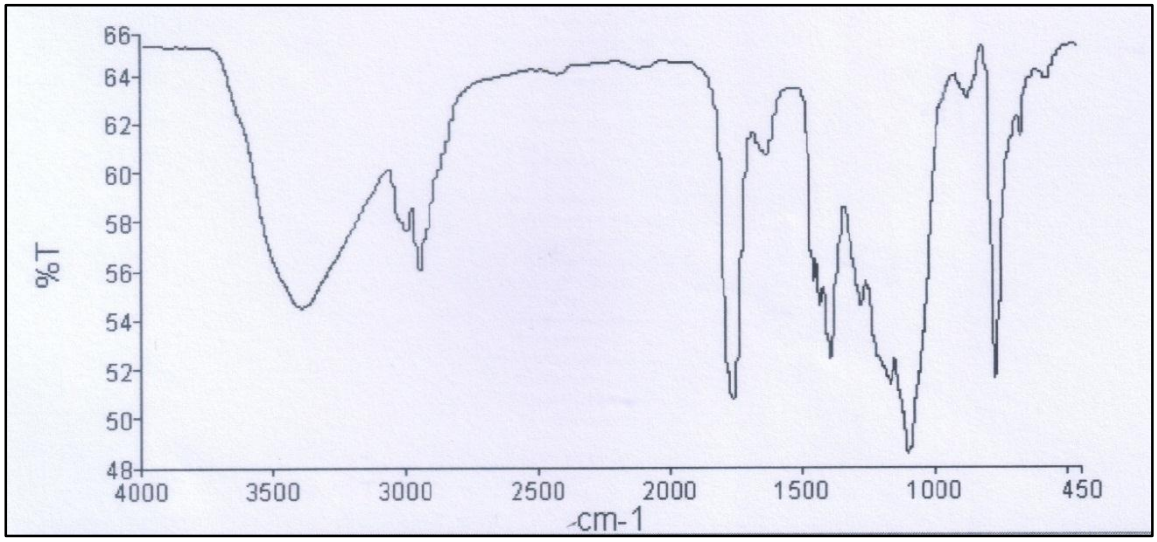

Figure 2.15 FTIR spectrum of PLGA

Table 2.9 Experimental and reported characteristic peaks of PLGA [72]

S.No.	Peak (cm^{-1})		Inference/ Responsible functional group
	Experimental	Literature	
1	3399	3450-3500	O-H bending
2	2954	2885-3010	C-H stretch
3	1757	1762	C=O stretch
4	1089	1186-1089	C-O stretch
5	1389	1450	C-H bending

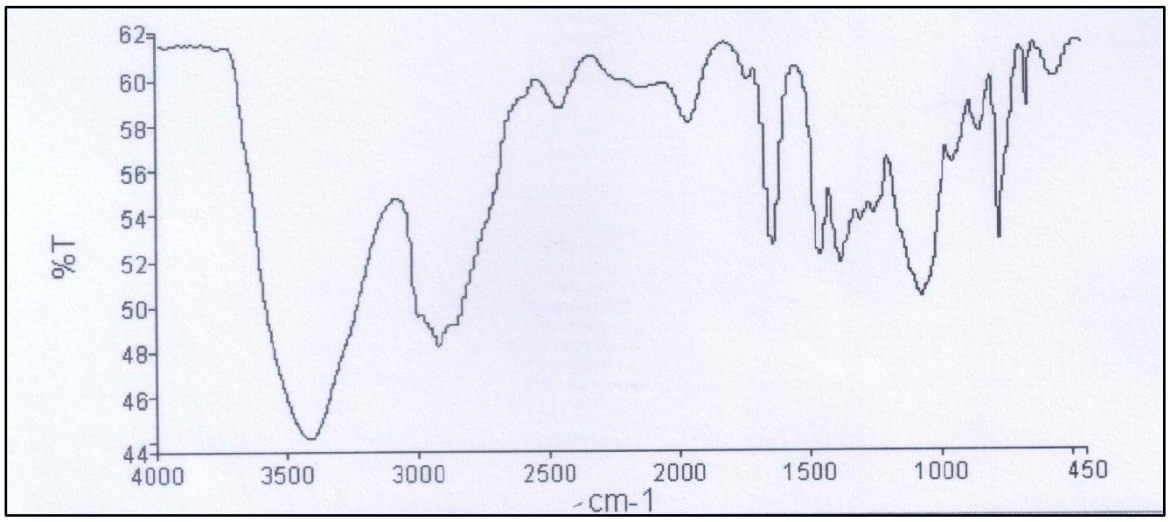

Figure 2.16 FTIR spectrum of Pluronic F127

Table 2.10 Experimental and reported characteristic peaks of Pluronic F127 [73]

S.No.	Peak (cm^{-1})		Inference/ Responsible functional group
	Experimental	Literature	
1	3413	3445	O-H Stretching
2	2926	2891	C-H bending
3	1641	1644	C=O

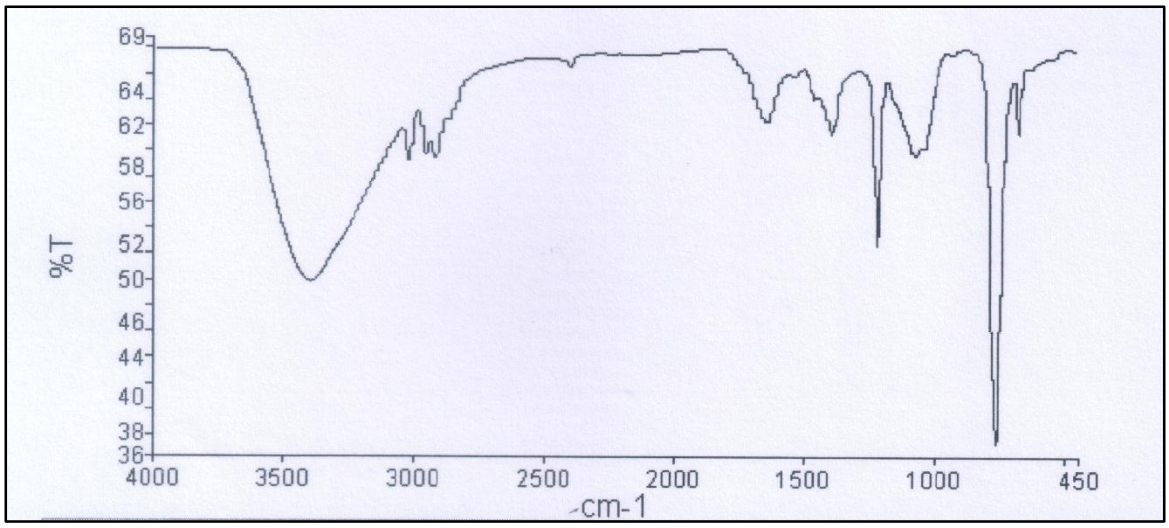

Figure 2.17 FTIR spectrum of cellulose acetate phthalate (CAP)

Table 2.11 Experimental and reported characteristic peaks of CAP [74]

S.No.	Peak (cm^{-1})		Inference /Responsible functional group
	Experimental	Literature	
1	2921	2924	C≡N stretch
2	1642	1747	C=O stretching
3	1384.16	1454	CH_2 group
4	1215	1119	C-O

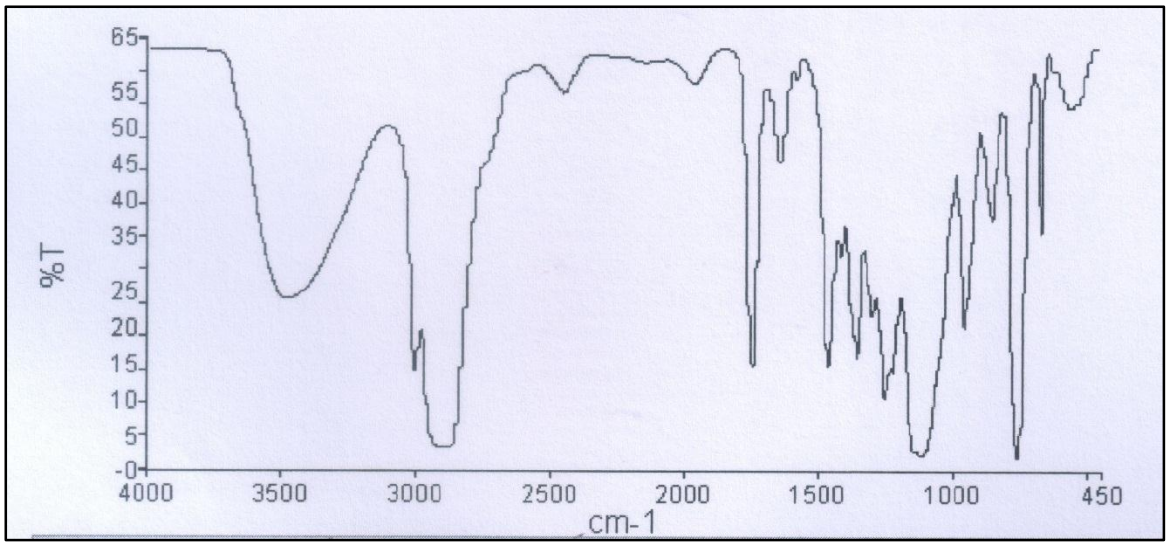

Figure 2.18 FTIR spectrum of TPGS

Table 2.12 Experimental and reported characteristic peaks of TPGS [75-77]

S.No.	Peak(cm^{-1})		Inference/ Responsible functional group
	Experimental	Literature	
1	1218	1293	C-O
2	3484	3426	OH
3	1639	1654	C=O
4	1742	1742	-CH

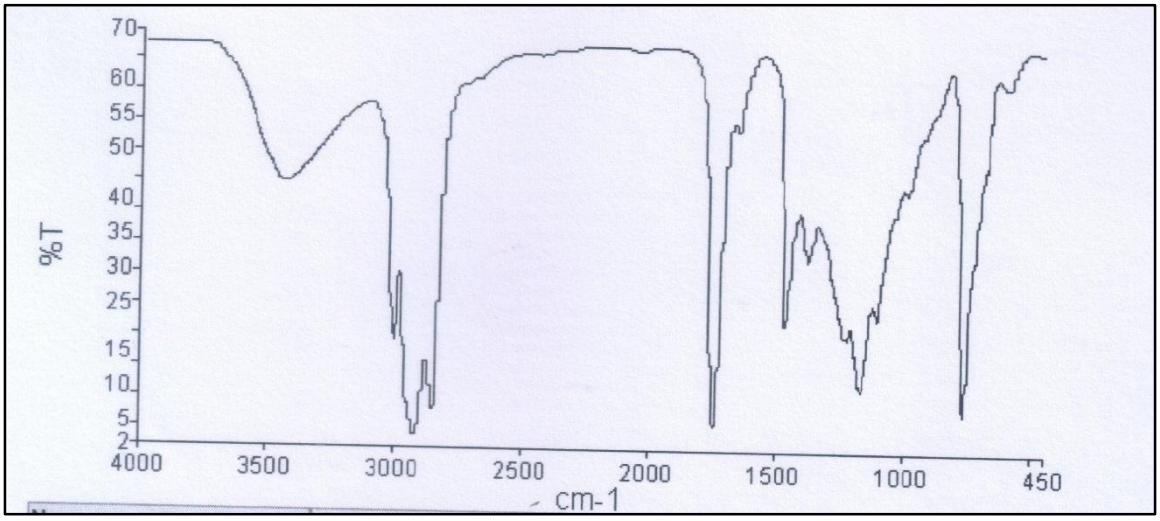

Figure 2.19 FTIR spectrum of linseed oil

Table 2.13 Experimental and reported characteristic peaks of linseed oil [78]

S.No.	Peak (cm^{-1})		Inference/ Responsible functional group
	Experimental	Literature	
1	3011	3011	(C-H)=CH stretching
2	2926	2926	(C-H)CH_2 asymmetric stretching
3	2856	2855	(C-H)CH_2 symmetric stretching
4	1742	1747	(C=O) stretching
5	1654	1658	(C=C) stretching
6	1460	1464	CH_2 bending
7	1164	1164	(CH_2) wagging
8	1100	1100	(O-CH_2-C) asymmetric stretching

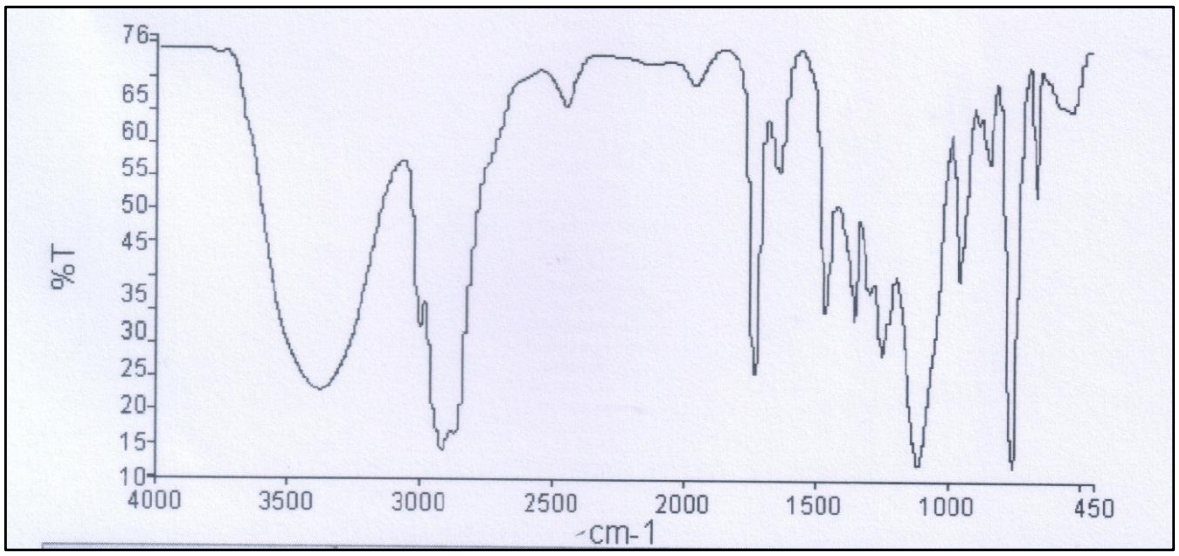

Figure 2.20 FTIR spectrum of physical mixture 1 (insulin, PLA-NH2, Pluronic F127 and CAP)

Table 2.14 Experimental and reported characteristic peaks of components of physical mixture 1

S.No.	Experimental Peak (cm^{-1})	Experimental Corresponding peak of respective component	Inference/ characteristic peak of compound
1	3388	3404	Characteristic O-H bends of PLA
2	1641	1641	Characteristic C=O stretch of PF127
3	2924	2921	Characteristic C≡N stretch of CAP
4	1108	1105	Characteristic C-N stretch of insulin
5	3007	3007	Characteristic N-H stretch of insulin

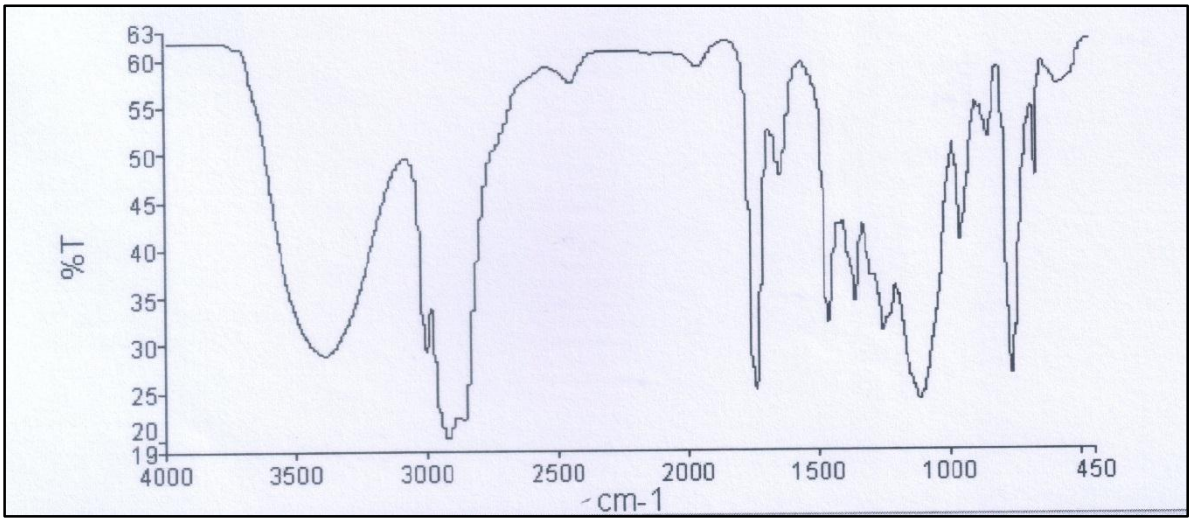

Figure 2.21 FTIR spectrum of physical mixture 2 (insulin, linseed oil, TPGS, Pluronic F127)

Table 2.15 Experimental and reported characteristic peaks of components of physical mixture 2

S.No.	Experimental Peak (cm^{-1})	Experimental Corresponding peak of respective component	Inference/ characteristic peak of each component of mixture
1	3395	3395	Characteristic H-N-H vibration of insulin
2	3009	3007	Characteristic N-H stretch of insulin
3	2926	2926	(C-H)CH_2 asymmetric stretching of Linseed oil
4	1740	1742	(C=O) stretching of Linseed oil
5	1640	1639 1641	C=O of TPGS; Characteristic C=O stretch of PF127
6	1460	1460	CH_2 bending of Linseed oil
7	1105	1105	Characteristic C-N stretch of insulin
8	1731	1742	-CH group of TPGS

2.4 REFERENCES

1. Weiss, M., D.F. Steiner, and L.H. Philipson, *Insulin biosynthesis, secretion, structure, and structure-activity relationships*, in *Endotext [Internet]*. 2014, MDText. com, Inc.
2. Weiss M, S.D., Philipson LH., *Insulin Biosynthesis, Secretion, Structure, and Structure-Activity Relationships.*, A.B. Feingold KR, Boyce A, et al., Editor. 2000, MDText.com: South Dartmouth (MA).
3. Ahmed, R., *Aspart Insulin: A Mealtime Insulin*. 2017, Molecular Anatomy Project Rutgers school.
4. Lima, L.M.T.R., Favero-Retto, M.P., Palmieri, L.C., *Crystal structure of aspart insulin at pH 6.5*. 2017.
5. Kahn, C.R. and A.S. Rosentha, *Immunologic Reactions to Insulin: Insulin Allergy, Insulin Resistance, and the Autoimmune Insulin Syndrome.* Diabetes Care, 1979. **2**(3): p. 283.
6. Schernthaner, G., *Immunogenicity and allergenic potential of animal and human insulins.* Diabetes Care, 1993. **16 Suppl 3**: p. 155-65.
7. Bzowyckyj, A.S. and A.M. Stahnke, *Hypersensitivity reactions to human insulin analogs in insulin-naïve patients: a systematic review.* Therapeutic advances in endocrinology and metabolism, 2018. **9**(2): p. 53-65.
8. Heinzerling, L., et al., *Insulin allergy: clinical manifestations and management strategies.* Allergy, 2008. **63**(2): p. 148-55.
9. Gentile, S., et al., *Lipodystrophy in Insulin-Treated Subjects and Other Injection-Site Skin Reactions: Are We Sure Everything is Clear?* Diabetes therapy : research, treatment and education of diabetes and related disorders, 2016. **7**(3): p. 401-409.
10. Mokta, J.K., K.K. Mokta, and P. Panda, *Insulin lipodystrophy and lipohypertrophy.* Indian journal of endocrinology and metabolism, 2013. **17**(4): p. 773-774.
11. Blanco, M., et al., *Prevalence and risk factors of lipohypertrophy in insulin-injecting patients with diabetes.* Diabetes & Metabolism, 2013. **39**(5): p. 445-453.
12. de Villiers, F.P.R., *Lipohypertrophy—a complication of insulin injections.* Journal of Endocrinology, Metabolism and Diabetes of South Africa, 2006. **11**(2): p. 64-66.
13. Hambridge, K., *The management of lipohypertrophy in diabetes care.* British Journal of Nursing, 2007. **16**(9): p. 520-524.
14. Kurtzhals, P., et al., *Correlations of receptor binding and metabolic and mitogenic potencies of insulin analogs designed for clinical use.* Diabetes, 2000. **49**(6): p. 999-1005.
15. Donner, T., *Insulin–pharmacology, therapeutic regimens and principles of intensive insulin therapy*, in *Endotext [Internet]*. 2015, MDText. com, Inc.
16. Yamada, S., *Insulin glulisine in the management of diabetes.* Diabetes, metabolic syndrome and obesity : targets and therapy, 2009. **2**: p. 111-115.
17. Neumiller, J.J. and S.M. Setter, *Pharmacologic management of the older patient with type 2 diabetes mellitus.* The American journal of geriatric pharmacotherapy, 2009. **7**(6): p. 324-342.
18. Rendell, M., *Technosphere inhaled insulin (Afrezza).* Drugs Today (Barc), 2014. **50**(12): p. 813-27.
19. Walsh, G., *Biopharmaceutical benchmarks 2018.* Nat. Biotechnol, 2018. **36**: p. 1136-1145.
20. Benson, E.A., et al., *Flocculation and loss of potency of human NPH insulin.* Diabetes Care, 1988. **11**(7): p. 563-566.
21. Nordisk, N., *Levemir [Package insert].* Plainsboro, NJ: Author, 2015.
22. Home, P.D. and S.G. Ashwell, *An overview of insulin glargine.* Diabetes Metab Res Rev, 2002. **18 Suppl 3**: p. S57-63.
23. Kalra, S. and Y. Gupta, *Clinical use of Insulin Degludec: Practical Experience and Pragmatic Suggestions.* North American journal of medical sciences, 2015. **7**(3): p. 81-85.

24. Olin, J.L. and K.B. Harris, *Expanded basal insulin options for type 2 diabetes mellitus.* The Journal for Nurse Practitioners, 2017. **13**(3): p. 210-215.
25. Clements, J.N., et al., *Clinical pharmacokinetics and pharmacodynamics of insulin glargine 300 U/mL.* Clinical pharmacokinetics, 2017. **56**(5): p. 449-458.
26. Expert, A.A., *Insulin–Pharmacology, Therapeutic Regimens And Principles Of Intensive Insulin Therapy.*
27. Beals, J.M., et al., *Insulin*, in *Pharmaceutical biotechnology*. 2019, Springer. p. 403-427.
28. Briggs, K.T., et al., *Nondestructive Quantitative Inspection of Drug Products Using Benchtop NMR Relaxometry—the Case of NovoMix® 30.* AAPS PharmSciTech, 2019. **20**(5): p. 189.
29. Segal, A.R. and N. El Sayed, *Are you ready for more insulin concentrations?* Journal of diabetes science and technology, 2015. **9**(2): p. 331-338.
30. Kahn, C.R., *The Molecular Mechanism of Insulin Action.* Annual Review of Medicine, 1985. **36**(1): p. 429-451.
31. Evans, M., et al., *A review of modern insulin analogue pharmacokinetic and pharmacodynamic profiles in type 2 diabetes: improvements and limitations.* Diabetes, obesity & metabolism, 2011. **13**(8): p. 677-684.
32. Cheng, A.Y.Y., et al., *Differentiating Basal Insulin Preparations: Understanding How They Work Explains Why They Are Different.* Advances in Therapy, 2019. **36**(5): p. 1018-1030.
33. Charman, S.A., et al., *Lymphatic absorption is a significant contributor to the subcutaneous bioavailability of insulin in a sheep model.* Pharm Res, 2001. **18**(11): p. 1620-6.
34. Kagan, L., et al., *The role of the lymphatic system in subcutaneous absorption of macromolecules in the rat model.* European Journal of Pharmaceutics and Biopharmaceutics, 2007. **67**(3): p. 759-765.
35. Rasmussen, C.H., et al., *Insulin aspart pharmacokinetics: an assessment of its variability and underlying mechanisms.* Eur J Pharm Sci, 2014. **62**: p. 65-75.
36. Soeborg, T., et al., *Absorption kinetics of insulin after subcutaneous administration.* Eur J Pharm Sci, 2009. **36**(1): p. 78-90.
37. Gradel, A.K.J., T. Porsgaard, and J. Lykkesfeldt, *Factors Affecting the Absorption of Subcutaneously Administered Insulin: Effect on Variability.* 2018. **2018**: p. 1205121.
38. Holleman, F. and J.B.L. Hoekstra, *Insulin Lispro.* New England Journal of Medicine, 1997. **337**(3): p. 176-183.
39. Duckworth, W.C., R.G. Bennett, and F.G. Hamel, *Insulin Degradation: Progress and Potential*.* Endocrine Reviews, 1998. **19**(5): p. 608-624.
40. Rubenstein, A.H. and I. Spitz, *Role of the Kidney in Insulin Metabolism and Excretion.* Diabetes, 1968. **17**(3): p. 161.
41. Alsahli, M. and J.E. Gerich, *Hypoglycemia in Patients with Diabetes and Renal Disease.* Journal of clinical medicine, 2015. **4**(5): p. 948-964.
42. Makadia, H.K. and S.J. Siegel, *Poly lactic-co-glycolic acid (PLGA) as biodegradable controlled drug delivery carrier.* Polymers, 2011. **3**(3): p. 1377-1397.
43. Lü, J.-M., et al., *Current advances in research and clinical applications of PLGA-based nanotechnology.* Expert Review of Molecular Diagnostics, 2009. **9**(4): p. 325-341.
44. Avgoustakis, K., *Polylactic-co-glycolic acid (PLGA).* Encyclopedia of biomaterials and biomedical engineering, 2005(Scheme 2): p. 1-11.
45. Anderson, J.M. and M.S. Shive, *Biodegradation and biocompatibility of PLA and PLGA microspheres.* Advanced Drug Delivery Reviews, 1997. **28**(1): p. 5-24.
46. Shibata, A., S. Yada, and M. Terakawa, *Biodegradability of poly(lactic-co-glycolic acid) after femtosecond laser irradiation.* Scientific Reports, 2016. **6**: p. 27884.
47. Mir, M., N. Ahmed, and A.u. Rehman, *Recent applications of PLGA based nanostructures in drug delivery.* Colloids and Surfaces B: Biointerfaces, 2017. **159**: p. 217-231.

48. Cui, F.-d., et al., *Preparation of insulin loaded PLGA-Hp55 nanoparticles for oral delivery.* Journal of Pharmaceutical Sciences, 2007. **96**(2): p. 421-427.
49. Zhang, X., et al., *Preparation and characterization of insulin-loaded bioadhesive PLGA nanoparticles for oral administration.* European Journal of Pharmaceutical Sciences, 2012. **45**(5): p. 632-638.
50. Schwendeman, S.P., *Recent Advances in the Stabilization of Proteins Encapsulated in Injectable PLGA Delivery Systems.* 2002. **19**(1): p. 26.
51. Liu, H. and T.J. Webster, *Bioinspired Nanocomposites for Orthopedic Applications*, in *Nanotechnology for the Regeneration of Hard and Soft Tissues*. p. 1-51.
52. Jamshidian, M., et al., *Poly-Lactic Acid: Production, Applications, Nanocomposites, and Release Studies.* Comprehensive Reviews in Food Science and Food Safety, 2010. **9**(5): p. 552-571.
53. Xiong, X.Y., et al., *Pluronic P85/poly(lactic acid) vesicles as novel carrier for oral insulin delivery.* Colloids Surf B Biointerfaces, 2013. **111**: p. 282-8.
54. Luo, Y.Y., et al., *A review of biodegradable polymeric systems for oral insulin delivery.* Drug Delivery, 2016. **23**(6): p. 1882-1891.
55. Martin, O. and L. Avérous, *Poly(lactic acid): plasticization and properties of biodegradable multiphase systems.* Polymer, 2001. **42**(14): p. 6209-6219.
56. Xiong, X.Y., K.C. Tam, and L.H. Gan, *Release kinetics of hydrophobic and hydrophilic model drugs from pluronic F127/poly(lactic acid) nanoparticles.* Journal of Controlled Release, 2005. **103**(1): p. 73-82.
57. Bohorquez, M., et al., *A Study of the Temperature-Dependent Micellization of Pluronic F127.* Journal of Colloid and Interface Science, 1999. **216**(1): p. 34-40.
58. *Reagents and Chemcals portfolio* Available from: https://www.gbiosciences.com/Buffers-Reagents-Chemicals/Pluronic_F-127.
59. Yan, A., et al., *Tocopheryl Polyethylene Glycol Succinate as a Safe, Antioxidant Surfactant for Processing Carbon Nanotubes and Fullerenes.* Carbon, 2007. **45**(13): p. 2463-2470.
60. Yang, C., et al., *Recent Advances in the Application of Vitamin E TPGS for Drug Delivery.* Theranostics, 2018. **8**(2): p. 464-485.
61. Tan, S., et al., *Recent developments in d-α-tocopheryl polyethylene glycol-succinate-based nanomedicine for cancer therapy.* Drug Delivery, 2017. **24**(1): p. 1831-1842.
62. Baka, E., J.E.A. Comer, and K. Takács-Novák, *Study of equilibrium solubility measurement by saturation shake-flask method using hydrochlorothiazide as model compound.* Journal of Pharmaceutical and Biomedical Analysis, 2008. **46**(2): p. 335-341.
63. Ravi, S., et al., *Development and Validation of an HPLC–UV Method for the Determination of Insulin in Rat Plasma: Application to Pharmacokinetic Study.* Chromatographia, 2007. **66**(9): p. 805-809.
64. Yilmaz, B., Y. Kadioglu, and I. Capoglu, *Determination of Insulin in Humans with Insulin-Dependent Diabetes Mellitus Patients by HPLC with Diode Array Detection.* Journal of Chromatographic Science, 2012. **50**(7): p. 586-590.
65. Roy, M., et al., *1H NMR spectrum of the native human insulin monomer. Evidence for conformational differences between the monomer and aggregated forms.* J Biol Chem, 1990. **265**(10): p. 5448-52.
66. Weiss, M.A., et al., *Heteronuclear 2D NMR studies of an engineered insulin monomer: assignment and characterization of the receptor-binding surface by selective 2H and 13C labeling with application to protein design.* Biochemistry, 1991. **30**(30): p. 7373-89.
67. Severcan, F., N. Kaptan, and B. Turan, *Fourier Transform Infrared Spectroscopic Studies of Diabetic Rat Heart Crude Membranes.* Journal of Spectroscopy, 2003. **17**.
68. Xie, L. and C.-L. Tsou, *Comparison of secondary structures of insulin and proinsulin by FTIR.* Journal of protein Chemistry, 1993. **12**(4): p. 483-487.

69. Sarmento, B., et al., *Characterization of insulin-loaded alginate nanoparticles produced by ionotropic pre-gelation through DSC and FTIR studies.* Carbohydrate Polymers, 2006. **66**(1): p. 1-7.
70. Xu, J., et al., *Preparation of chitosan/PLA blend micro/nanofibers by electrospinning.* Materials Letters, 2009. **63**(8): p. 658-660.
71. Yang, S.-l., et al., *Thermal and mechanical properties of chemical crosslinked polylactide (PLA).* Polymer Testing, 2008. **27**(8): p. 957-963.
72. Singh, G., et al., *Recent biomedical applications and patents on biodegradable polymer-PLGA.* International Journal of Pharmacology and Pharmaceutical Sciences, 2014. **1**: p. 30-42.
73. Chatterjee, S., et al., *Dual-responsive (pH/temperature) Pluronic F-127 hydrogel drug delivery system for textile-based transdermal therapy.* Scientific Reports, 2019. **9**(1): p. 11658.
74. Roy, A., P. Bhunia, and S. De, *Solvent effect and macrovoid formation in cellulose acetate phthalate (CAP)–polyacrylonitrile (PAN) blend hollow fiber membranes.* Journal of Applied Polymer Science, 2017. **134**(1).
75. Ha, P.T., et al., *The synthesis of poly (lactide)-vitamin E TPGS (PLA-TPGS) copolymer and its utilization to formulate a curcumin nanocarrier.* Advances in Natural Sciences: Nanoscience and Nanotechnology, 2010. **1**(1): p. 015012.
76. Khare, V., et al., *Synthesis and characterization of TPGS–gemcitabine prodrug micelles for pancreatic cancer therapy.* RSC Advances, 2016. **6**(65): p. 60126-60137.
77. Gaonkar, R.H., et al., *Garcinol loaded vitamin E TPGS emulsified PLGA nanoparticles: preparation, physicochemical characterization, in vitro and in vivo studies.* Scientific Reports, 2017. **7**(1): p. 530.
78. Lazzari, M. and O. Chiantore, *Drying and oxidative degradation of linseed oil.* Polymer Degradation and Stability, 1999. **65**(2): p. 303-313.

CHAPTER 3

Thermo-responsive size shifting polymeric nanoparticles for oral delivery of insulin

3.1 INTRODUCTION

A dawning era of proteomics has provided number of biologics i.e. proteins and peptides with wide range of applications in diagnostics as disease bio-markers, and as therapeutics for various diseases in bio-medical field. Since last two decades, many pharmaceutical companies have jumped in to the business of bio-macro-molecules like proteins and peptides due to their specific biological actions and high potency. Proteins and peptides have been delivered by conventional, invasive parenteral routes such as intravenous, subcutaneous, and intramuscular depot which limit their use in chronic disease conditions like diabetes, cancer, osteoporosis, and hormonal disorders etc., due to inadequate patient compliance. Though oral route is the most preferred and patient friendly, oral delivery of labile proteins and peptides remains challenging due to hostile physiology of gastro-intestinal tract such as harsh acidic pH, proteolytic enzymes and absorption barriers [1]. Therefore, essential endeavours are needed to formulate an alternative pulmonary, nasal or oral drug delivery system that can protect the labile macromolecule from all the physiological barriers and deliver it at desired site in therapeutically viable form.

Adroit nano-sized materials have gained inordinate attention in variety of sciences including biological, medical, pharmaceutical, agricultural, material, and environmental science due to their elite and unique features [2]. Nanoparticulate drug delivery systems have been emerged as promising tool to deliver various small and macro molecular therapeutic agents at targeted site with additional benefits such as controlled release, avoidance of dose related toxicity, and better pharmacokinetic profile that can manage the disease condition efficiently. Many nano systems such as polymeric nanoparticles [3, 4], liposomes [5], nano-emulsions [6], solid lipid nanoparticles [7] etc., have been deeply investigated and found suitable for oral delivery of proteins and peptides, however, none of them have attained commercial success till date. Polymeric nanoparticles (NPs) have particularly been effective platform for protein delivery due to the ease of fine-tuning their overall bio-physicochemical properties in addition to their capability to protect and release proteins in a controlled manner [8]. These nano materials are generally formulated by methods like salting out or nano-precipitation, emulsification-solvent evaporation, emulsification-solvent diffusion, emulsion polymerization, interfacial poly-condensation, solvent displacement and interfacial deposition, phase separation coacervation, double

emulsification – solvent evaporation etc [9, 10]. All of the above mentioned methods of preparation somewhere involve mechanical energy in the form of stirring, homogenization and/or ultra-sonication to make nano sized droplets and organic solvents which after evaporation will form hard nanoparticles. This mechanical energy and organic solvents can adversely affect the structure and biological activity of labile proteins and peptides and make them partially or fully inactive. Thus, one of the great challenges in the formulation development of proteins and peptide is to keep them intact and viable during process of nanoparticle preparation. Hence, a novel solvent free platform has been developed which can load the labile macromolecules (with positive or negative charge) in the nanoparticulate system.

The charged core of polymeric material covered by thermo-sensitive shell has been architected to incorporate hydrophilic proteins. It involves two steps, the first one is preparation of polymeric nanoparticles by nano-precipitation method and the second one is loading of labile protein molecules by solvent free method. In the first step for making nanoparticles, the negatively charged polymer like poly (lactic-co-glycolic acid) (PLGA) with carboxyl group at terminal and positively charged poly lactic acid (PLA-NH_2) with amine group at terminal end have been utilised which can incorporate positively charged proteins (such as interleukin 10, erythropoietin) and negatively charged proteins (such as insulin), respectively, by electrostatic interaction. The employment of hydrophobic polymers like PLGA and PLA have following reasons:

- biodegradable and biocompatible nature
- provides controlled release of hydrophilic protein molecules due to potential electrostatic binding force

To employ a thermo-sensitive shell various pluronics (PF 127, PF 68 and P 123) have been studied. Pluronics are tri-co-block polymer cum surfactants containing hydrophilic poly (ethylene oxide) (PEO) and hydrophobic poly (propylene oxide) (PPO) blocks arranged in PEO-PPO-PEO manner. Additionally they possess thermo responsive swelling behaviour depending on PEO residues in various grades. Depending on content of PEO pluronics possess different thermal properties and hence, PF 127 and PF 68 containing 70% and 80% PEO blocks, respectively, were selected for trial [11]. Additionally, Pluronic P 123 having poly (ethylene glycol)-poly (proplylene glycol)- poly (ethylene glycol) was also taken in consideration due to the presence of hydrophilic blocks. While preparation of NPs by nano-

precipitation method, pluronics are used as surfactant which make shell on the polymeric core made up of PLGA or PLA.

The shell made up of pluronic with distinct property of loosening their assembly of block molecules at lower temperature (4°C) and condensing at high temperature (37°C) provided the basis of solvent free loading of protein molecules. During incubation of NPs in protein solution at 4°C, the loosened state of shell allows the charged protein molecules to bind to the oppositely charged hydrophobic core by electrostatic interaction. Then, at 37°C temperature in body it provides controlled release of protein molecules due to entrapment in tightly shrunk shell. The schematic diagram of thermo-responsive NPs is shown in figure 3.1.

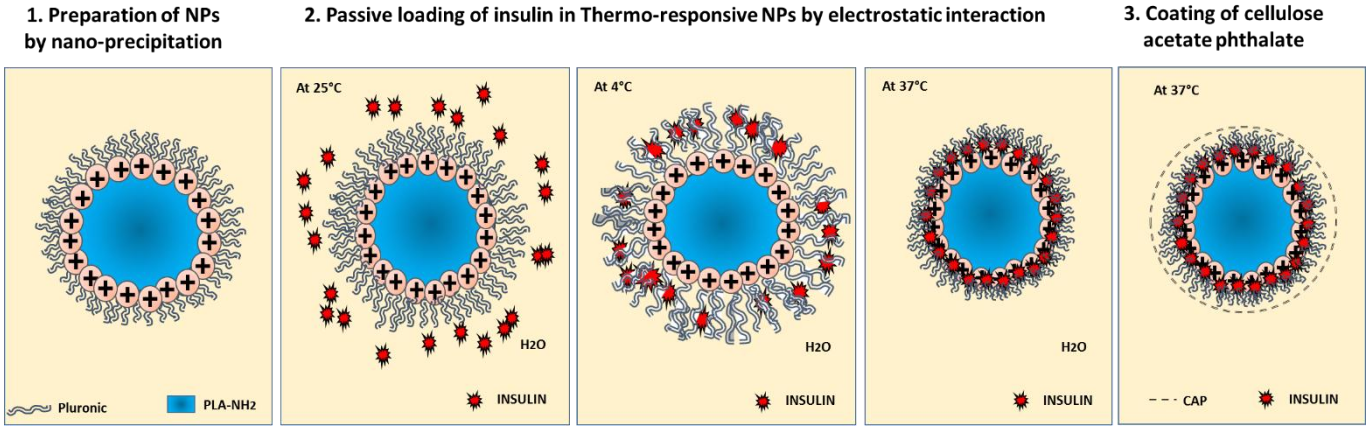

Figure. 3.1 Schematic illustration of positively charged PLA-NH_2 thermo-responsive size sifting NPs bearing negatively charged protein insulin

Despite of being first recombinant protein with early discovery in 1921, insulin delivery yet requires invasive and painful subcutaneous injections offering a great discomfort to patients of diabetes [12]. Insulin suffers from various difficulties such as short biological half-life, degradation by protease in GIT and poor absorption due to higher molecular weight (5808 daltons) and hydrophilic nature. In patients with diabetes mellitus type I, insulin needs to be injected at high frequency to maintain blood glucose in euglycaemic range. To imitate natural levels of insulin, injection of long acting insulin to maintain basal insulin level supplemented with bolus injections of fast acting insulin at meals are being prescribed by the physicians [13]. In well-developed stage of diabetes mellitus type II also, the insulin therapy is needed in addition to oral hypoglycaemic agents to maintain tight glycaemic control [14]. Maintaining tight glycaemic control is the long-term goal of

diabetes treatment and hence, oral nanoparticulate formulation that can provide insulin in its biologically active form in a controlled manner would be highly recommended to meet the unmet medical need. Keeping above mentioned facts in mind insulin was selected as model protein for the thermo-responsive nanoparticles. Insulin possesses slightly negative charge at physiological pH (7.4) and hence NPs with hydrophobic core of positively charged PLA-NH_2 were selected for its delivery. Then, NPs were coated by an enteric coating material cellulose acetate phthalate to protect them from upper part of GIT. Cellulose acetate phthalate is well-established cellulose ester being used as an enteric coating material due to its pH dependent solubility. It is insoluble in buffer systems with pH less than 5.5 but as pH value increases it gets solubilized due to swelling in the intestinal fluid [15, 16].

3.2. EXPERIMENTAL

3.2.1. Materials

Human recombinant insulin (regular), amine group terminated Poly -l-lactide (PLA- NH_2), Poly lactide co-glycolide (PLGA) 50:50, Pluronic F127, Pluronic F68, Pluronic F123, dialysis membrane (MWCO 100KDa), Human recombinant insulin ELISA kit (RAB0327) DNase and RNase free distilled water were purchased from Sigma Aldrich , St. Louis, MO, USA. Dulbecco's modified Eagle's medium (GIBCO, Grand Island, NY) was purchased from Thermo Fischer Scientific.

3.2.2. Preparation of thermo-responsive NPs

Thermo-responsive NPs were prepared by nano-precipitation method as depicted in flow diagram in figure 3.2. NPs without pluronic surfactant were also prepared for comparison purpose.

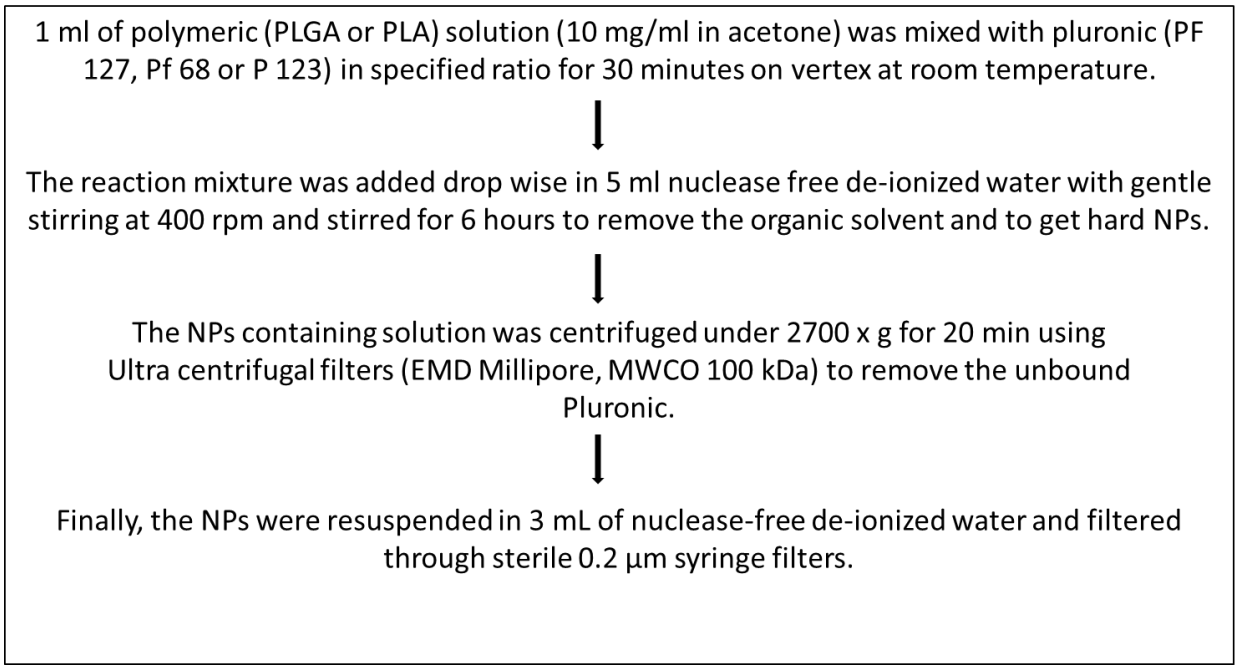

Figure 3.2 Preparation of thermo-responsive NPs by nano-precipitation method.

3.2.3 Solvent free loading of insulin

Positively charged thermo-responsive NPs of PLA-NH_2 were selected for loading of negatively charged protein, insulin, as a model candidate. 5 mg insulin was dissolved in 5 ml de-ionised water and the prepared PLA NPs were incubated in the protein solution for 2 hours at 4°C. After incubation, centrifugation at 2700 x g for 10 min was done, with ultra-centrifugal millipore filter (MWCO 12 KDa) to remove unloaded insulin. The percentage entrapment and loading were calculated by measuring unloaded or free insulin by validated RP-HPLC method.

3.2.4 Cellulose acetate phthalate (CAP) coating on NPs

Prepared insulin loaded thermo-responsive PLA NPs were coated with enteric coating material CAP by simple incubation of NPs in CAP solution for 2 hours. Coating was assured by change in size and zeta potential value.

3.2.5 Optimization of formulation

3.2.5.1 Selection of suitable pluronic

Different pluronics; PF 127, PF 68 and P 123 in different ratios [polymer (PLGA) to pluronic 1:0, 1:2, 1:5, 1:10, 1:12, 1:15, 1:20], were tried to manufacture NPs with thermo-responsive shell which can swell and de-swell in high range (nm) to allow higher loading of protein. The suitable pluronic to be used for architecting thermo-responsive shell was selected on the basis of particle size, PDI and zeta potential.

3.2.5.2 After selection of the suitable pluronic from screening procedure done with PLGA polymer, the most appropriate pluronic polymer was exploited in different ratios to formulate optimized thermo-responsive PLA NPs for delivery of negatively charged model protein insulin. The optimization was done with respect to mean hydrodynamic diameter, PDI, zeta potential and percentage entrapment efficiency.

3.2.6 Physicochemical characterization

Mean particle hydrodynamic diameter (nm), polydispersity index and zeta potential (mV) was assessed by zetasizer (nano ZS, Malvern Instruments, UK). In addition, the thermo-responsive swelling/de-swelling behavior of NPs was analyzed from 4°C to 37°C. All measurements were carried out in triplicate. Shape and surface morphology was characterized by atomic force microscopy to check the swelled spongy structure of shell at 4°C and de-swelled hard shell at 37°C.

3.2.7 RP-HPLC method for insulin

A validated RP-HPLC method was used with subtle fine tuning [17]. Briefly, the chromatographic separation of the analyte was achieved at ambient room temperature using Lichrospher® 100 RP-18e, C18 HPLC column (4.6 X 250 mm, 5 µm). The mobile phase consisted of 0.2 M sodium sulphate anhydrous adjusted to pH 2.3 with ortho phosphoric acid and acetonitrile (70:30, v/v), filtered through a 0.45µm Millipore membrane filter under vacuum and degassed by sonication prior to use. The analysis was run at a flow rate of 1.0 mL/min. The detector was set at a wavelength of 214 nm. The injection volume was 20 µL.

3.2.8 Entrapment efficiency

The protein entrapment efficiency and the loading content were determined by separation of unloaded proteins from NPs using centrifugation through ultra-centrifugal filters (MWCO 100 kDa). Unloaded protein (i.e. insulin) was measured using validated RP-HPLC method.

3.2.8.1 Enhancement of entrapment efficiency

To suffice our drug delivery system with more payload, we tried several approaches and found a best way to enhance the entrapment without affecting structural integrity and conformational stability of the insulin. Insulin is having isoelectric point of 5.8 which means it is neutrally charge and insoluble at pH 5.4. If the pH of the insulin solution is being varied it turns out into a significant change in its net charge. At pH below 5.4 it becomes more positively charged as the pH is decreased and above pH 5.4 it becomes more negatively charged as the pH is increased. As the developed PLA-NH2 TNPs are positively charged, more negatively charged molecules of insulin can bind strongly due to an electrostatic interaction. Based on this rationale, the insulin loading process was performed at different pH conditions i.e. pH 7.4, pH 8.0, pH 9.0 and pH 10.0. Entrapment efficiency was assessed as discussed earlier. However, not being lured by the high entrapment efficiency, any possible detrimental effect of varied pH condition on insulin was also checked by conforming structural integrity as well as secondary structure by CD spectroscopy.

Our aim was to enhance the encapsulation of model protein insulin in our previously developed thermo responsive size shifting NPs. Generally, in passive loading by electrostatic interaction between protein molecules and oppositely charged core of the NPs, the extent of encapsulation is dependent on charge difference between them. The positive core made up of PLA-NH2 have positive charge which imparts zeta potential ranging from +15.7 to +26.1 mV, approximately, to the NPs. Insulin have isoelectric point (net charge is zero) at pH 5.4 so drug loading process at this pH may result in lesser protein loading but as we increase the pH, net negative charge of insulin increases, for example, at pH 7.4, pH 8 and pH 10 insulin have net charge of -3.06, -5.7 and -12 respectively. Now, to take most advantage of this positive charge of NPs, it was hypothesized to change the pH of insulin solution during loading of insulin into NPs and to get enhanced protein loading. At

physiological pH (7.4) insulin have slight negative -3.06 mV charge so that when we performed the encapsulation process (incubation of TNPs in insulin solution in PBS) at pH 7.4, approximately 72% entrapment efficiency was obtained. Hence, to increase the encapsulation we performed the encapsulation process at various pH and observed the effect of pH on encapsulation efficiency.

3.2.8.2 Method of incubation at different pH

The optimized formulation of TNPs made up of PLA-NH_2 was incubated for 2 hours at 4 °C with insulin solutions at different pH. Different pH solutions were made by adjusting the pH of phosphate buffer saline with NaOH and HCl. Insulin solution (1mg/ml) at pH 7.4, 8, 9, and 10 were made and TNPs were incubated in each insulin solution.

3.2.8.3 Protein confirmation and stability study

We tried to increase the encapsulation efficiency of insulin in the developed formulation. This may lead to conformational change in secondary structure of insulin which is not desired. We performed CD spectroscopy in order to check the conformational change in secondary structure of insulin after loading in formulations. The insulin released from TNPs incubated at different pH conditions (pH 7.4, 8, 9 and 10) was analyzed.

3.2.9 *In Vitro* Release Study

CAP coated thermo-responsive PLA NPs bearing insulin were re-dispersed in 1 ml phosphate buffer saline and filled in hermitically sealed sac of previously activated dialysis membrane (MWCO 12 KDa). Dialysis membrane sac was immersed in 50 ml of simulated gastric fluid (pH 1.2) for initial two hours followed by 6 hours in 50 ml of simulated intestinal fluid (pH 6.8) at 100 rpm and 37°C. Then release media was changed to phosphate buffer saline pH 7.4. At different time interval aliquots were withdrawn and the same amount of fresh media was added to maintain the sink condition. Withdrawn samples were analysed by RP-HPLC method after suitable dilutions.

3.2.10 Transmission Electron Microscopy (TEM)

For TEM study, optimized TNPs formulation was dialyzed with dialysis membrane (pore size: 100 KDa) to remove the excessive surfactant and properly diluted, to get fine quality image. Thereafter, the diluted TNPs solution was put onto a 300-mesh copper grid to

develop a thin film. The grid was covered with a small drop of staining solution (2% w/v uranyl acetate) and excess solution was removed. Sample was allowed to dry thoroughly in air and examined under a transmission electron microscope to capture photomicrographs (JEOL, JEM-2100, Japan).

3.2.11 Stability study

To check the stability profile, the selected optimized formulations were stored at room temperature (25±2 °C) as well as cool temperature (4±2 °C) for three months and evaluated for change in size and zeta potential at specific intermittent time points i.e. 0, 30, 60, 90 days. Malvern Zetasizer 2000 nano ZS instrument was employed.

3.2.12 Protein confirmation and stability study

Because proteins and peptides are most vulnerable towards heat, mechanical energy, sonication and organic solvents, it becomes necessarily important to monitor whether the insulin is intact without any conformational change after going through the entrapment process. So to evaluate the secondary structure, folding and binding properties of insulin, circular dichroism technique was employed. The TNPs were centrifuged at 12000 rpm in Nanosap® centrifugal device (MW cut off 10 KDa) to remove the free insulin. Then, TNPs were membrane (MW cut off 10 KDa) dialyzed by dialysis bag method in PBS pH 7.4. The released insulin was quantified by RP HPLC method and proper dilution was made in the range of 5-10 µmol/ml. Samples were analyzed by CD spectrophotometer (Jasco J-1500). Insulin solution (5 µmol/ml) in PBS 7.4 was considered as standard protein solution for comparison.

3.2.13 *In vitro* cell uptake study

Fluorescence assisted cell sorting (FACS) was used to quantitatively measure the cellular uptake of FITC (Fluorescein iso-thiocynate) loaded TNPs in human intestinal cell lines: HCT116 and Caco-2 cells. Cell lines were maintained in Dulbecco's modified eagle's medium (DMEM) pH 7.4 supplemented with 10% FBS and 1% penicillin-streptomycin (antimycotic-antibiotic solution). Cells (1×10^6 cells per well) were seeded in six well plate and allowed to adhere for overnight period. Subsequently, FITC loaded TNPs formulation and control FITC solution was incubated for 6 hours and then washed repeatedly with

phosphate buffer (pH 7.4) to remove any surface adhered formulation. Uptake of TNPs was assessed by measuring cell associated mean fluorescence intensity using flow cytometer BD FACS Caliber and software cell Quest Pro.

3.2.14 Trans Epithelial Electrical Resistance (TEER)

Trans-epithelial electrical resistance of Caco-2 cell monolayer was measured to check whether the developed TNPs (uncoated and coated) have the ability to open the tight cellular junction between epithelial cells of intestinal membrane. To form the monolayer cells were seeded in 6 well Transwell ® filters (3.0 µm pore size, 12 mm diameter, Corning Costar, USA) at a density of 5×10^4 cells/well and media was replaced with fresh media for 21 days. The monolayer formation was considered optimum when the electrical resistance reached 350-400 Ω*cm^2 measured using Millicell RES meter (Millipore, Milano, Italy) [18, 19]. The decrement in resistance value (TEER) was measured every 30 minutes up to 2 hours after the treatment with free insulin, insulin loaded uncoated TNPs and insulin loaded CAP coated TNPs (having equivalent concentration of insulin 100 µg/ml). Thereafter, the treatment solution was removed by washing with PBS pH 7.4 and recovery of TEER was measured hourly up to 6 hours. The relative percentage change in resistance value with reference to zero time point was calculated and plotted against time scale.

3.2.15 *In vitro* bio-activity

MCF-7 cell line was obtained from institutional cell repository and cultured in RPMI 1640 medium supplemented with 10% FBS, 1% L- glutamine per liter, 100 unit/ml penicillin and 100 µg/ml streptomycin at 37°C in humidified atmosphere of 5 % (v/v) CO2 per air mixture. The *in vitro* bio-activity of insulin was determined by the gold standard MTT cell viability assay. It is well reported that MCF-7 cells express IGF-1 (Insulin like growth factor) receptors on its surface [20]. Therefore, in the presence of insulin, MCF-7 cells proliferate rapidly. Briefly, MCF-7 cells (0.5×10^4 cells per well) were seeded in 96-well culture plate and kept overnight in BOD incubator for restoration of metabolic activity. Thereafter, cells were treated with pure insulin, blank TNPs, CAP coated TNPs, insulin bearing TNPs and insulin bearing CAP coated TNPs dispersed in culture medium equivalent to different concentrations (0.5, 1, 2, 3, 4, 5 µg/ml) of pure insulin. After 24 hours, used culture media was aspirated off and fresh media was supplemented. 48 hours

post-treatment again the used media was aspirated off and fresh media containing MTT dye (0.5 mg/ml) was added and incubated for 4 hours in dark. Herein, the yellow tetrazolium MTT i.e. 3-[4,5-dimethylthiazole-2-yl]-2,5-diphenyltetrazolium bromide is converted to MTT-formazan crystals (purple-blue colored), which is catalyzed by mitochondrial succinate dehydrogenase enzyme [21]. Therefore, only viable cells with metabolic activity will form the formazan crystals. The formazan crystals were then dissolved by adding 0.2 ml of DMSO to each well and gentle shaking for 2 minutes was done on 96-well plate shaker. Finally, the absorbance was analyzed at 570 nm using a multi-well scanning spectrophotometer (PowerWave XS, Biotek, VT, USA). Thus, proliferation level of MCF-7 under pure insulin, blank TNPs, CAP coated TNPs, insulin bearing TNPs and insulin bearing CAP coated TNPs was calculated with comparison to control MCF-7 cells growing without any treatment. The experiment was performed in triplicate.

3.2.16 Animal experiments

The Male Sprague Dawley rats, 6 – 8 weeks old and weighing 180 – 200 grams, were acquired and handled as per the protocols approved by Institutional Animal Ethics Committee, National Animal Laboratory Center, CSIR – Central Drug Research Institute, Lucknow, India.

3.2.16.1 Induction of diabetes

Diabetes was induced by well-established streptozotocin induced model, wherein single moderate dose of 75 mg/kg (dissolved in 10 mM citrate buffer pH 4.5) was given, intraperitonealy [22]. One week post STZ treatment, animals with fasting blood glucose >300 mg/dl were considered diabetic.

3.2.16.2 Hypoglycemic activity, Plasma insulin level and Pharmacokinetics

In order to assess the in vivo activity of insulin loaded formulations, this study was carried out in STZ induced diabetic rats. The animals were fasted for 6 hours prior to start of study and stratified in to three groups of five rats in each group, according to the fasting blood glucose level. Administration of the insulin containing CAP coated TNPs, positive control, and diabetic control was done according to the information mentioned below:

Group I: PBS pH 7.4 via oral route (diabetic control)

Group II: Insulin solution in PBS pH 7.4 via sub cutaneous route at the dose of 2 IU/kg (Positive control)

Group III: Insulin bearing TNPs (INS-CAP@TNPs) via oral route at the dose of 10 IU/kg

Blood samples (200 µl) were withdrawn at selected time intervals (0, 0.25, 0.5, 1, 2, 4, 8, 12, 24 hours) via ta il vein puncture. At the same time single drop of blood was put on glucometer strip inserted in the glucometer (AccuCheck) to read the blood glucose level. Blood samples were collected in micro centrifuge tubes (MCT) pre-coated with EDTA solution as anti-coagulant. All the samples were centrifuged at 3000 rpm to separate the plasma. The plasma samples were stored at -20°C until being analyzed by Insulin Elisa kit (Sigma Aldrich) according to the manufacturer's protocols. Pharmacokinetic parameters were analyzed by WinNonlin 6.0 (Pharsight Co., Mountain View, CA, USA) software and oral bio-availability was calculated in comparison to SC insulin. The relative oral bio-availability was calculated from below given formula:

$$\boldsymbol{Relative\ Bioavailability} = \mathbf{100} * \frac{\boldsymbol{AUC\ (Oral) x\ Dose\ (SC)}}{\boldsymbol{AUC\ (SC) x\ Dose\ (Oral)}}$$

3.2.17 Statistical Analysis

All the experiments were performed at least thrice with three independent samples (n=3) unless otherwise stated. *In vitro* data have been represented as Mean ± SD whereas in vivo data were represented as Mean ± SEM (standard error of means). The statistical comparisons between the groups were done by employing one-way analysis of variance (ANOVA) followed by Bonferroni's multicomparison post-hoc analysis test using GraphPad Prism 5 software (Graph Pad Software Inc., CA, USA). Statistically significant difference was considered if p value was less than 0.05 at 95% confidential interval.

3.3 RESULTS AND DISCUSSION

3.3.1 Selection of suitable pluronic and optimization of polymer: pluronic ratio

The desired NPs should have high swelling of thermo-responsive layer at 4°C and de-swelling at 37°C which imparts better loading and controlled release, respectively. NPs prepared by employing pluronic F 127 (in all the ratio tried) showed higher degree of swelling at 4°C and de-swelling at 37°C temperature in comparison to NPs prepared by PF 68 and P 123 as shown in figure 3.3, 3.5 and 3.6. The maximum degree of swelling/de-swelling property with good PDI was obtained with pluronic F 127 at 1:20 polymer to pluronic ratio. This NPs showed mean hydrodynamic diameter of 47.39±4.66 nm at room temperature (25°C) which was increased to 115.53±14.23 nm at 4°C due to swelling in thermo-responsive shell and at 37°C, mean hydrodynamic diameter was reached to 34.33±5.46 nm due to de-swelling. This phenomena of unpacking and packing with significant change in diameter of NPs helps in proper and higher loading of proteins. Furthermore, the change in zeta potential at different temperature also promotes higher encapsulation of proteins. At 4°C PLGA NPs with pluronic F 127 attained more negative surface charge than at room temperature which helps in high electrostatic interaction with positively charged proteins and enhance the loading efficiency as shown in figure 3.4. In case of pluronic F 68 somewhat swelling was seen at ratio of 1:12 and 1:20 but de-swelling phenomena was absent which may lead to moderate failure in achieving better controlled release. Pluronic 123 proved to be as good surfactant which gave NPs with lesser diameter (83.26±5.423 nm) at very low concentration (ratio 1:2), but it could not show significant swelling/de-swelling phenomena. Hence, based on above results pluronic F 127 was considered as best, amongst pluronics tried, to form thermo-responsive shell in NPs.

Here, PLGA was only used for screening of different pluronics for its thermo-responsive property. But it can be efficiently used to load positively charged proteins such as erythropoietin and interleukin -10.

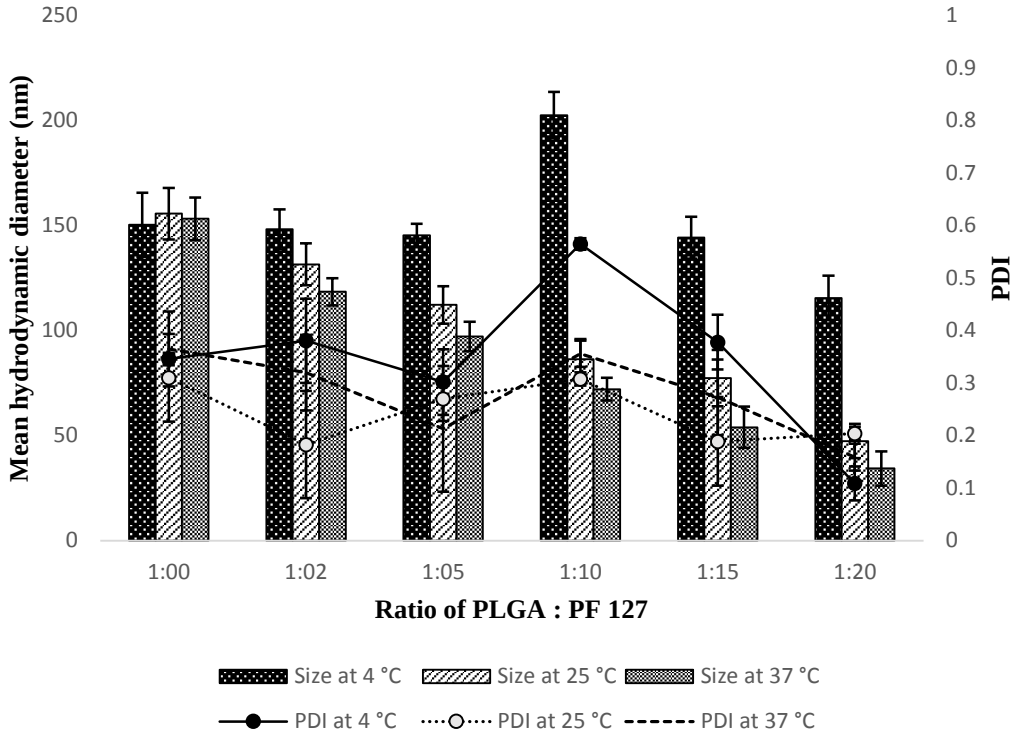

Figure. 3.3 Thermo-responsive behaviour of pluronic F 127: Effect of various temperatures (4°C, 25°C, and 37°C) on mean hydrodynamic diameter (nm) and polydispersity index of thermo-responsive NPs (n=3)

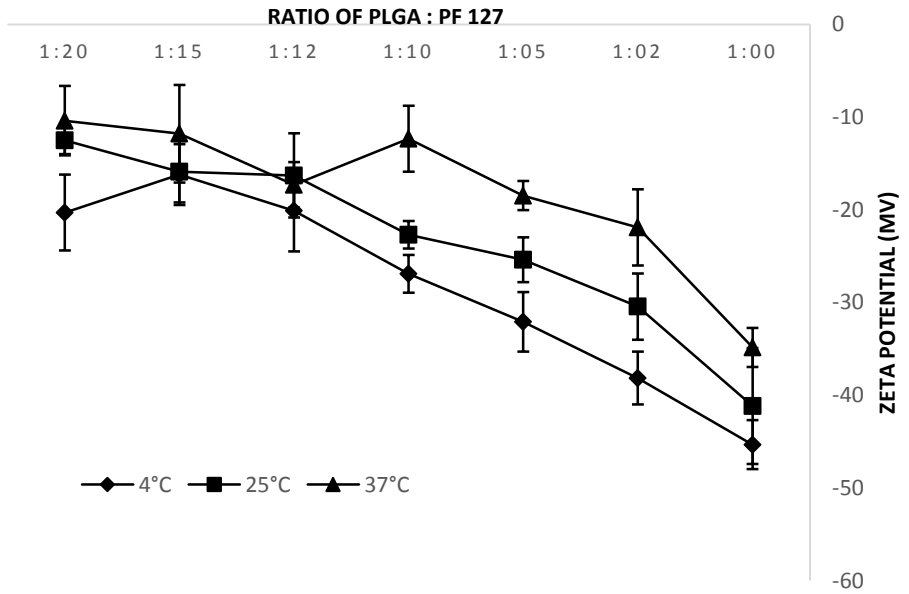

Figure. 3.4 Thermo-responsive behavior of pluronic F 127: Effect of various temperatures(4°C, 25°C, and 37°C) on zeta potential (mV) of thermo-responsive NPs (n=3)

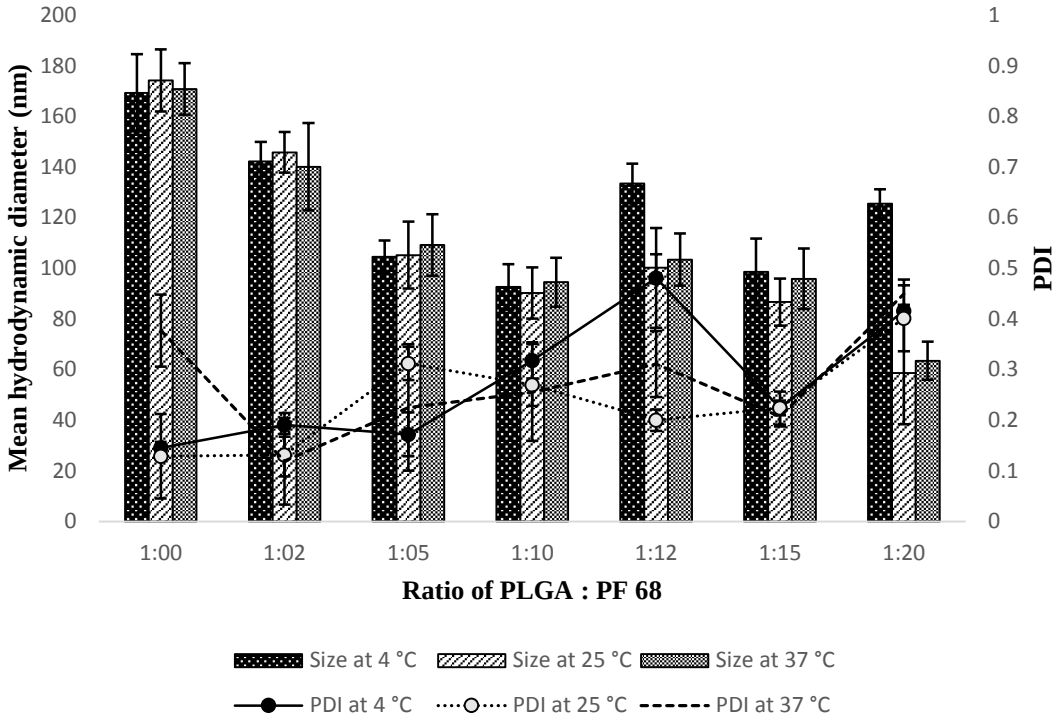

Figure. 3.5 Thermo-responsive behaviour of pluronic F 68: Effect of various temperatures (4°C, 25°C, and 37°C) on mean hydrodynamic diameter (nm) and polydispersity index of thermo-responsive NPs (n=3)

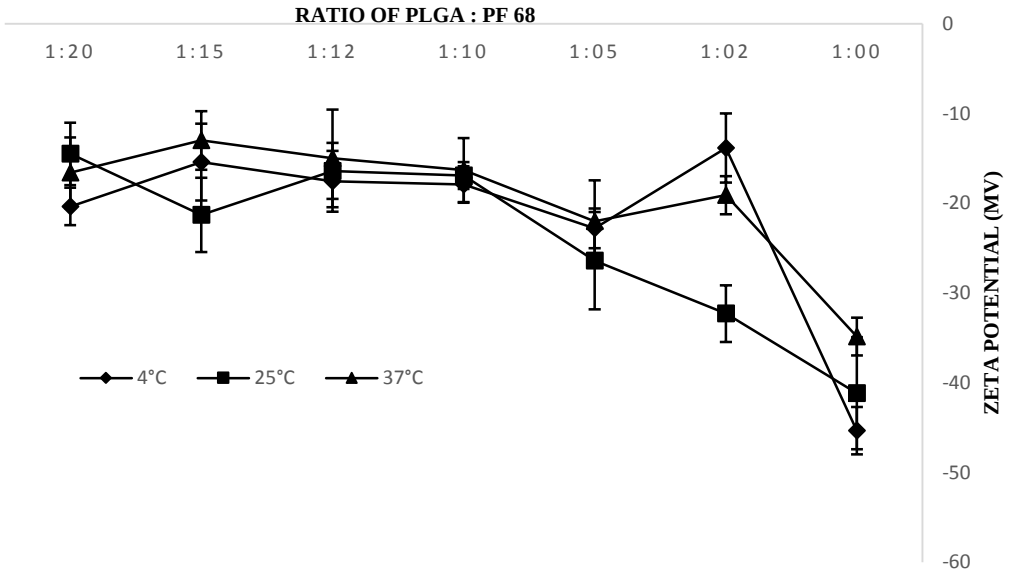

Figure. 3.6 Thermo-responsive behaviour of pluronic F 68: Effect of various temperatures (4°C, 25°C, and 37°C) on zeta potential (mV) of thermo-responsive NPs (n=3)

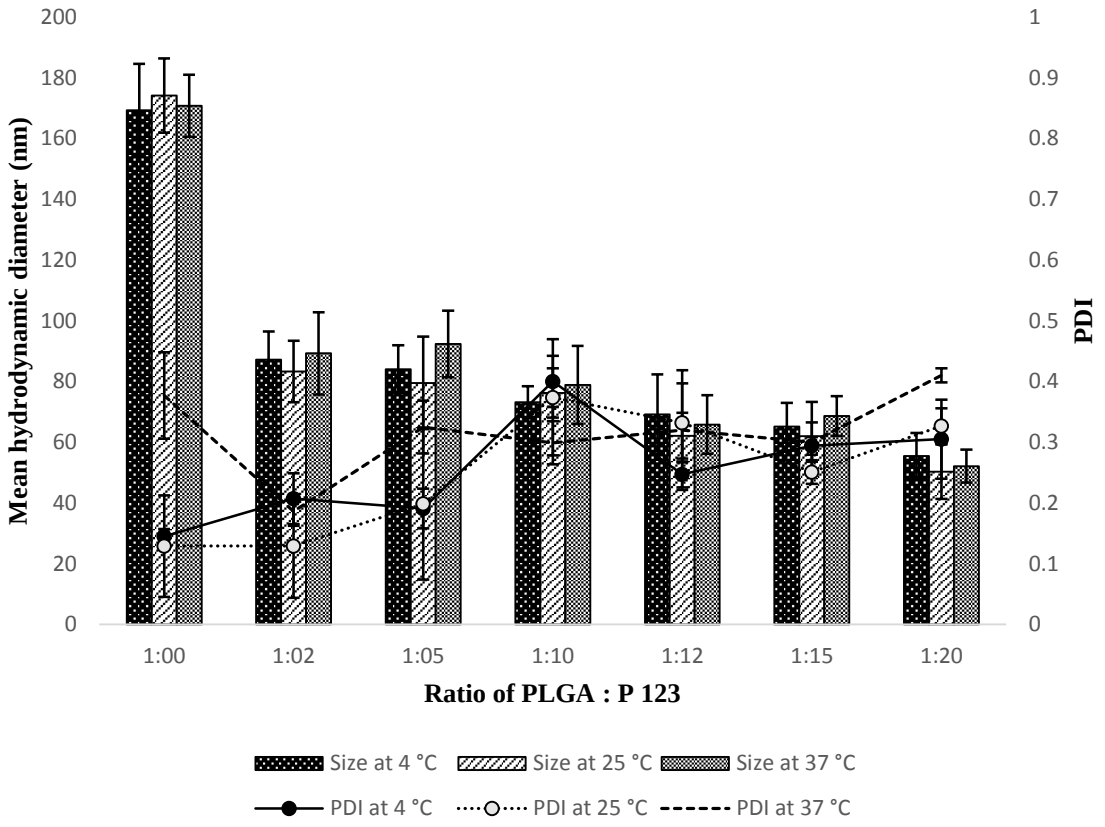

Figure. 3.7 Thermo-responsive behaviour of pluronic P 123: Effect of various temperatures (4°C, 25°C, and 37°C) on mean hydrodynamic diameter (nm) and polydispersity index of thermo-responsive NPs (n=3)

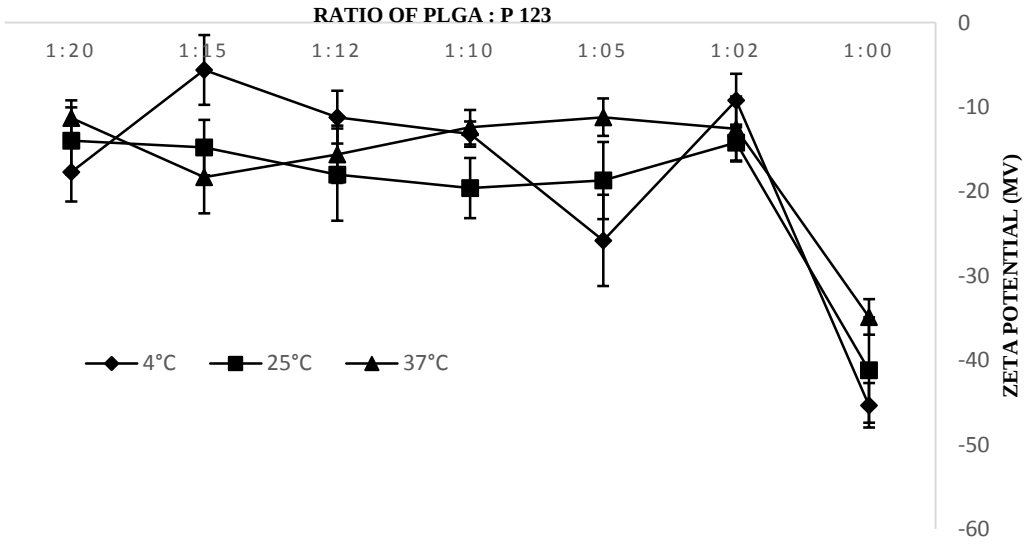

Figure. 3.8 Thermo-responsive behaviour of pluronic P 123: Effect of various temperatures (4°C, 25°C, and 37°C) on zeta potential (mV) of thermo-responsive NPs (n=3)

3.3.2 Optimization of PLA NPs:

After selection of pluronic F 127 from above obtained results, the nanoparticles with positively charged core of PLA-NH_2 were prepared by nanoprecipitation method as discussed above. The thermo-sponge nanoparticles were manufactured using different ratios of PLA: Pluronic F 127, such as 1:0, 1:2, 1:5, 1:10, 1:15 and 1:20. The obtained positively charged thermo-responsive NPs then further incubated with insulin solution at 4°C to load the proteins in solvent free manner. Prepared formulations were optimized based on size, PDI, zeta potential and percentage entrapment efficiency.

3.3.3 CAP coating: effect of on size and zeta potential

In order to confirm coating of CAP on insulin loaded thermo-responsive PLA NPs, the change in size and zeta potential after coating were compared to uncoated formulation. Increment in size and reversal of zeta potential from positive (12.1 mV) to negative (-11.4 mV) was observed, as shown in figure 3.9.

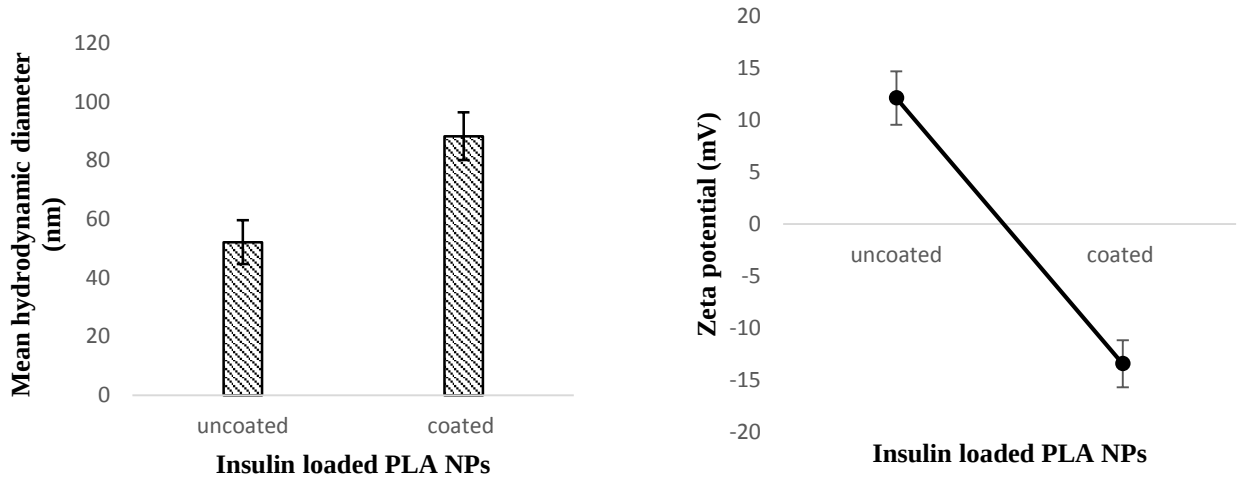

Figure. 3.9 Increase in mean hydrodynamic diameter (left) and reversal of zeta potential (mV) showing effective coating of CAP on insulin loaded thermo-responsive PLA NPs (n=3)

3.3.4 Physico-chemical characterization of uncoated PLA NPs

3.3.4.1 Size, PDI and zeta potential

From figure 3.10 it is visible that as amount of pluronic F 127 was increased, degree of swelling/de-swelling was also increased with good PDI which may be due to more availability of pluronic F 127 molecules to form thermo-responsive layer. In the absence of pluronic F 127, nanoparticles with 155.68 ± 13.24 nm size and 32 ± 6.25 mV zeta potential were formed but with poor stability and least degree of swelling/de-swelling phenomena. At ratio 1:20 the NPs have shown highest degree of swelling/de-swelling phenomena wherein, the size of nanoparticles at 25°C was 48.96 ± 8.14 nm and shifted to 125.23 ±10.36 nm at 4°C due to swelling of pluronic F 127 layer. However, when temperature of the same formulations was changed to 37 °C, the nanoparticles showed size of 32.56 ±7.01 nm which confirms the temperature controlled de-swelling of pluronic F 127.

From figure 3.11, we can notice that in the absence of pluronic F 127, PLA-NH2 nanoparticles had 32 ± 6.25 mV zeta potential but at polymer to surfactant (PLA-NH2: Pluronic F 127) ratio of 1:2, comparatively less positive surface charge was observed with value of 26.7 ± 2.88 mV. The reason behind is non-ionic nature of pluronic F 127. The multi-molecular layer of non-ionic pluronic F 127 shell is reducing the net surface charge of PLA-NH2 core of the nano-particles due to shielding effect. In accordance with aforementioned fact it can be observed from the data that as PLA-NH2 to pluronic F 127 ratio was increased from 1:2 to 1: 20, the zeta potential value (positive surface charge) was decreased.

More interestingly, it was observed that temperature regulated shifts in zeta potential was also noted apart from the primary shifts in size of the thermo-responsive nanoparticles. As temperature decreased from 37°C to 25°C to 4°C a stepwise increment in zeta potential value was observed and this trend was persistent at different polymer (PLA-NH2) to surfactant (pluronic F 127) ratios above 1:2. Let's discuss this event for the ratio 1:20 which was considered optimum. Herein, at 37°C, 25°C and 4°C, observed zeta potential values are 10.8 ± 1.77 mV, 12.1 ± 1.05 mV and 14.31 ± 2.25 mV, respectively. In another way we can say that the surface charge lowering capability (shielding effect) of pluronic F 127 is comparatively lesser at lower temperature. Fortunately, this phenomenon inadvertently, favored the loading of insulin by electrostatic interaction. At 4°C when pluronic F 127 shell

is in loosened and swelled state and comparatively more positive surface charge is present, negatively charged insulin molecules will easily bind with positively charged core.

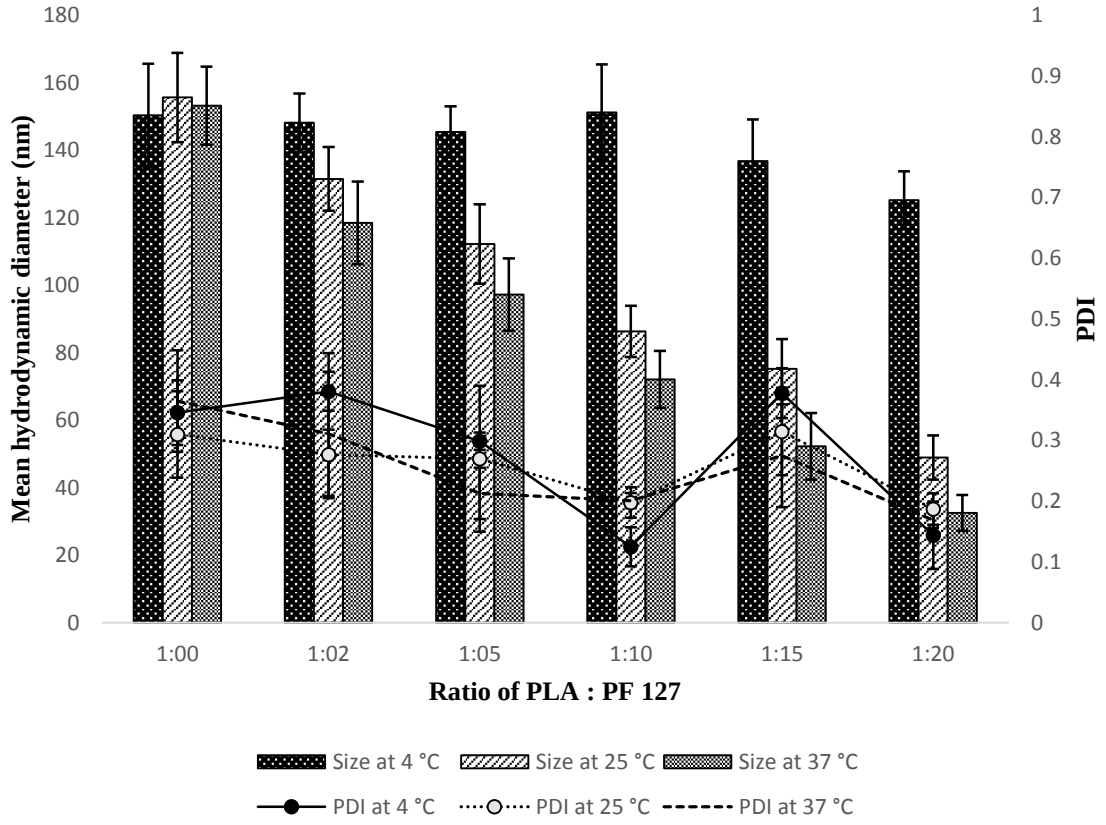

Figure. 3.10 Mean hydrodynamic diameter (nm) and polydispersity index of insulin loaded thermo-responsive PLA-NH2 NPs (n=3)

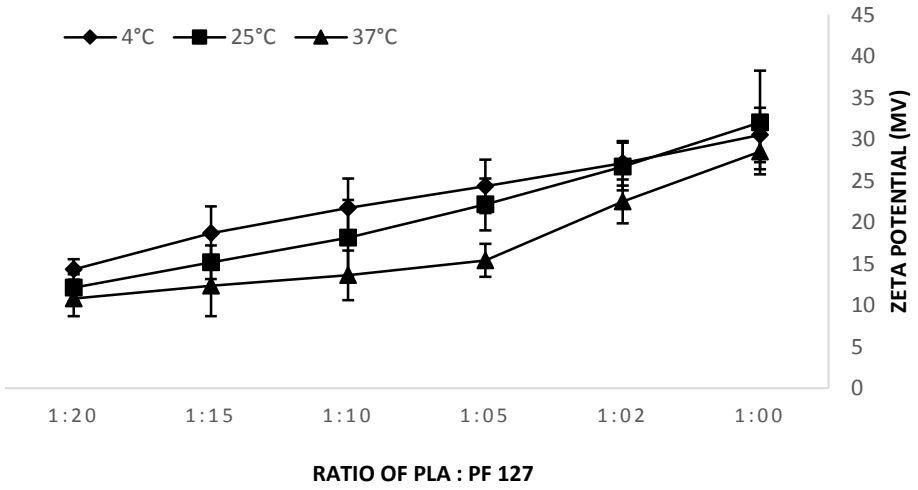

Figure. 3.11 Zeta potential (mV) of insulin loaded thermo-responsive PLA-NH2 NPs (n=3)

3.3.4.2 Shape and surface morphology by atomic force microscopy

Atomic force microscopy (AFM) images revealed the phenomena of swelling and de-swelling at 4°C and 37°C, respectively, as shown in figure 3.12.

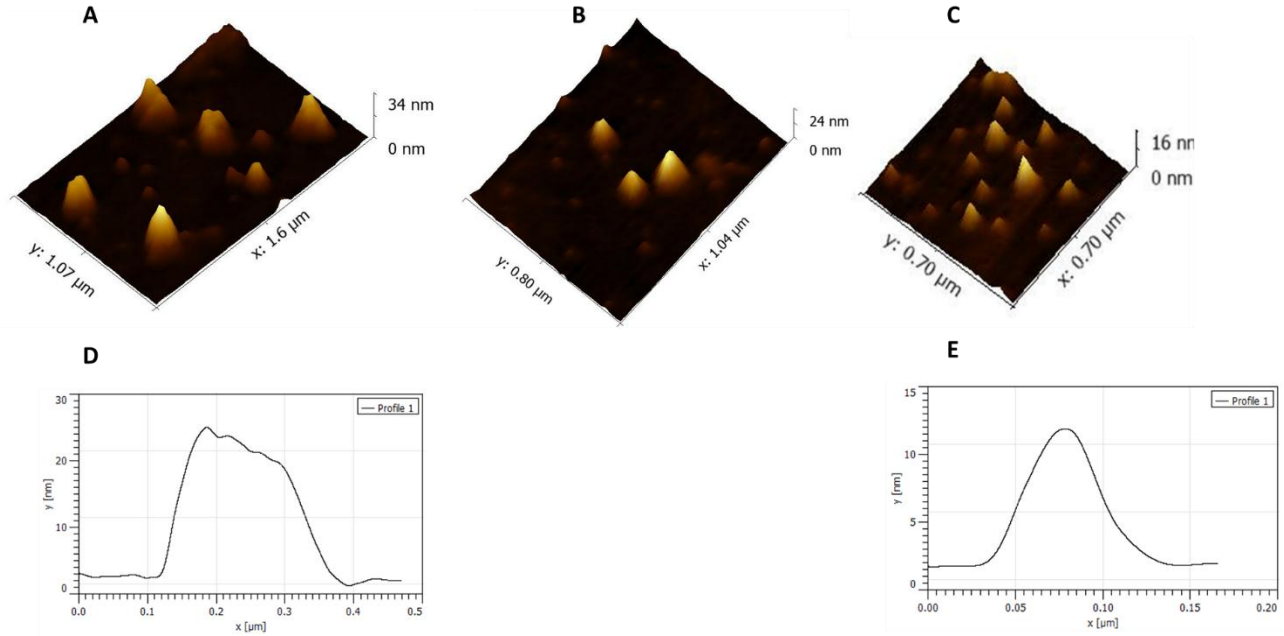

Figure. 3.12 AFM images of optimized thermo-responsive PLA NPs revealing the swelling and de-selling phenomena. **A]** NPs in swelled state at 4°C **B]** NPs at ambient room temperature **C]** NPs in de-swelled state at 37°C. **D]** The graph showing average height and diameter (nm) of NPs at 4°C. **E]** The graph showing average height and diameter (nm) of NPs at 37°C.

3.3.5 RP-HPLC method for insulin quantification

The method was found linear in the range of 0.05 µg to 5 µg/ml concentration with R^2 value of 0.9978 as shown in figure 3.13. Figure 3.14 shows the chromatogram obtained for 4 µg/ml concentration of insulin.

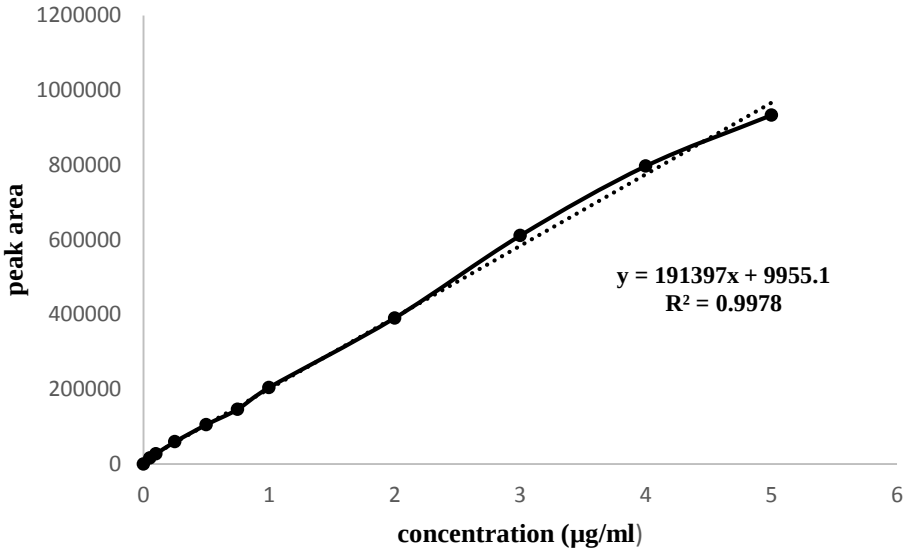

Figure 3.13. Calibration curve of insulin

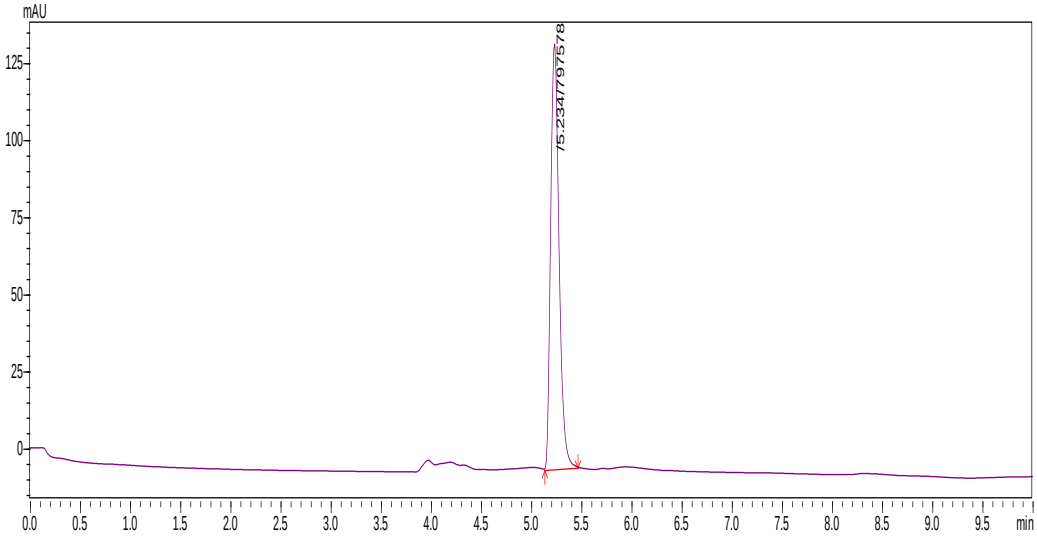

Figure. 3.14 The chromatogram obtained for 4 µg/ml concentration of insulin.

3.3.6 Percentage entrapment proficiency

As the PLA: PF 127 ratio increased, percentage entrapment efficiency was also increased due to increase in surface area and higher degree of swelling/de-swelling of thermo-responsive shell. NPs with 1:20 ratio of PLA: PF 127 showed highest entrapment and was considered as optimum formulation to carry forward for *in vitro* and in vivo performance (figure 3.15).

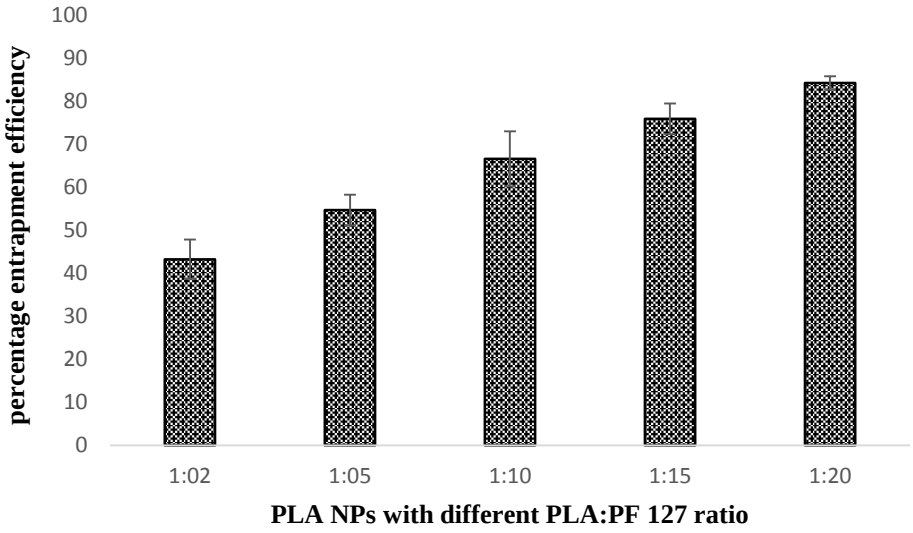

Figure. 3.15 Percentage entrapment efficiency of different PLA NPs formulations to incorporate insulin (n=3)

3.3.6.1 An approach for enhancement of entrapment efficiency

It was found that as the pH of insulin solution was increased, the net negative charge of insulin was also increased as shown in table 3.1. As the net negative charge on insulin molecules increases, their electrostatic interaction to positively charged TNPs becomes strong resulting in augmented encapsulation efficiency. As shown in table 3.1 and figure 3.16, when pH was increased from 7.4 to 9, % EE was upraised to 12 to 15% while at pH 10 the highest encapsulation efficiency of 91% was achieved.

Table 3.1. Effect of pH of insulin solution on insulin charge and entrapment efficiency

pH of insulin solution during incubation	**charge of insulin**	**Entrapment efficiency (Mean±S.D ; n = 3)**
pH 7.4	-3.06	78.89±4.56
pH 8	-5.7	82.5±3.16
pH 9	-9.5	86.8±6.38
pH 10	-12	91.4±3.57

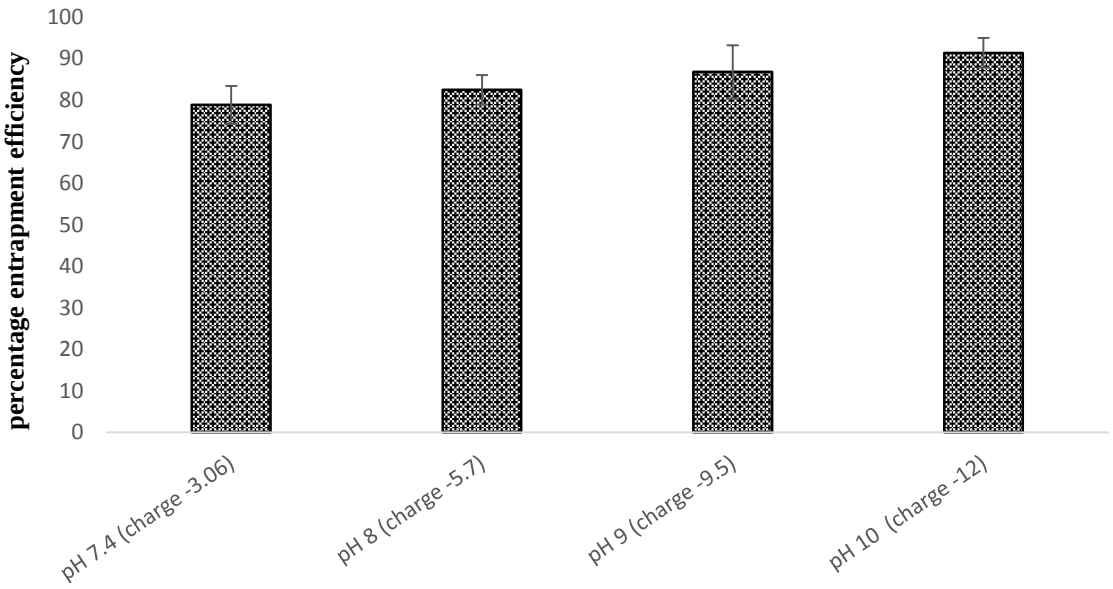

Figure. 3.16. Effect of insulin charge at different pH on its entrapment efficiency

3.3.6.2 Protein confirmation and stability

The retention of insulin in its active and stable secondary structure form is very important when it comes to its delivery through oral route. Though encapsulation of insulin in TNPs has provided the impeccable shelter to this protein molecules, in voracity of enhancing the encapsulation efficiency the native structure of insulin should not be compromised. Therefore, the confirmation stability of insulin released from TNPs incubated at different pH condition was checked with CD spectrometry. According to the obtained results as shown in figure 3.17, insulin released at all the pH conditions has showed almost overall retention of their alpha helix (negative band at 208 nm) as well as beta sheet structure (negative band at between 220 and 223 nm) as compared to standard insulin solution. But it is worth to note that the both characteristic bands of α helix as well as β sheet got shifted 4-5 nm in the opposite direction of each other which suggest that there might be a change in folding of coil structure. Therefore, their $([\Theta]_{208}/[\Theta]_{223}$ ratios were found 1.42 for insulin released at pH 9 and 1.58 for insulin released at pH 10.

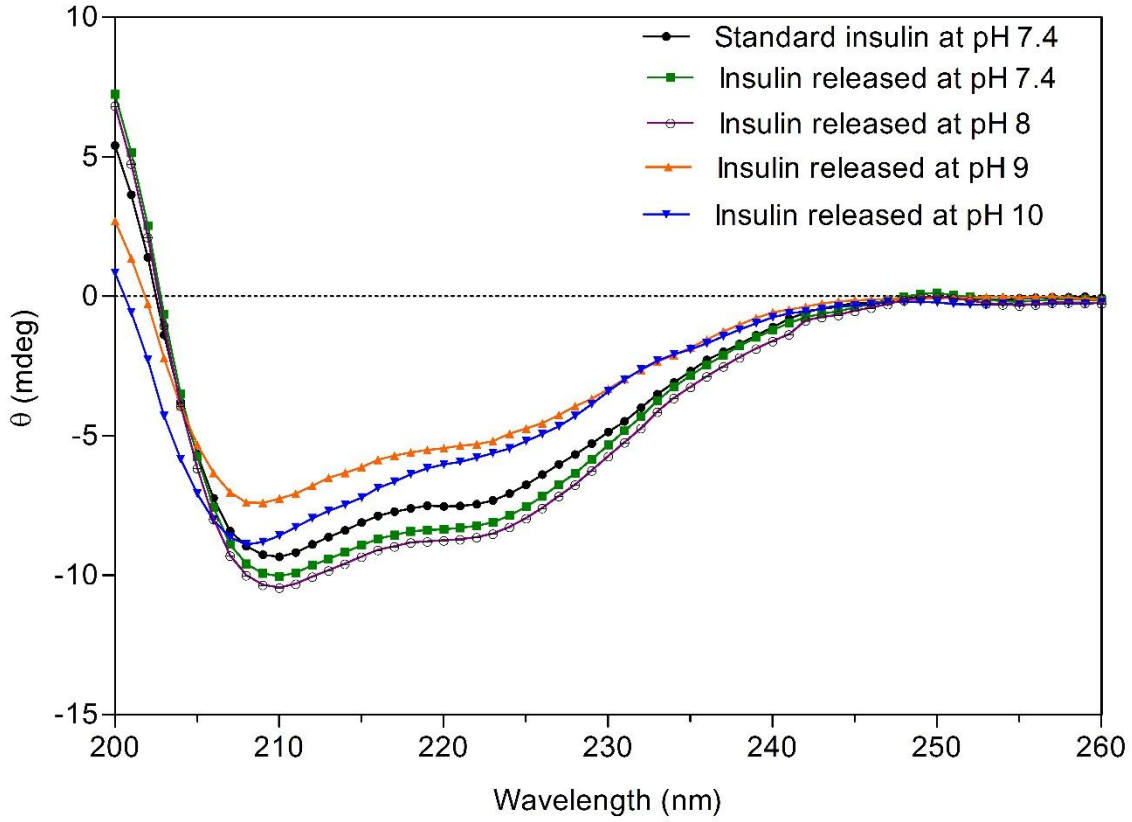

Figure. 3.17. UV-CD spectra of standard insulin and released insulin at different pH

3.3.7 Transmission Electron Microscopy (TEM)

To see the morphology and structure characteristic of developed TNPs, High resolution transmission electron microscopy was used. The obtained microscopic image (figure 3.18) revealed that TNPs are roughly spherical in shape, well dispersed without aggregation, and have ultra-fine size (approx. 50 nm) less than 100 nm as in support with the results of mean hydrodynamic diameter.

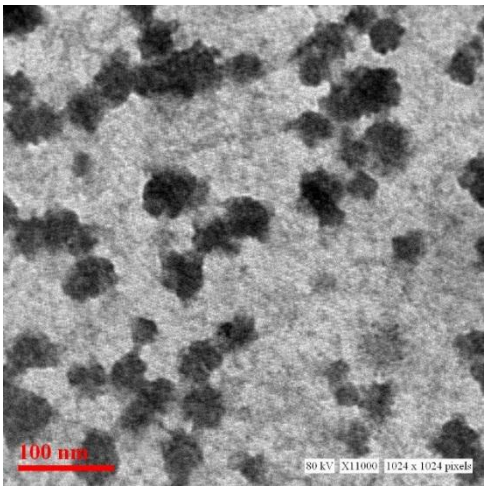

Figure 3.18. Transmission electron microscopic image with 11000x magnification.

3.3.8 Stability study

During the stability study at room temperature (25°C) as well as 4 °C, TNPS showed no significant change in size of the particles up to 60 days but after that there was subtle increase in particle size when analyzed at 90th day (Figure 3.19). Herein, at 25°C the average size remained near 60.18 ± 6.8 nm during the study period, while for the same formulations stored at 4°C temperature it was observed nearby 127.03 ± 10.87 nm. This drastic change was due to comparatively shrunken or de-swelled state of thermo-responsive PF127 shell at 25°C than 4°C. The change in zeta potential was also non-significant and the optimized formulation was found stable with good PDI (Figure 3.20).

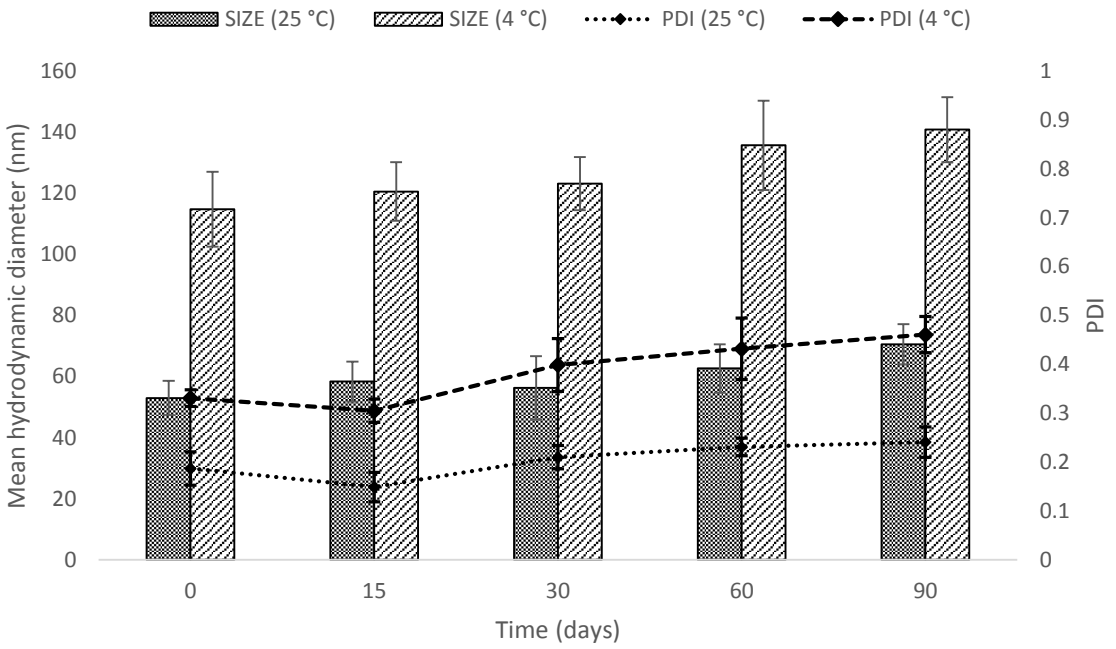

Figure 3.19. Effect of storage at 25 °C and 4 °C on mean hydrodynamic diameter (nm) and polydisersityindex (PDI) of the TNPs formulation.

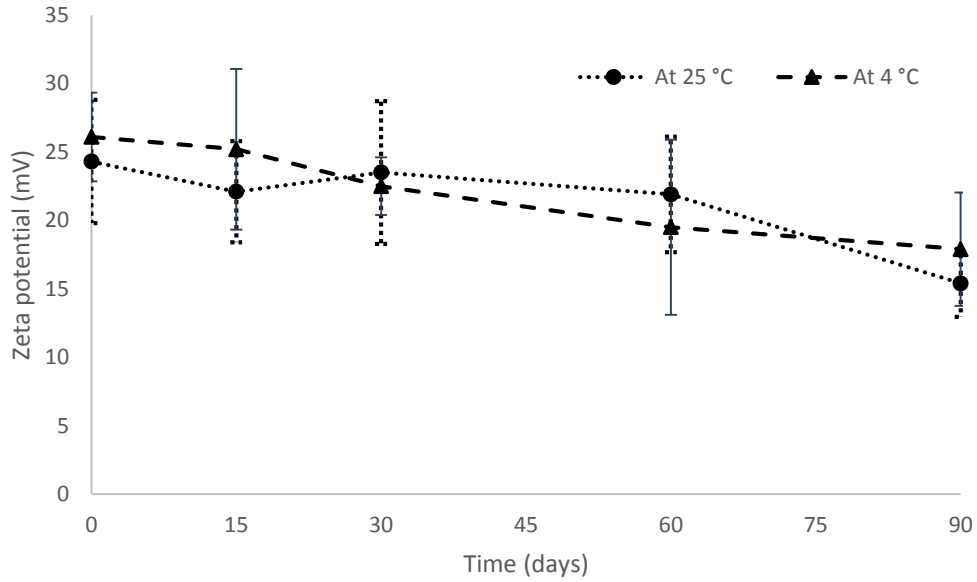

Figure 3.20. Effect of storage at 25 °C and 4 °C on zeta potential (mV) of the TNPs formulation.

3.3.9 Protein confirmation and stability study

Proteins are dynamic bio-macro-molecules and their therapeutic activity is primarily dependent on their secondary structure and confirmation. Circular dichroism technique was used to know the conformational changes, secondary structure, folding and binding properties of insulin. After encapsulation of insulin in TNPs what conformational changes have been occurred were analyzed. The negative band at 208 nm primarily arise from component of α helical structure while a band at 223 nm is due to β structure of insulin [23]. Here, it was found that released insulin also showed representative CD bands at 208 nm and 223 nm as of standard insulin which suggest that the released insulin was intact with proper secondary structure confirmation and folding (figure 3.21). The ratio of Θ (mdeg) value at two wavelengths; 208 and 223 ($[\Theta]_{208}/[\Theta]_{223}$) is used as tool to know about the secondary structure retention of proteins [24]. The $[\Theta]_{208}/[\Theta]_{223}$ ratio was found 1.22 for standard insulin and 1.18 for insulin released from TNPs which indicates that there is very subtle and negligible confirmation conversion but overall secondary structure and tertiary structure of native protein is retained.

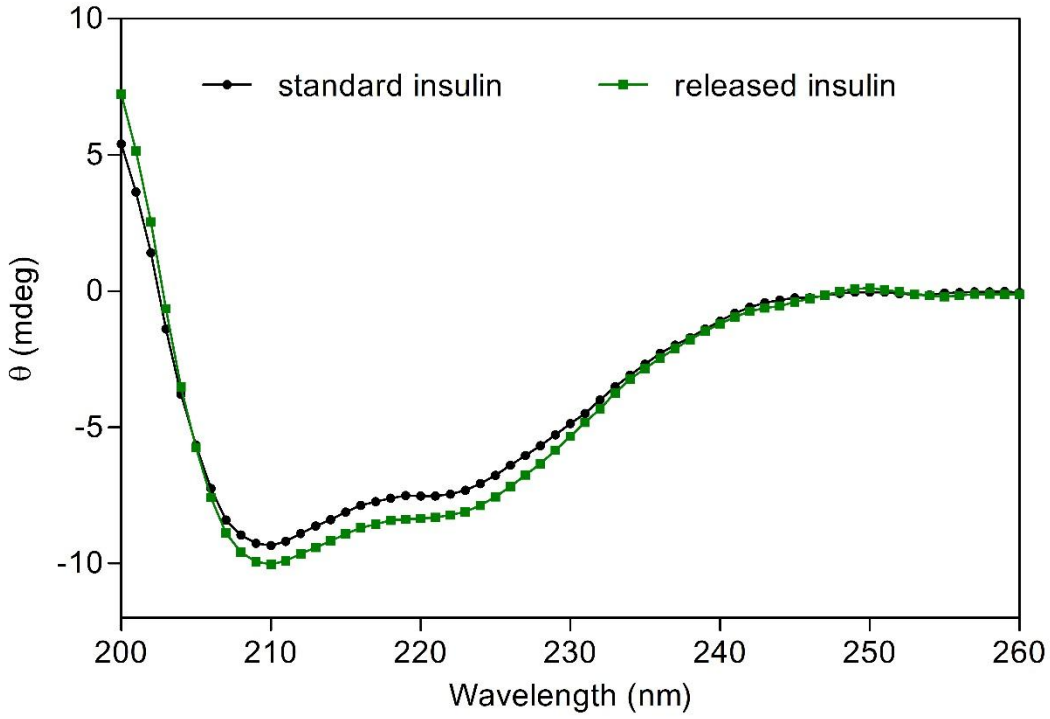

Figure 3.21. UV-CD spectra of standard insulin and insulin released from TNPs.

3.3.10 *In vitro* cell uptake study

To check the ability of NPs to carry forward entrapped insulin through intestinal membrane, quantitative cell uptake study was executed in HCT 116 and Caco2 cell lines by FACS. From the figure 3.22, it is visible that FITC loaded NPs (mean fluorescent intensity 286.76) has shown approximately 17 fold higher uptake then FITC solution (mean fluorescent intensity 16.54) in HCT 116 cells. In Caco-2 cells the FITC loaded TNPs (mean florescent intensity 246.40) has shown approximately 15 fold higher uptake then FITC solution (mean fluorescent intensity 37.61) as shown in figure 3.23.

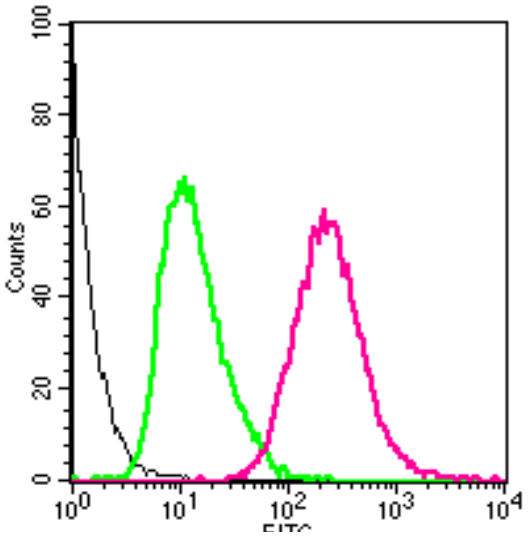

Figure 3.22. Histogram showing cell uptake of NPs in HCT 116 cells

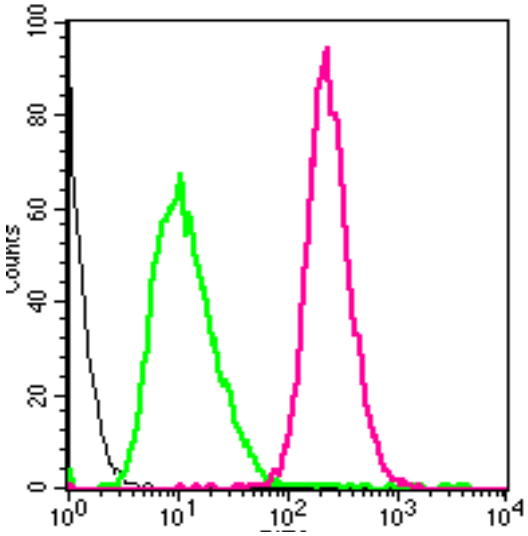

Figure 3.23. Histogram showing cell uptake of NPs in Caco2 cells

Note: [Black line denotes control untreated cells, green line denotes cells treated with FITC solution and pink line denotes cells treated with FITC loaded NPs]

3.3.11Trans Epithelial Electrical Resistance (TEER)

Trans-epithelial electrical resistance is the epitome of tight epithelial junction present at intestinal membrane which restrict the para cellular transport of high molecular weight, hydrophilic bio-macromolecules like insulin. Therefore, this study was performed to check that if uncoated TNPs (made up of PLA –NH2) or CAP coated TNPs have the property of opening the tight junction. Generally, caco-2 cell monolayer has a TEER value between 350-400 $\Omega*cm^2$ and when the tight junction opens up the resistance (TEER) value decreases. According to the obtained results, the free insulin did not show any significant

decrement in percent TEER compared to zero time point but insulin bearing uncoated TNPs showed sharp decrease up to 60% TEER 1.5 hour post treatment which may be due to re-organization of membrane proteins by positively charged TNPs (PLA-NH_2 core as well as shell of pluronic F 127). The highest decrement in percent TEER was observed 2 hours post treatment with insulin bearing CAP coated TNPs where the percent TEER reached approximately 48% as shown in figure 3.24. Here, the reason may be the phthalate moieties of CAP which is reported to have property of opening the tight epithelial junction. Therefore, it can be inferred that the opening of tight junction will facilitate para cellular transport resulting in enhanced bioavailability of insulin. After removal of treatment, at 6 hour time point recovery of TEER was observed up to 75–85% TEER. The recovery in TEER value is important to note because it signifies the transient opening of tight junction and not the permanent damage. However, 100% recovery in TEER was not obtained.

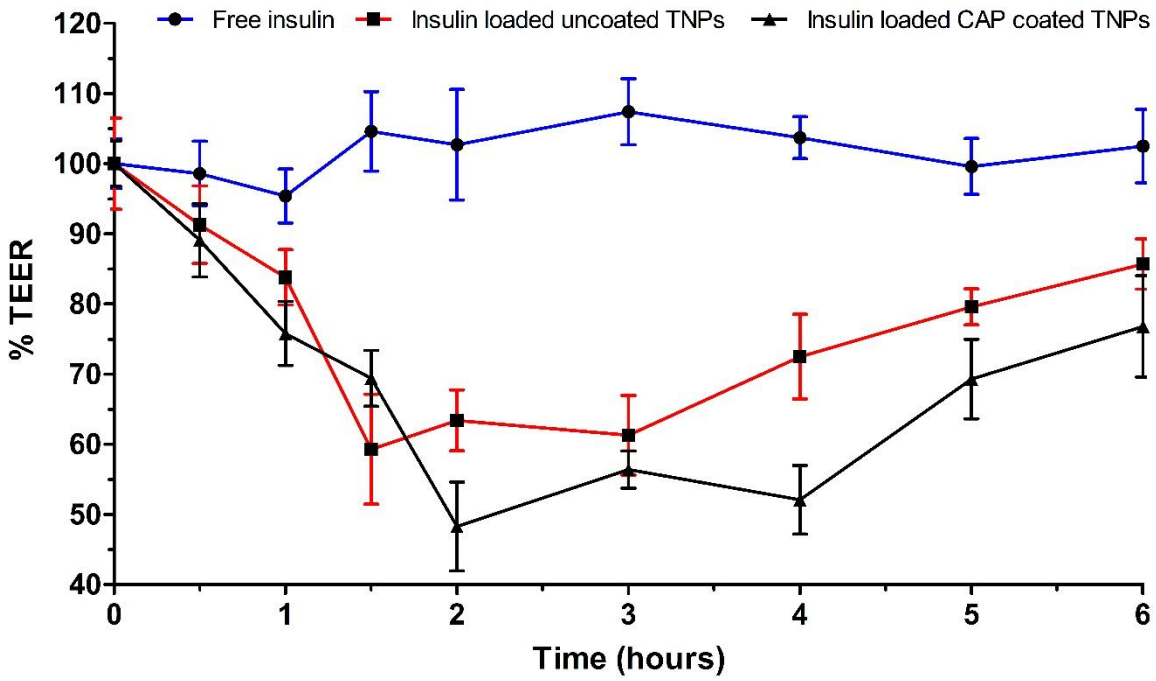

Figure 3.24. Change in percentage TEER of Caco-2 monolayer after treatment with free insulin, insulin loaded uncoated TNPs and insulin loaded CAP coated TNPs. Results are represented as percent TEER of the basal value at zero time point (t_0). (**Mean ± S.D; n=6**)

3.3.12 *In vitro* release

Optimized formulation, CAP coated PLA NPs with 1:20 ratio of PLA: PF 127, was selected for *in vitro* drug release study. Due to coating of CAP, no release of insulin was observed in initial 2 hours in simulated gastric fluid but release was started after 30 minutes in simulated intestinal fluid and continued up to 72 hours with initial burst release followed by controlled release as shown in figure 3.25. Here, it is presumed that after removal of CAP coating, the insulin having PLA NPs would be uptaken by M cells present in Payer's patches leading to entry into systemic circulation and that is the reason that release study was considered for 72 hours.

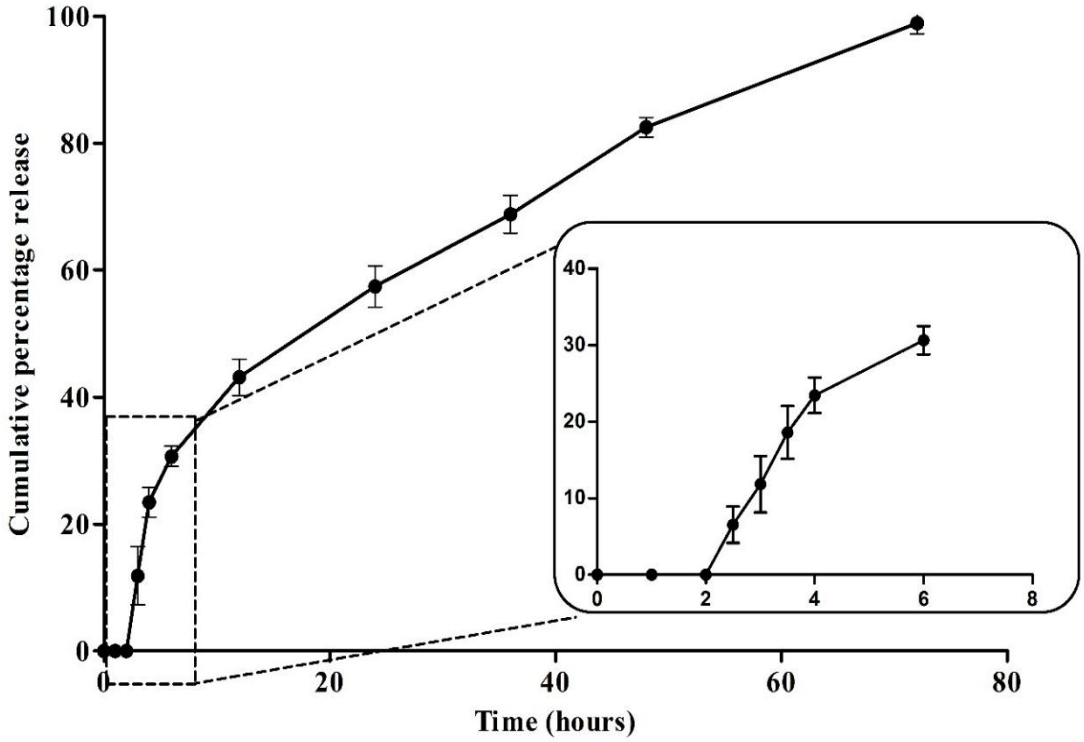

Figure. 3.25 *In vitro* release profile of CAP coated PLA NPs bearing insulin (n=3)

3.3.13 MALDI-TOF of insulin released *in vitro*

MALDI-TOF was performed to check whether the insulin released from formulation is in intact form without any degradation. Peak at 5809 as shown in mass spectra (figure 3.26) of insulin revealed that released insulin was intact and did not show degradation at acidic pH. Hence, it can be concluded that developed CAP coated thermo-responsive PLA NPs have the potential to deliver insulin without degradation.

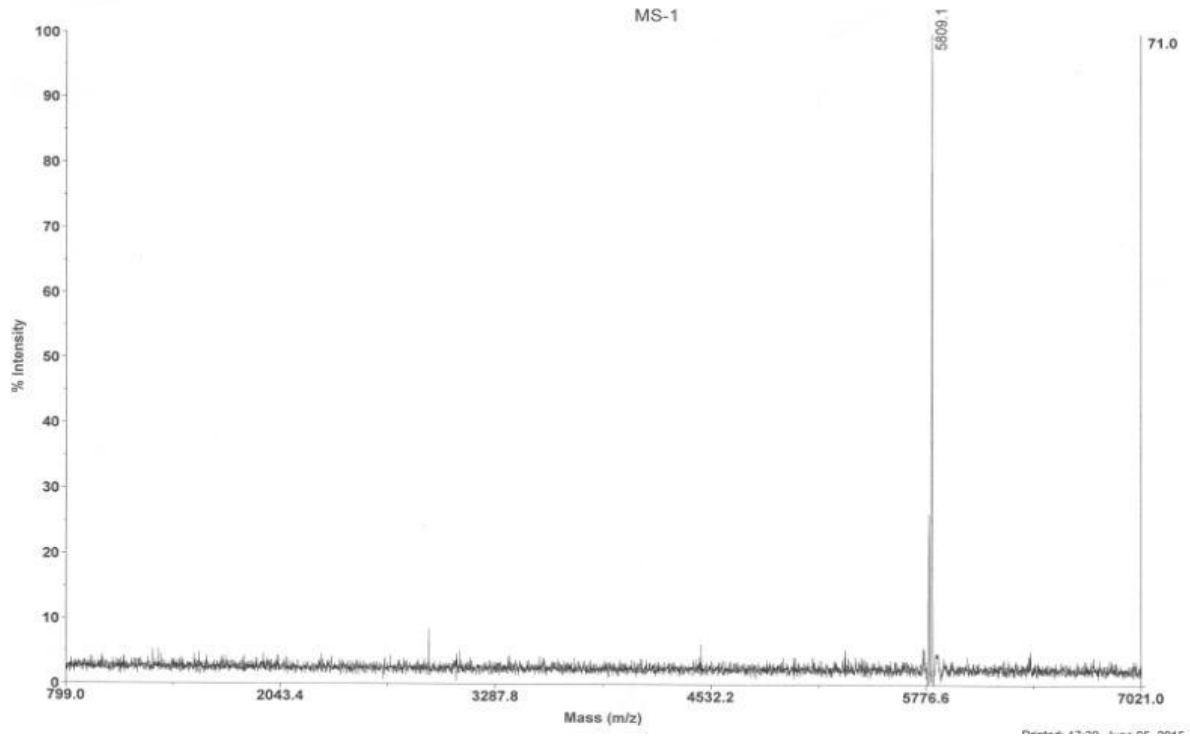

Figure. 3.26 Mass spectra of insulin released from CAP coated thermo-responsive PLA NPs

3.3.14 *In vitro* bio-activity

Despite of the positive advocacy showcased by results of conformational stability (CD spectroscopic results) and structural integrity (MALDI TOF results) of insulin released from developed thermo-responsive size shifting nanoparticles, the critical aspect which questions that whether this drug delivery system is capable to deliver the insulin in its therapeutically viable form or not, remains the prime concern. Therefore, we employed MCF-7 cell lines which can show insulin dependent proliferation due to the presence of IGF-1 receptors on its cell membrane. Approximately 50,000 MCF-7 cells were seeded in each well of 96 well plate, supplemented with excess of RPMI 1640 culture medium. The

cells were treated with different concentrations (0.5, 1, 2, 3, 4, 5 µg/ml) of pure insulin (positive control), Blank TNPs, Blank CAP-TNPs, Insulin bearing INS@TNPs and INS@CAP-TNPs. Herein, control wells wherein, cells were not treated with insulin but only same volume of culture medium was added served as reference growth. The cell viability was measured by gold standard MTT assay. As shown in the figure 3.27 pure insulin exhibited significantly high proliferation than INS@TNPs and INS@CAP-TNPs at all the concentrations which may be due to direct availability of insulin in dissolved form. In case of INS@TNPs and INS@CAP-TNPs, at same concentration uncoated INS@ TNPs showed high proliferation as compared to coated INS@CAP-TNPs suggesting lesser availability of released insulin from the INS@CAP-TNPs. Herein, we can conclude that released insulin from both INS@TNPs and INS@CAP-TNPs formulations, is in therapeutically active form. Moreover, the data showcased that developed formulations are capable to protect the labile insulin molecule in its bio-active form.

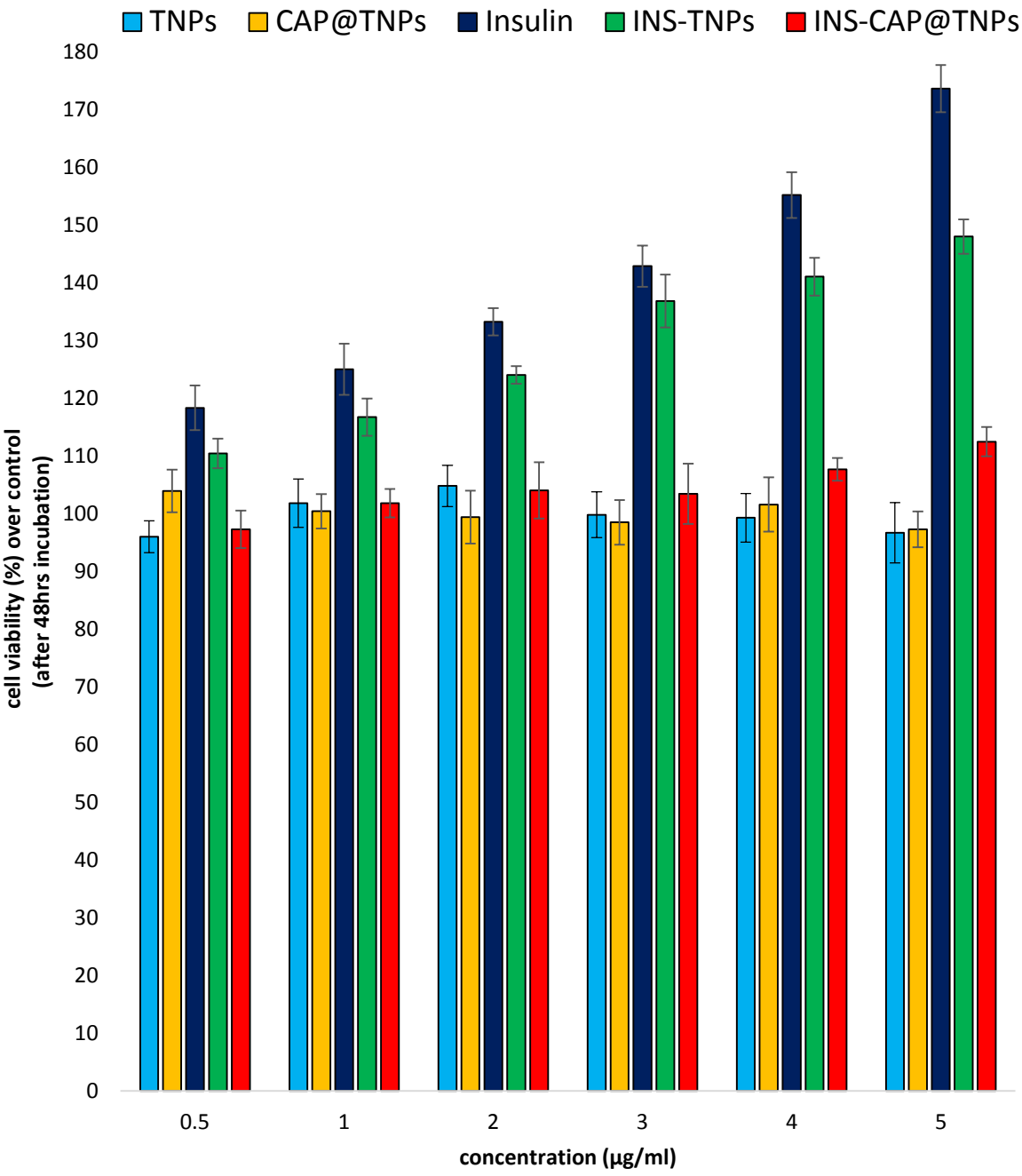

Figure 3.27. *In vitro* bio-activity of pure insulin (positive control), Blank TNPs, Blank CAP-TNPs, Insulin bearing INS@TNPs and INS@CAP-TNPs confirmed by MTT cell proliferation assay on MCF-7 cells (**Mean ± S.D; n=3**)

3.3.15 Animal experiments

3.3.15.1 Hypoglycemic activity: In vivo efficacy

STZ induced diabetic Male SD rats were fasted for 6 hours and then treated with PBS pH 7.4 via oral route (diabetic control or negative control), insulin solution in PBS pH 7.4 via sub-cutaneous route at the dose of 2 IU/kg and insulin incorporated thermo-responsive size shifting NPs (INS-CAP@TNPs) via oral route at the dose of 10 IU/kg. The blood glucose data obtained at different time intervals (figure 3.28) demonstrated that in case of SC insulin, onset of action started after 15 minutes of treatment. The maximal blood glucose decrement up to 49.4 ± 4.20 mg/dl was attained 2 hours post-treatment and thereafter blood glucose level kept rising up to 12 hours and reached above 300 mg/dl. It is worthy to note that SC insulin led to sudden fall of blood glucose level but fails to maintain it for more than 4 hours. Meanwhile, INS@CAP-TNPS managed to lower the blood glucose to 156.4 ± 15.29 mg/dl at 4 hours and maintained it below 200 mg/dl up to 12 hours. Blood glucose management with approximately 50% decrement for more than 12 hours is attributed to the controlled release, better cell uptake from intestine and enhanced para-cellular transport due to opening of tight epithelial junction of intestine offered by thermo-responsive size shifting nanoparticles.

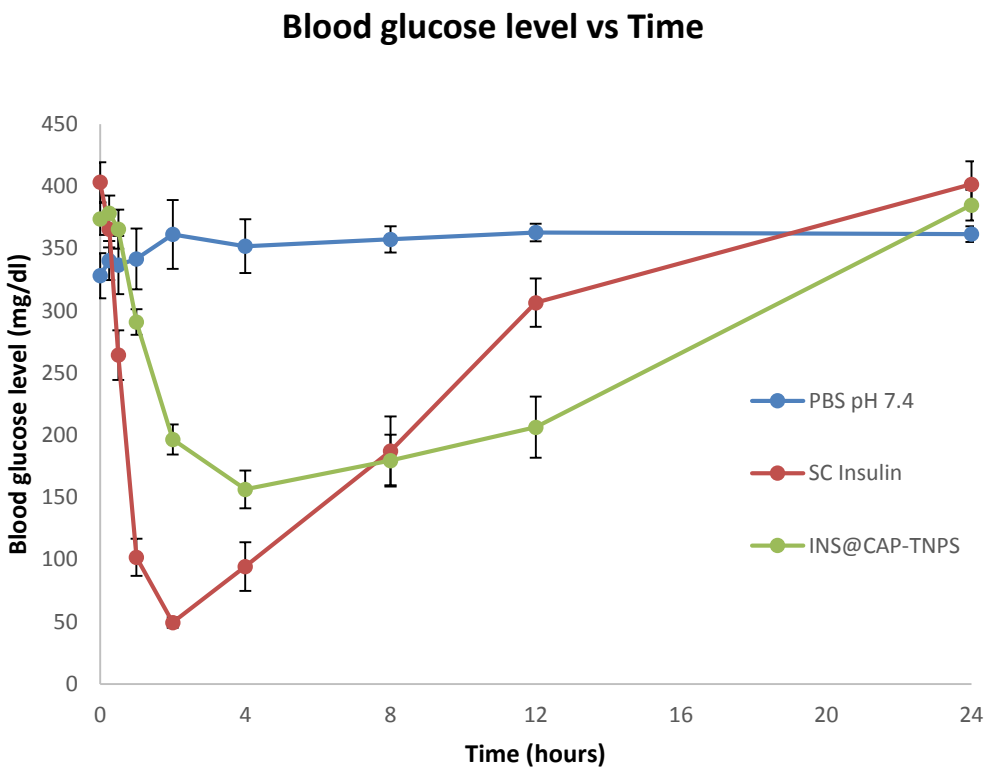

Figure 3.28. Blood glucose levels in diabetic rats after oral administration CAP coated thermo-responsive size shifting nanoparticles (INS@CAP-TNPS) at the dose equivalent to 10 IU/Kg of insulin and sub-cutaneous administration of insulin solution in PBS 7.4 at the dose of 2 IU/Kg. DC stands for diabetic control group which received PBS pH 7.4 orally and served as baseline for plasma insulin level (n=5, Mean ± SEM)

3.3.15.2 Plasma Insulin level and Pharmacokinetics

The plasma was separated from the blood samples withdrawn at different time intervals and stored at -80°C. Prior to analysis, the samples were allowed to attain the room temperature and then analysed by ELISA kit –RAB0327 (Sigma Aldrich Inc.) after proper dilution according to the assay protocols given by the manufacturer. The change in plasma insulin level with respect to time after administration of SC insulin and oral INS@CAP-TNPS is represented in figure 3.29. We observed a basal plasma insulin level of 64.63 ± 4.02 µIU/ml over 24 hours in diabetic rats. The peak plasma insulin concentration (Cmax) after 30 minutes (Tmax) of SC insulin treatment was observed to be 669.34 ± 23.54 µIU/ml. Then, the plasma insulin level fell down to 115.99 ± 10.44 µIU/ml at 4 hours, remained below up to 12 hours and reached to basal diabetic level of 62.54 ± 9.68 µIU/ml after 24

hours. The INS@CAP-TNPS offered plasma insulin level of 143.53 ± 13.55 µIU/ml after 1 hour (onset) of oral administration and deliver the insulin to get a hike of 236.64 ± 26.31 µIU/ml at 4 hours' time point. Moreover, INS@CAP-TNPS managed to keep the plasma insulin level above ~100 µIU/ml up to 8 hours. The pharmacokinetic parameter achieved after non compartmental analysis via WinNonlin 6.0 software are shown in table 3.2. According to the pharmacokinetic modelling, orally delivered INS@CAP-TNPS showed significantly lower Cmax 236.64 µIU/ml as compared to 669.35 µIU/ml for sub-cutaneously delivered insulin, which is mainly due to the controlled release provided by INS@CAP-TNPS and route of administration derived advantage. The area under the curve (AUC) observed after administration of INS@CAP-TNPS is 5140.07 hr* µIU/ml as compared to 6231.11 hr* µIU/ml observed for SC insulin, suggesting almost similar AUC values but at 5 times more dose than SC insulin. The relative bio-availability of developed INS@CAP-TNPS (10 IU/kg) with reference to sub-cutaneously administered insulin (2IU/kg) was calculated and observed to be 16.49%.

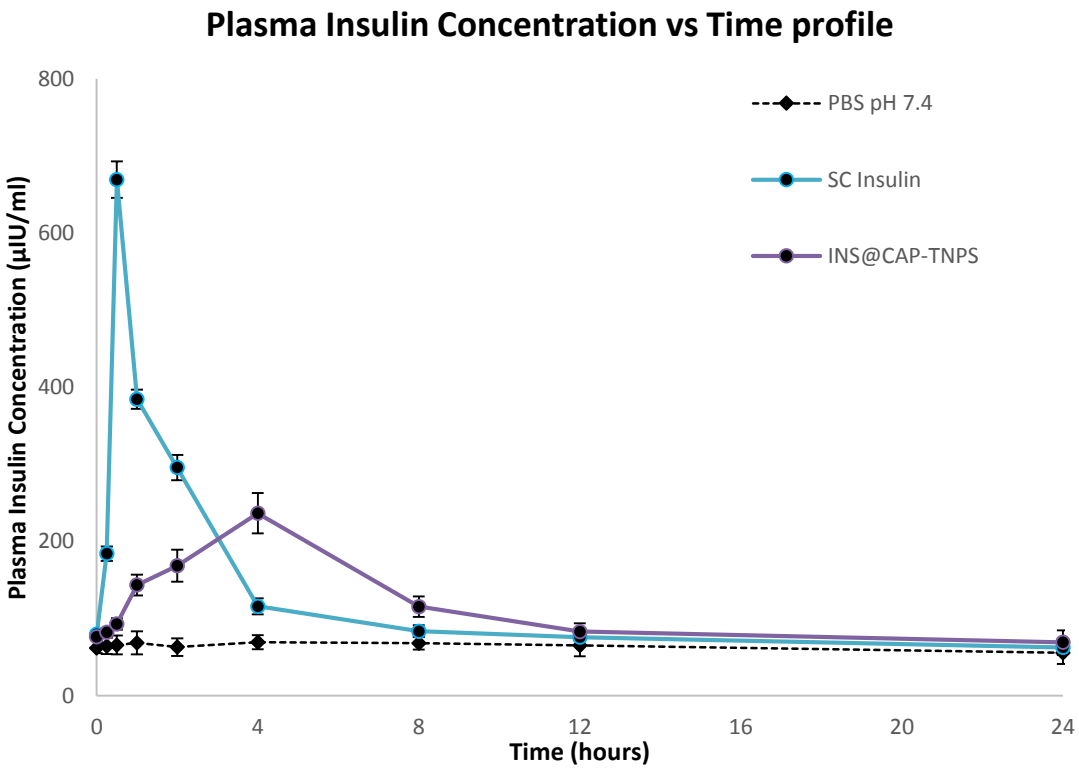

Figure 3.29. Plasma Insulin levels in diabetic rats after oral administration CAP coated thermo-responsive size shifting nanoparticles (INS@CAP-TNPS) at the dose equivalent to 10 IU/Kg of insulin and sub-cutaneous administration of insulin solution in PBS 7.4 at the

dose of 2 IU/Kg. DC stands for diabetic control group which served as baseline for plasma insulin level (n=5, Mean ± SD)

Table 3.2. Pharmacokinetic parameters after oral administration CAP coated thermo-responsive size shifting nanoparticles (INS@CAP-TNPS) at the dose equivalent to 10 IU/Kg of insulin and sub-cutaneous administration of insulin solution in PBS 7.4 at the dose of 2 IU/Kg.

Pharmacokinetic Parameter (Unit)	Sub-cutaneous insulin	INS@CAP-TNPS
Dose (IU/kg)	2	10
Tmax (hr)	**0.5**	**2**
Cmax (µIU/ml)	669.35	236.64
AUC (hr* µIU/ml)	6231.11	5140.07
Relative oral bioavailability (%)	**100**	**16.49**

3.4 CONCLUSION

Thermo-responsive size shifting polymeric nanoparticles for oral delivery of insulin were successfully architected and evaluated for *in vitro* and *in vivo* performances. The unique thermo-responsive property of pluronic F 127 facilitated swelling/de-swelling phenomena which enabled temperature based passive loading of insulin without any detrimental effects. Moreover, entrapment efficiency of insulin was enhanced to maximum by playing with negative charge of insulin and its electrostatic interaction between positively charged PLA $–NH_2$. CAP coating provided a stubborn barrier to hostile acidic pH of upper GIT and protected the insulin. Therefore, from the results obtained after *in vitro* and in vivo analysis, it can be collectively concluded that the envisaged formulation worked very well and delivered the insulin in its viable form with relative oral bio-availability of 16.49 percentage as compared to SC insulin. The positive results ignited a hope that the most awaited as well as most challenging breakthrough of oral insulin may be achieved in coming future.

3.5 REFERENCES

1. Pawar, V.K., et al., *Targeting of gastrointestinal tract for amended delivery of protein/peptide therapeutics: strategies and industrial perspectives.* J Control Release, 2014. **196**: p. 168-83.
2. Roco, M., *The Long View of Nanotechnology Development: The National Nanotechnology Initiative at 10 Years*, in *Nanotechnology Research Directions for Societal Needs in 2020*. 2011, Springer Netherlands. p. 1-28.
3. des Rieux, A., et al., *Nanoparticles as potential oral delivery systems of proteins and vaccines: A mechanistic approach.* Journal of Controlled Release, 2006. **116**(1): p. 1-27.
4. Ensign, L.M., R. Cone, and J. Hanes, *Oral drug delivery with polymeric nanoparticles: The gastrointestinal mucus barriers.* Advanced Drug Delivery Reviews, 2012. **64**(6): p. 557-570.
5. Swaminathan, J. and C. Ehrhardt, *Liposomal delivery of proteins and peptides.* Expert Opin Drug Deliv, 2012. **9**(12): p. 1489-503.
6. Venkata Ramana Rao, S. and J. Shao, *Self-nanoemulsifying drug delivery systems (SNEDDS) for oral delivery of protein drugs: I. Formulation development.* International Journal of Pharmaceutics, 2008. **362**(1–2): p. 2-9.
7. Fan, T., et al., *Design and evaluation of solid lipid nanoparticles modified with peptide ligand for oral delivery of protein drugs.* Eur J Pharm Biopharm, 2014. **88**(2): p. 518-28.
8. Yan, M., et al., *A novel intracellular protein delivery platform based on single-protein nanocapsules.* Nat Nanotechnol, 2010. **5**(1): p. 48-53.
9. Rao, J.P. and K.E. Geckeler, *Polymer nanoparticles: Preparation techniques and size-control parameters.* Progress in Polymer Science, 2011. **36**(7): p. 887-913.
10. Pinto Reis, C., et al., *Nanoencapsulation I. Methods for preparation of drug-loaded polymeric nanoparticles.* Nanomedicine: Nanotechnology, Biology and Medicine, 2006. **2**(1): p. 8-21.
11. Seymour, M., *Coal-aqueous mixtures having a particular coal particle size distribution*. 1986, Google Patents.
12. Sabetsky, V. and J. Ekblom, *Insulin: a new era for an old hormone.* Pharmacol Res, 2010. **61**(1): p. 1-4.
13. *Continuous Glucose Monitoring and Intensive Treatment of Type 1 Diabetes.* New England Journal of Medicine, 2008. **359**(14): p. 1464-1476.
14. Hermann, L.S., *Combination therapy with insulin and metformin.* Endocr Pract, 1998. **4**(6): p. 404-12.
15. Malm, C.J., J. Emerson, and G.D. Hiait, *Cellulose Acetate Phthalate as an Enteric Coating Material.* Journal of the American Pharmaceutical Association (Scientific ed.), 1951. **40**(10): p. 520-525.
16. Chaturvedi, K., A.R. Kulkarni, and T.M. Aminabhavi, *Blend Microspheres of Poly(3-hydroxybutyrate) and Cellulose Acetate Phthalate for Colon Delivery of 5-Fluorouracil.* Industrial & Engineering Chemistry Research, 2011. **50**(18): p. 10414-10423.
17. Ravi, S., et al., *Development and Validation of an HPLC–UV Method for the Determination of Insulin in Rat Plasma: Application to Pharmacokinetic Study.* Chromatographia, 2007. **66**(9-10): p. 805-809.
18. Sharma, S., et al., *Investigating the role of Pluronic-g-Cationic polyelectrolyte as functional stabilizer for nanocrystals: Impact on Paclitaxel oral bioavailability and tumor growth.* Acta Biomater, 2015. **26**: p. 169-83.
19. Yu, S.H., et al., *Nanoparticle-induced tight-junction opening for the transport of an anti-angiogenic sulfated polysaccharide across Caco-2 cell monolayers.* Acta Biomater, 2013. **9**(7): p. 7449-59.

20. Dupont, J. and D. Le Roith, *Insulin-like growth factor 1 and oestradiol promote cell proliferation of MCF-7 breast cancer cells: new insights into their synergistic effects.* Molecular pathology : MP, 2001. **54**(3): p. 149-154.
21. Chacon, E., D. Acosta, and J.J. Lemasters, *9 - Primary Cultures of Cardiac Myocytes as In Vitro Models for Pharmacological and Toxicological Assessments*, in *In Vitro Methods in Pharmaceutical Research*, J.V. Castell and M.J. Gómez-Lechón, Editors. 1997, Academic Press: San Diego. p. 209-223.
22. Deeds, M.C., et al., *Single dose streptozotocin-induced diabetes: considerations for study design in islet transplantation models.* Laboratory animals, 2011. **45**(3): p. 131-140.
23. Greenfield, N.J., *Using circular dichroism spectra to estimate protein secondary structure.* Nat Protoc, 2006. **1**(6): p. 2876-90.
24. Lee, S., et al., *Synthesis and biological properties of insulin-deoxycholic acid chemical conjugates.* Bioconjug Chem, 2005. **16**(3): p. 615-20.

CHAPTER 4

Poly-l-lysine coated oral nano-emulsion for combined delivery of insulin and c-peptide

4.1 INTRODUCTION

From discovery, proteins and peptides have been administered invasively via parenteral routes such as intra venous, sub cutaneous, and intra muscular depot which render their pleasant use in chronic disease conditions. Though oral route is the utmost preferred and patient compliant, oral delivery of labile proteins and peptides remains perplexing due to opponent physiology of gastro-intestinal tract such as acidic pH, destructive enzymes and absorption barriers [1]. Therefore, attempts are made to address the issues in most rational way so that labile macromolecule can be saved from all the physiological barriers and delivered at required site in biologically active form.

In the case of diabetes type I, wherein insulin secretion is dampened due to loss of beta cells, delivery of external recombinant insulin becomes mandatory to keep blood glucose level in normal range [2]. While, in diabetes type II the early treatment with mono or combinative oral hypoglycemic agents (metformin, pioglitazone, glimepride) transition into insulin injection as the disease progresses [3]. Thus, either in diabetes type I or II at certain stage, delivery of external recombinant insulin is inevitable [4]. However, just mere control of blood glucose level by insulin administration is not sufficient in patient with diabetic complications. Major proportion of diabetes lead illness and death are due to the complications with vascularization (micro and micro) regardless of the type of diabetes [5]. Generally, the detrimental effects of high blood glucose are classified into macro-vascular diseases (coronary artery disorder, peripheral arterial disease, and stroke) and micro-vascular complications (diabetic nephropathy, neuropathy, and retinopathy). Yet now there is no such drug available in the market that can manage the earlier mentioned complications. Recent studies have reported physiological role and beneficial properties of c-peptide which was earlier considered as byproduct of insulin biosynthesis [6, 7]. According to the meta-analysis, external recombinant insulin therapy lacks c-peptide maintenance in body and hence it's beneficial physiological effects which play pivotal role in managing the diabetic complications. [8, 9] C-peptide exerts its action through G-protein coupled receptors to activate calcium channel and increases Na^+-K^+-ATPase activity, which is usually found decreased in the patients having advanced micro-vascular complications (nephropathy and retinopathy) of diabetes [10]. Moreover, c-peptide enhances actions of eNOS (endothelial nitric oxide synthase). Study done by Wahren, Ekberg [11] et al, reports that c-peptide administration in type I diabetes patients, who lacks

natural c-peptide, promoted blood flow to skeletal muscle and skin, diminished glomerular hyper-filtration, dampened urinary albumin excretion, and improved nerve function without any such effects in healthy subjects. Several clinical studies have been done by Johansson et al. evaluating short term replacement of c-peptide in type I diabetes patients. They inspected low dose c -peptide infusion for renal function and glucose uptake (in whole body) with comparison to sodium chloride infusion and found that c-peptide increased whole body glucose utilization by 25 percent while decreased glomerular hyper-filtration by 6 percent [12]. In a follow up study they knew that one month administration of c-peptide decreased HbA1C level in type I diabetics by 9 to 16 percent versus control suggesting improved glycemic control. They also reported 55 percent decrease in albuminuria after 4 weeks indicating its potential to ameliorate diabetic nephropathy [13]. A randomized double-blind trial with placebo control was executed by Ekberg et al, and found that three month therapy of c-peptide, in type I diabetic patients with neuropathy, improved sensory nerve conduction and vibration perception illustrating its indication in diabetic neuropathy [14]. Diabetics are vulnerable to heart disorders and usually have diastolic dysfunction and myocardial perfusion abnormalities. A randomized double-blind crossover study was done by Hansen et al. in which they compared the effect of c-peptide infusion with saline infusion for myocardial dysfunction in type I diabetics. They found that during c-peptide administration the diastolic velocities and myocardial blood flow of the diabetics was increased to the levels observed in the healthy controls showing myocardial benefits [15]. Therefore, combined delivery of insulin and c-peptide has been envisaged with a view to provide tight glycemic control without any diabetic complications. Now, to deliver the protein insulin and c-peptide by oral route of administration, help of adroit nano-formulation was taken. Many nano systems such as polymeric nanoparticles [16, 17], liposomes [18], nanoparticles[16], solid lipid nanoparticles [19] etc., have been heavily scrutinized and found suitable for prompt delivery of proteins/peptides like macromolecules through oral route, however, none of them have attained commercial success till date. Nano-emulsions provide promising avenue for the said purpose of conveying proteins/peptides in therapeutic form via GIT [20]. Oral w/o/w nano-emulsion has been architected to shelter hydrophilic insulin and c-peptide in internal aqueous droplets housed inside oil droplet - dispersed in external aqueous phase. The hydrophobic boundary created by oil will provide controlled release to the hydrophilic insulin and c-peptide house in the aqueous core. Poly-arginine has been exploited as coating material for

oral insulin delivery via oleic acid nano-emulsion [21]. To protect the labile insulin and c-peptide from hostile acidic condition oil globules were coated with positively charged poly-l-lysine [22] in addition to the surfactant layer of pluronic F 127 at the interface. The mechanistic sketch of proposed formulation is shown in figure 4.1.

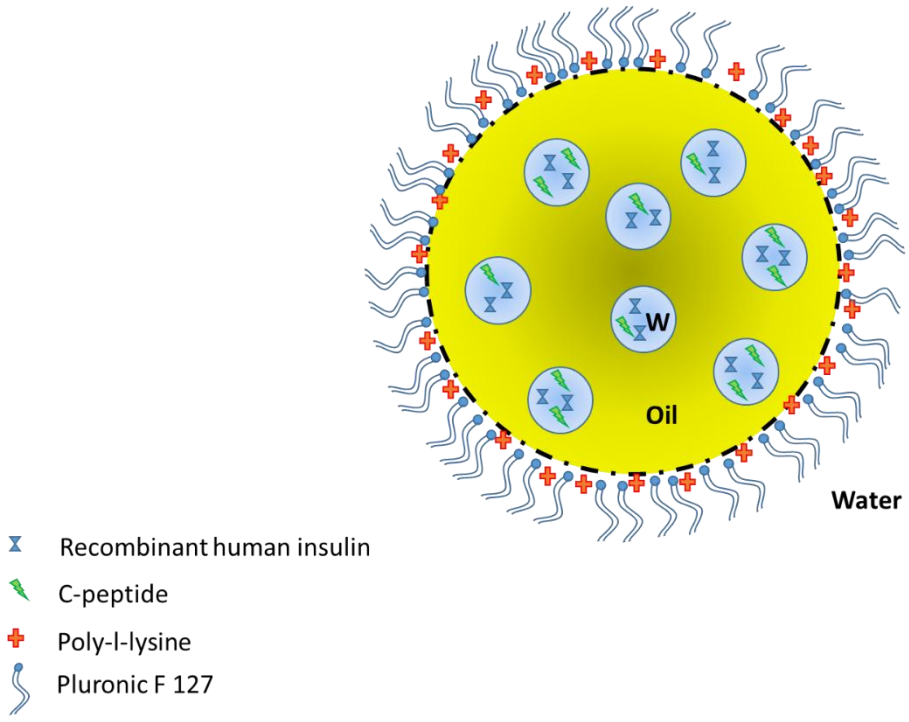

Figure 4.1 Mechanistic sketch of poly-l-lysine coated w/o/w nano-emulsion.

Herein, the architected poly-l-lysine coated nano-emulsion will protect and release proteins in a controlled manner at intestinal membrane due to adhesive property of poly-l-lysine to cell membrane [23].

4.2 MATERIALS AND METHODS

4.2.1 Materials

4.2.2 Method of preparation of nano-emulsion

To incorporate hydrophilic protein and peptide moieties like insulin and c-peptide, w/o/w nano-emulsion was envisaged and manufactured by double emulsification method as illustrated in figure 4.2. Briefly, calculated quantities of insulin and c-peptide were dispersed in nuclease free triple distilled water (pH 7.0) and the dispersion was added drop

wise in to organic phase (containing oil such as sesame, linseed, palm or olive oil and mixture of surfactant and co-surfactant) under ultra-sonication at 20% amplitude to get the primary (w/o) nano-emulsion. Herein, the aqueous dispersion of insulin and c-peptide was advertently made rather than its solution as we intended to keep both the peptide with its physiological molecular state and surface charge at neutral pH 7.0 in housed in internal aqueous droplet of w/o/w nano-emulsion [24, 25]. Thereafter, prepared primary nano-emulsion was poured drop wise in aqueous phase containing pluronic F 127 with stirring at 800 rpm for 30 minutes. For preparation of coated nano-emulsions, poly-l-lysine (0.01% v/v) solution was added in to the aqueous phase containing pluronic F 127 in the ratio 1:10. Finally, the w/o/w nano-emulsions were obtained and characterized for different physico-chemical parameters. Formulations were made in triplicate.

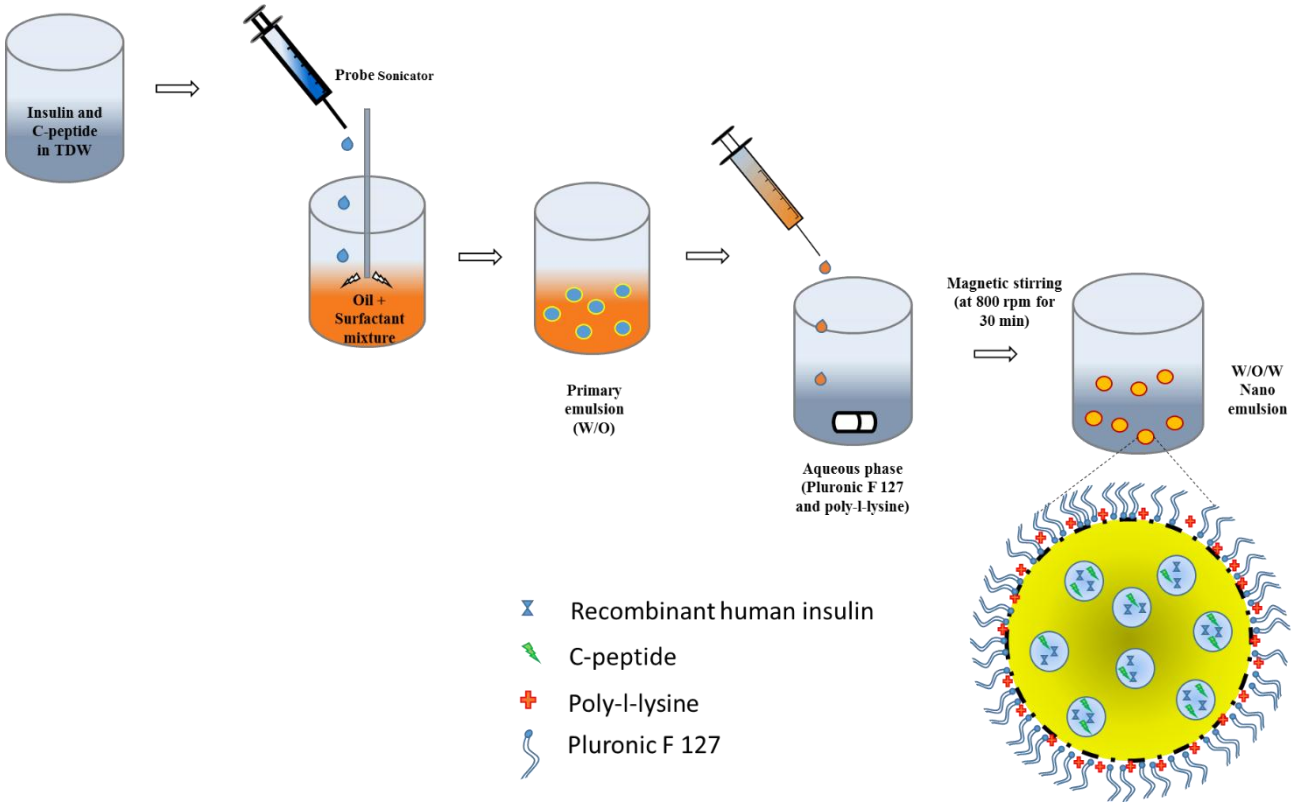

Figure 4.2 Schematic diagram illustrating preparation of poly-l-lysine coated nano-emulsion containing insulin and c-peptide.

4.2.3 Method for Selection of the formulation components

4.2.3.1 Selection of oil

Selection of the oil was prime concern while formulating oral nano-emulsion bearing labile protein insulin and c-peptide. Therefore, instead of selecting an inert oil that just provide oil droplet with hydrophobic boundaries to contain hydrophilic peptide molecules inside, biologically active purified natural oils were chosen. Four oils having either anti-diabetic effect and/or helpful to reduce diabetic complication were screened from the array of naturally occurring resources. After this primary screening four oils such as olive oil, sesame oil, palm oil and linseed oil were found suitable due to their below mentioned specific and special properties.

A) Olive oil: It improves diabetic complications at enzymatic level by rehabilitating hepatic arylsulfatase B and hepatic catalase enzyme level due to its antioxidant activity [26].
B) Sesame oil: sesame oil contains lignans (sesamin, sesamol, episesamin, and sesamolin) responsible for its antioxidant and anti-diabetic properties. Moreover, it contains 43% and 40% of poly and mono unsaturated fatty acids, respectively, which reduces the cardiovascular risk in diabetic-hypertensive patients by lowering blood pressure and lipids [27].
C) Linseed oil: The major component of linseed oil, alpha linolenic acid increases the GLUT4 membrane receptor present on skeletal muscles and thereby enhance insulin sensitivity facilitating glucose uptake in skeletal muscle which in turn reduces the blood glucose level [28].
D) Palm oil: Study has reported its blood glucose lowering and cholesterol lowering effects in diabetic mice [29].

Nano-emulsions were made from all the above selected natural oils and the oil which showed compatibility with surfactant mixture as well as good stability was selected.

4.2.3.2 Selection of surfactant and co-surfactant

Suitable surfactant was selected from the range of surfactants with suitable hydrophilic lipophilic balance (labrafac, solutol, tween80, labrasol, migliol, cremophore EL, Gelucire 44/14) based on its miscibility and compatibility with co-surfactant and oil. Co-surfactant

was selected from the range of co-surfactants (propylene glycol, glycerine, transcutol p and vitamin E TPGS) based on their phase compatibility with surfactant and oil.

4.3 Optimization process

4.3.1 Optimization of nano-emulsion components

Several batches of formulation were prepared as part of preliminary studies to determine the effects of formulation and process variables on formulation characteristics.

4.3.1.1 Optimization of surfactant: co-surfactant ratio

Surfactant: cosurfactant ratios were manually set from the literature as 70:30, 50:50 and 30:70. Prepared nano-emulsions were evaluated on the scale of globule size, PDI and zeta potential (Malvern zetasizer nanoZS) for selection of optimum surfactant: co-surfactant ratio.

4.3.1.2 Optimization of oil: surfactant mixture ratio

Different batches of the nano-emulsions were formulated with 70:30, 50:50 and 30:70 ratios of oil to surfactant mixture and were assessed for the globule size, polydispersity index and zeta potential.

4.3.1.3 Optimization of aqueous surfactant

Different batches of nano-emulsions with 1%, 2% and 3% aqueous surfactant pluronic F 127 were prepared and the globule size, PDI and zeta potential were ascertained.

4.3.2 Optimization of process variables

4.3.2.1 Effect of sonication time

Various nano-emulsions were prepared by ultra-sonication at 20% amplitude (kept minimum to avoid any detrimental effects to labile protein and peptide). Sonication time was set at 2 min, 5 min, and 10 min for preparing primary w/o nano-emulsion. After obtaining final w/o/w nano-emulsion, formulations were evaluated for mean globule size, polydispersity index and zeta potential. Furthermore, insulin and c-peptide released from the formulations were evaluated for any break-down or structural/conformational change by MALDI-TOF and circular dichroism spectroscopy, respectively.

4.4 Characterization of formulations

4.4.1 Visual inspection

It was simply done by visually checking the nano-emulsions stored in glass bottles at room temperature without any centrifugation force. This study was conducted for 60 days. Formulations were prepared and 10 ml batches were taken in glass bottles. These glass bottles were kept at room temperature without any disturbance. The formulations were observed daily for phase separation and creaming, if any. The formulation was considered stable if no sign of phase parting or creaming during 60 days was observed. Formulations were prepared in triplicate

4.4.2 Physicochemical characterization

Mean globule size, polydispersity index and zeta potential of the prepared nano-emulsions were measured by the dynamic light scattering (DLS) method using Zetasizer Nano ZS (Malvern instruments). The analyses were performed with max 4mW He-Ne laser (633nm) at a scattering angle of 173˚ at 25˚C temperature. One drop of freshly prepared formulations were added into 1ml of triple distilled water and sample was put in to the suitable cuvette and analyzed. The measurements were reported in triplicate as a mean globule size ± SD.

4.4.3 Entrapment efficiency

Entrapment efficiency was measured by direct method. In 500 µl nano-emulsion, 100 µl triton X 100 solution was added and vortexed to break down the oil droplets. Then 1 ml chloroform was added and vortexed to solubilize oil part. After that, centrifugation at 5000 rpm for 10 min was done to apart aqueous and chloroform part. Aqueous portion was subjected to analysis by respective ELISA kit (Sigma-aldrich) for estimation of insulin and c-peptide. Protocols for ELISA were used accordingly.

4.4.4 *In vitro* drug release study

The release of the drug from the optimized Nano-emulsion formulation was inspected by dialysis sac method. 1 ml of poly-l-lysine coated optimized nano-emulsion formulation (LNE7) bearing insulin and c-peptide was filled in hermitically sealed sac of previously activated dialysis membrane (MWCO 12 KDa). Dialysis membrane sac was immersed in 50 ml of SGF pH 1.2 for initial two hours, followed by 6 hours in 50 ml of SIF pH 6.8 at

100 rpm and 37°C and then after in PBS pH 7.4 up to 24 hours. At different time points sample aliquots were removed and the same amount of fresh dissolution medium was supplemented for conservation of the sink condition. The samples were assayed for the quantification of insulin and c-peptide by enzyme immunoassay (EIA) method according to protocols of ELISA assay after suitable dilutions. The cumulative percentage release was plotted against time in hours to get the drug release profiles of insulin and c-peptide.

4.4.5 Transmission Electron Microscopy (TEM)

First of all, extra surfactant was detached by dialyzing optimized nano-emulsion formulation with the help of dialysis membrane (pore size: 100 KDa). Afterwards, formerly obtained sample solution was diluted and its thin film was made onto a 300-mesh copper grid. Now, the appropriately formed thin film was enclosed with a little quantity of 2% w/v uranyl acetate solution and surplus solution was drained. Sample was air dried followed by examination under transmission electron microscope (JEOL, JEM-2100, Japan) and photomicrographs were captured.

4.4.6 Protein confirmation and stability study

The proteins and peptides are highly vulnerable against heat, mechanical energy, sonication and organic solvents, therefore it becomes important to examine the impact of these factors on the insulin and c-peptide for any possible conformational changes during encapsulation process. For such evaluation, circular dichroism technique was utilized to confirm the secondary structure. Firstly, triton X 100 solution was added to the nano-emulsion for breaking down the oil droplets facilitating the release of insulin and c-peptide from the formulation. Secondly, the obtained solution was centrifuged in Nanosap® centrifugal device (MW cut off 10 KDa) to separate the released insulin and c-peptide. Thereafter the amount of insulin and c-peptide was calculated by EIA (enzyme immuno-sorbate assay) method and suitable dilutions were made in the range of 5-10 µmol/ml. A pure solution of insulin and c-peptide (5 µmol/ml) in PBS 7.4, were considered as standard solutions for comparison. Finally, samples were analysed by CD spectrophotometer (Jasco J-1500) and MALDI-TOF, and obtained spectrums were checked to identify any conformational or structural anomaly in insulin and c-peptide.

4.4.7 *In vitro* cell uptake study

To quantitate the cellular uptake of FITC (Fluorescein iso-thiocynate) loaded nano-emulsion in HCT116 and Caco-2 human intestinal cell lines, *In vitro* cell uptake study was performed by using flow cytometer (BD Fluorescence assisted cell sorting (FACS) Caliber, software – CellQuest Pro). HCT116 and Caco-2 cells were supplemented with DMEM (pH 7.4) complemented with 10% FBS and 1% penicillin-streptomycin (antimycotic-antibiotic solution). The HCT116 and Caco-2 cells were added in six well plate at density of 1 x 10^5 cells/well and kept overnight for adhesion and priming. Subsequently selected wells were incubated with DMEM media containing FITC control solution and FITC loaded Nano-emulsion formulations for 6 hours followed by repeated washing with PBS (pH 7.4) to remove free FITC and FITC loaded nano-emulsion. Cells were then trypsinized, pelleted, resuspended in PBS and analyzed for mean fluorescence intensity produced by internalized FITC loaded nano-emulsion in comparison to free FITC solution as control.

4.4.8 Trans Epithelial Electrical Resistance (TEER)

The tight epithelial junction at intestine work as barricade to insulin and c-peptide like macromolecules and hence block their absorption after oral administration. Therefore it is necessary to investigate whether the formulated nano-emulsions (uncoated and coated with poly-l-lysine) have ability of loosening the tight cellular junction of epithelial cells in intestine. Thereby, TEER of caco-2 cell monolayer and any changes in that by prepared formulations were assessed. The Caco-2 cells were seeded in 6 well Transwell ® filters (3.0µm pore size, 12 mm diameter, Corning Costar, USA) at a density of 5×10^4 cells per each well. For 21 days, fresh cell culture media was supplied and cells were allowed to form a monolayer. When the electrical resistance reached 350-400 Ω*cm^2 then formed monolayer was considered as optimum and it was measured by using Millicell ERS meter (Millipore, Milano, Italy) [30, 31]. A subsequent decrease in the value of (TEER) was observed every 30 minutes up to 2 hours after treatment with free insulin and c-peptide solution, insulin and c-peptide loaded uncoated nano-emulsion, and poly-l-lysine coated nano-emulsion bearing insulin and c-peptide (having equivalent concentration of insulin 100 µg/ml). Afterwards, the treatment solution was drained by washing with PBS pH 7.4, fresh culture media was added and recovery of the monolayer was calculated hourly up to

6 hours. Finally the relative percentage changes in TEER values were calculated and graph was plotted against time.

4.4.9 *In vitro* bio-activity of insulin

It is well reported that MCF-7 (Michigan Cancer Foundation-7) cells showcase overexpression of IGF-1 (insulin like growth factor) receptors on its surface [32]. Therefore, in the presence of insulin, MCF-7 cells proliferate rapidly on the basis of which this study was planned to estimate the activity of insulin *in vitro*. Briefly, MCF-7 cell line was obtained from institutional cell repository and cultured in RPMI 1640 medium supplemented with 10% FBS, 1% L- glutamine per liter, 100 unit/ml penicillin and 100 µg/ml streptomycin at 37°C in humidified atmosphere of 5 % (v/v) CO2 per air mixture. The gold standard MTT cell viability assay was exercised for investigating *in vitro* bio-activity of insulin. Herein, MCF-7 cells (5 x 10^3 cells/well) were seeded in 96-well plate and kept for 12 hours in BOD incubator for refurbishment of metabolic activity. Thereafter, cells were treated with pure insulin, blank uncoated LNE (ULNE), blank PLL coated LNE (CLNE), insulin and c-peptide bearing INS-ULNE and INS-CLNE dispersed in culture medium equivalent to different concentrations (0.5, 1, 2, 3, 4, 5 µg/ml) of pure insulin. Used culture media was aspirated off from the wells and fresh media was added after 24 hours. 48 hours post-treatment, again the used media was aspirated off and fresh media containing MTT dye (0.5mg/ml) was added and incubated for 4 hours in dark. During this phase, mitochondrial succinate dehydrogenase enzyme plays its role and converts the yellow tetrazolium MTT i.e. 3-[4,5-dimethylthiazole-2-yl]-2,5-diphenyltetrazolium bromide to MTT-formazan crystals (purple-blue colored) [33]. Thus, formazan crystals were only formed in the viable MCF-7 cells with metabolic activity which were then dissolved by adding 0.2 ml of DMSO to each well and gentle shaking for 2 minutes on 96-well plate shaker. Finally, the absorbance was analyzed at 570 nm using a multi-well scanning spectrophotometer (PowerWave XS, Biotek, VT, USA). Ultimately, proliferation level of MCF-7 under pure insulin, blank uncoated LNE (ULNE), blank PLL coated LNE (CLNE), insulin and c-peptide bearing INS-ULNE and INS-CLNE was calculated with comparison to control MCF-7 cells growing without any treatment. The experiment was performed thrice (n=3) to get valid results with minimal errors.

4.4.10 Stability study

Stability of developed LNE formulations was also the critical aspect to account for. Therefore, the stability profiles of the selected optimized formulations were obtained at room temperature (25±2 °C) as well as in cool temperature (4±2 °C) for three months. The samples were withdrawn at different time intervals i.e. 0, 30, 60, 90 days. Then samples were assessed for variation in mean globule size, PDI and zeta potential.

4.4.11 Animal experiments

6 – 8 weeks old male Sprague Dawley rats, weighing 180 – 200 grams, were received and handled as per the guidelines granted by IAEC, National Animal Laboratory Center, CSIR – Central Drug Research Institute, Lucknow, India.

4.4.11.1 Induction of diabetes

A well-established streptozotocin induced model for diabetes was considered appropriate and single moderate dose of 75 mg/kg of streptozotocin (dissolved in 10mM citrate buffer pH 4.5) was given intraperitonealy [34]. After one week of STZ treatment, the animal's fasting blood glucose level was measured daily and after attainment of > 300 mg/dl blood glucose level, rats were considered diabetic

4.4.11.2 Hypoglycemic activity, Plasma insulin level and Pharmacokinetics

In vivo study was designed in such way that main three attributes such as hypoglycemic activity, plasma insulin level and pharmacokinetics of the released insulin from optimized LNE formulations can be assessed in a single experiment and animal usage can be rationally minimized. Diabetic rats were kept on fasting for 6 hours and grouped according to their fasting blood glucose level and while taking care that each group had 5 rats with close proximity in their blood glucose level. Insulin and c-peptide containing nano-emulsion formulations, positive control and reference control were administered according to the information mentioned below:

Group I: Insulin solution in PBS pH 7.4 via sub cutaneous route at the dose of 2 IU/kg (Positive control)

Group II: Insulin solution in PBS pH 7.4 via oral route at the dose of 10 IU/kg (reference control)

Group III: Insulin and c-peptide bearing uncoated LNE7 (ULNE7) via oral route at the dose of 10 IU/kg

Group IV: Insulin and c-peptide bearing PLL coated LNE7 (CLNE7) via oral route at the dose of 10 IU/kg

At specified time points i.e. 0, 0.25, 0.5, 1, 2, 4, 8, 12 hours blood samples were withdrawn via tail vein puncture. During the blood withdrawal, a single drop of blood sample was placed on glucometer strip pre-inserted in the glucometer (AccuCheck) and blood glucose level was noted from the reading. The blood samples were collected in micro centrifuge tubes pre-coated with EDTA solution (anti-coagulating agent). Then the blood samples were centrifuged at 3000 rpm for 3 minutes to separate plasma and kept at -20°C. Moreover, the samples were analyzed by insulin Elisa kit (Sigma Aldrich) and c-peptide EIA kit according to the manufacturer's protocols. The data obtained from above analyses was calculated using WinNonlin 6.0 (Pharsight Co., Mountain View, CA, USA) software. For calculating relative oral bioavailability of insulin as compared to SC insulin, below mentioned equation was used:

$$\boldsymbol{Relative\ Bioavailability} = \mathbf{100} * \frac{\boldsymbol{AUC}\ (\boldsymbol{Oral})\boldsymbol{x}\ \boldsymbol{Dose}\ (\boldsymbol{SC})}{\boldsymbol{AUC}\ (\boldsymbol{SC})\boldsymbol{x}\ \boldsymbol{Dose}\ (\boldsymbol{Oral})}$$

4.4.12 Statistical Analysis

The statistical analysis between the groups was done by applying one-way analysis of variance (ANOVA) test followed by Bonferroni's multiple comparison post-hoc analysis. GraphPad Prism 5 software (Graph Pad Software Inc., CA, USA) was used to perform all the statistical tasks. Statistically significant difference was considered if p value was less than 0.05 at 95% confidential interval. All the experiments were executed thrice with three independent samples (n=3). *In vitro* data are signified as Mean ± SD whereas *in vivo* data are signified as Mean ± SEM (standard error of means).

4.5 RESULTS AND DISCUSSION

4.5.1 Selection of nano-emulsion components

From preliminary studies, it was observed that linseed oil NE is more stable by visual inspection with comparatively better characteristics in terms of globule size, PDI and zeta potential value (table 4.1). Based on the compatibility and miscibility (visible clarity after mixing) study surfactant labrasol with co-surfactant vitamin E TPGS was found to be most suitable surfactant mixture **(**table 4.2). For external aqueous phase pluronic F 127 was chosen.

Table 4.1 Selection of oil for nano-emulsion preparation by using surfactant (labrasol): co-surfactant (vitamin E TPGS) in ratio of 50:50 and 1% pluronic F 127 solution

Batch code	**Oil**	**Surfactant**	**Co-surfactant**	**Surfactant: co-surfactant ratio**	**Oil: Smix ratio**	**Mean globule size (nm) Mean ± S.D**	**PDI Mean ± S.D**	**Zeta potential (mv) Mean ± S.D**	**Stability (After 30 days)**
1.	palm oil	Labrasol	Vitamin E TPGS	50:50	50:50	524.35 ± 45.9	0.658 ± 0.110	-4.7 ± 5.6	Creaming
2.	Olive oil	labrasol	Vitamin E TPGS	50:50	50:50	645.6 ± 80.3	0.426 ± 0.097	-9.56 ± 3.9	Phase separation
3.	Sesame oil	labrasol	Vitamin E TPGS	50:50	50:50	326.8 ± 26.7	0.321 ± 0.054	-12.68 ± 3.55	Phase separation
4.	Linseed oil	labrasol	Vitamin E TPGS	50:50	50:50	259.6 ± 18.4	0.220 ± 0.023	-19.3 ± 7.6	Stable

*Formulations were made in triplicate (n=3)

Table 4.2 Surfactant and co-surfactant compatibility

SURFACTANT	**CO- SURFACTANT**	**OBSERVATION (at 25 °C)**
Cremophor EL	Transcutol P	Turbid
Tween 80	Glycerin	Phase separation
Solutol	Propylene glycol	Insoluble
Gelucire 44/14	Vitamin E TPGS	Turbid
Labrasol	**Vitamin E TPGS**	**Soluble**

4.5.2 Optimization and effect of different parameters

4.5.2.1 Effect of oil: surfactant mixture ratio

To check the effect of oil: surfactant mixture ration on mean globule size, PDI and zeta potential, surfactant to co-surfactant (labrasol and vitamin E TPGS:: 50:50) ratio was kept constant and oil: surfactant mixture ratio was varied from 30:70, 50:50 and 70:30. From the table 4.3, it can be concluded that as the percentage of oil increase in Smix ratio, large globule size with high PDI and increased zeta potential and vice versa was observed. Herein, oil: surfactant mixture ratio of 70:30 was considered optimum which provided approximately 200 nm globule size, fair enough PDI and zeta potential with minimum use of surfactants.

Table 4.3 Effect of oil: surfactant mixture ratio on globule size, PDI and zeta potential

Batch code	**Oil**	**Surfactant**	**Co-surfactant**	**Surfactant: co-surfactant ratio**	**Oil: Smix ratio**	**Mean globule size (nm) Mean ± S.D**	**PDI Mean ± S.D**	**Zeta potential (mv) Mean ± S.D**
LNE1	Linseed oil	labrasol	Vitamin E TPGS	50:50	30:70	84.5 ± 15.6	0.158 ± 0.08	-11.7 ± 3.6
LNE2	Linseed oil	labrasol	Vitamin E TPGS	50:50	50:50	145.7 ± 23.3	0.267 ± 0.12	-15.56 ± 2.9
LNE3	Linseed oil	labrasol	Vitamin E TPGS	50:50	70:30	230.2± 16.7	0.208 ± 0.035	-18.5 ± 6.55

*Formulations were made in triplicate (n=3)

4.5.2.2 Optimization of surfactant: co-surfactant ratio

Surfactant to co-surfactant ratios were optimized while keeping the optimum oil: surfactant ratio fixed at 70: 30 according to table 3. Three ratios of surfactant to co-surfactant 30: 70, 50:50, and 70:30 were used to formulate the nano-emulsion and evaluate its effect on mean globule size, PDI and zeta potential. When surfactant (labrasol) to co-surfactant (vitamin E TPGS) ratio 30: 70 was used to formulate the nano-emulsion, comparative larger globule size and high PDI were observed which may be due to low percentage of surfactant and high percentage of co-surfactant in the surfactant mixture. However, zeta potential was more on negative side which may be attributed to succinate terminal moieties of vitamin E TPGS. Therefore it may provide better storage stability. As the percentage of labrasol

surfactant is increasing in the surfactant mixture ratio globule size are getting smaller and zeta potential is decreasing as visible from table 4.4.

Table 4.4 Effect of surfactant: co-surfactant ratio on globule size, PDI and zeta potential

Batch code	**Oil**	**Surfactant**	**Co-surfactant**	**Surfactant: co-surfactant ratio**	**Oil: Smix ratio**	**Mean globule size (nm) Mean ± S.D**	**PDI Mean ± S.D**	**Zeta potential (mv) Mean ± S.D**
LNE4	Linseed oil	labrasol	Vitamin E TPGS	30:70	70: 30	423.5 ± 46.6	0.225 ± 0.056	-22.7 ± 9.6
LNE5	Linseed oil	labrasol	Vitamin E TPGS	50:50	70: 30	324.7±19.8	0.187 ± 0.01	-16.56 ± 4.9
LNE6	Linseed oil	labrasol	Vitamin E TPGS	70:30	70: 30	187.1± 12.2	0.133 ± 0.014	-15.8 ± 5.46

*Formulations were made in triplicate (n=3)

4.5.2.3 Optimization of aqueous surfactant

The aqueous non-ionic surfactant pluronic F 127 (tri-block co-polymer) was chosen due to its structural property providing centric hydrophobic block of PPG bordered by two hydrophilic blocks of PEG. Herein, it is envisaged that hydrophobic block of polypropylene glycol will remain towards lipophilic oil droplet and the hydrophilic blocks remain in aqueous phase. This arrangement provides stealthy layer to protect the peptide housed oil droplets against hostile acidic condition. Three concentrations; 1%, 2% and 3% w/v were tried to manufacture the nano-emulsions. As a representative formulation, globule size, PDI and zeta potential data of linseed oil nano-emulsion made with oil: surfactant mixture ratio 70:30 (optimized as discussed above) and surfactant: co-surfactant ratio 70:30 (optimized as discussed above) is shown in table 4.5. 1% w/v concentration of pluronic F 127 was found efficient enough to result the desired formulation with globule size near around 200 nm and good PDI of 0.145 ± 0.033 and zeta potential of -21.7 ± 4.5. Therefore, LNE7 was considered optimized formulation to be reproduced as poly-l-lysine coated nano-emulsion as described in the method of preparation. This formulation was employed for further characterization and *in vitro* evaluation.

Table 4.5 Effect of pluronic F127 concentrations on globule size, PDI and zeta potential

Batch code	Oil	Surfactant	Co-surfactant	Surfactant : co-surfactant ratio	Oil: Smix ratio	Pluronic F 127 conc. (% w/v)	Mean globule size (nm) Mean ± S.D	PDI Mean ± S.D	Zeta potential (mv) Mean ± S.D
LNE7	Linseed oil	labrasol	Vitamin E TPGS	70: 30	70: 30	1%	210.6±9.87	0.145 ± 0.033	-21.7 ± 4.5
LNE8	Linseed oil	labrasol	Vitamin E TPGS	70: 30	70: 30	2%	125.7±12.3	0.097 ± 0.040	-17.5 ± 7.23
LNE9	Linseed oil	labrasol	Vitamin E TPGS	70: 30	70: 30	3%	84.5± 16.9	0.103 ± 0.058	-18.8 ± 3.33

*Formulations were made in triplicate

4.5.2.4 Effect of poly-l-lysine coating and its confirmation

For the optimized formulation, batches were re-manufactured with involvement of poly-l-lysine solution (0.01%) as coating material mixed in aqueous phase containing 1% pluronic F 127, used in last step of process. After coating by positively charged poly-l-lysine, negatively charged linseed oil nano-emulsion faced charge reversal phenomena as visible from figure 4.3. The globule size was also somewhat increased without significant change in PDI value.

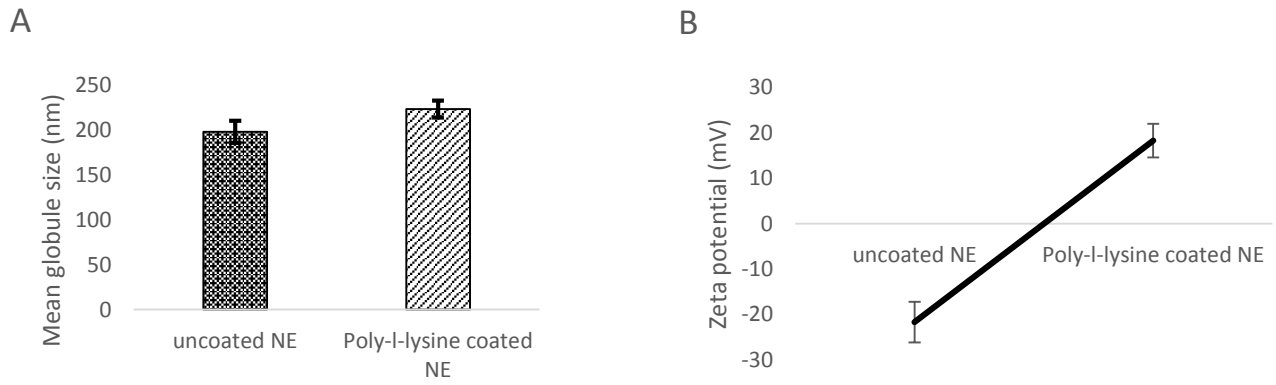

Figure 4.3 Effect of poly-l-lysine coating on (A) mean globule size and (B) zeta potential of linseed oil nano-emulsion (LNE7).

4.5.2.5 Optimization of sonication time: Effects on confirmation and structural integrity of insulin and c-peptide

To protect the labile proteins and peptide, formulation scientist always have to think about energy exposure during manufacturing process. Herein, ultra-sonication at lowest amplitude (20%) with pulse mode (5 sec on/ 5 sec off) process was selected for fabrication of primary w/o emulsion to avoid any chances of damage to insulin and c-peptide by intense sonication energy. Therefore, it was of prime concern to evaluate confirmation and structural integrity of both peptides as a check-point to further manufacturing by magnetic stirring which is not that much detrimental comparatively. For this purpose, linseed oil nano-emulsions were made by deploying ultra-sonication energy for 2min, 5 min and 10 min during primary emulsion formation and the further process remained common. After preparation of nano-emulsion, insulin and c-peptide both were allowed to release in PBS 7.4 after breaking the oil droplets by triton X 100 and chloroform. The released insulin and c-peptide samples were checked for secondary structure confirmation stability and structural integrity by circular dichroism and MALDI-TOF, respectively.

Results have shown that 2 minute of sonication did not affect the secondary structure of insulin but beyond that after 5 or 10 minutes of sonication, some detrimental change might have been occurred (figure 4). The negative band at 208 nm basically arise from component of α helical structure while a band at 223 nm is due to β structure of insulin [35]. Here, it was found that released insulin from nano-emulsion made with 2 min ultra-sonication showed representative CD bands at 208 nm and 223 nm as identical to the bands of standard insulin which suggest that the released insulin was intact with proper secondary structure confirmation and folding. The ratio of Θ (mdeg) value at two wavelengths; 208 and 223 ($[\Theta]_{208}/[\Theta]_{223}$) is used as tool to know about the secondary structure retention of proteins [36]. Structural factor ($[\Theta]_{208}/[\Theta]_{223}$) was found 1.18 for insulin released after 2 min sonication which was almost near to 1.22 for standard insulin but with 5 min and 10 min sonication structural factor ratio was found 0.93 and 0.74 respectively, indicating structural change. MALDI-TOF spectra of standard insulin and released insulin from nano-emulsion made with different sonication time has been shown in figures 4.5 to 4.8. Data of MALDI-TOF and CD spectroscopy together suggest that 2 min sonication is safe compared to 5 or 10 min which may result in subtle confirmation change. However, in any case break down of insulin has not been observed from MALDI-TOF spectra.

C-peptide being linear peptide chain, no secondary structure attributes were noted in CD spectra but though c-peptide released from NE made with 2 min showed identical spectrum to that of standard c-peptide solution (figure 4.9). MALDI-TOF of c-peptide released from NE made with 10 min sonication was found identical to the standard spectra showing identical molecular weight 3615.8 and 3615.9, respectively, indicating no damage to the peptide (figure 4.10 and 4.11). Finally, 2 min of flash sonication at amplitude 20% with pulse mode (5 sec on/ 5 sec off) was considered as optimum sonication time and used while preparation of formulations.

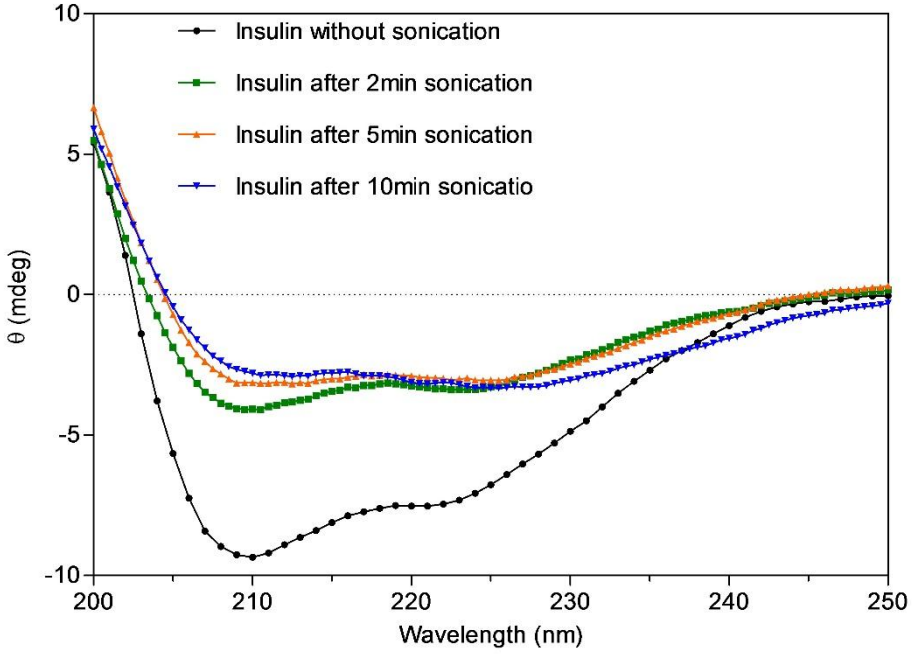

Figure 4.4 UV-CD spectra of standard insulin and insulin released from nano-emulsions made with 2 min, 5 min and 10 min of sonication.

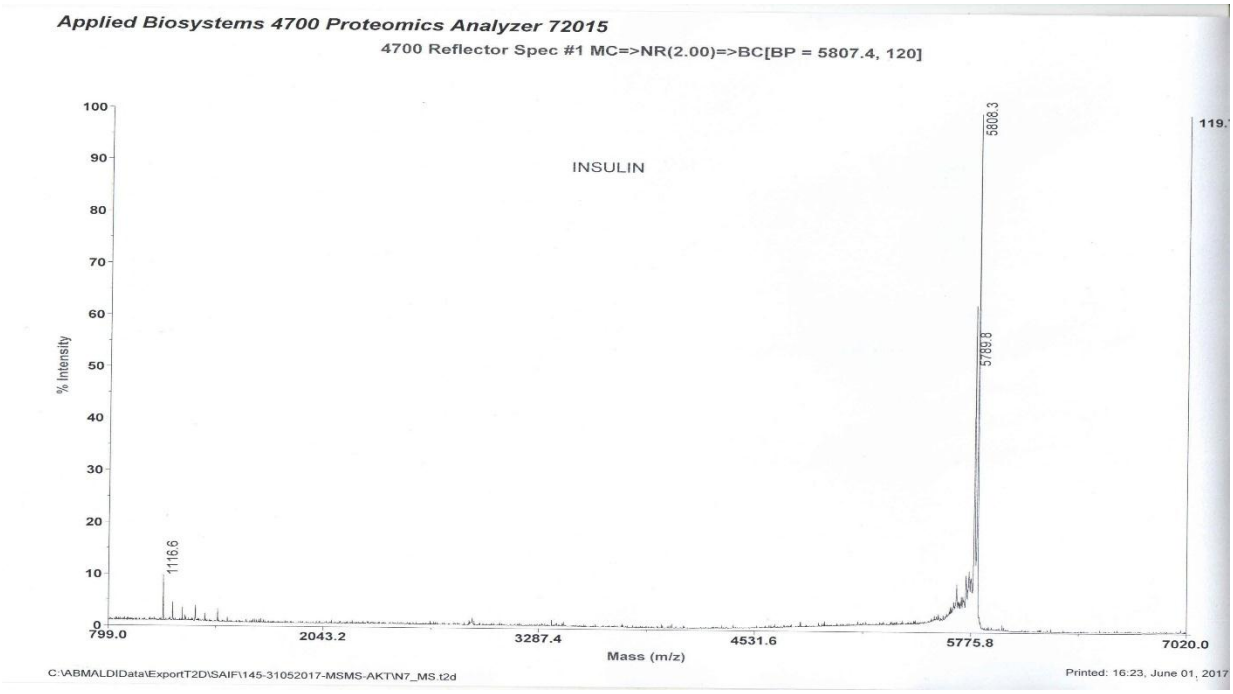

Figure 4.5 MALDI-TOF spectra of standard insulin with molecular weight showing 5808.3 Daltons

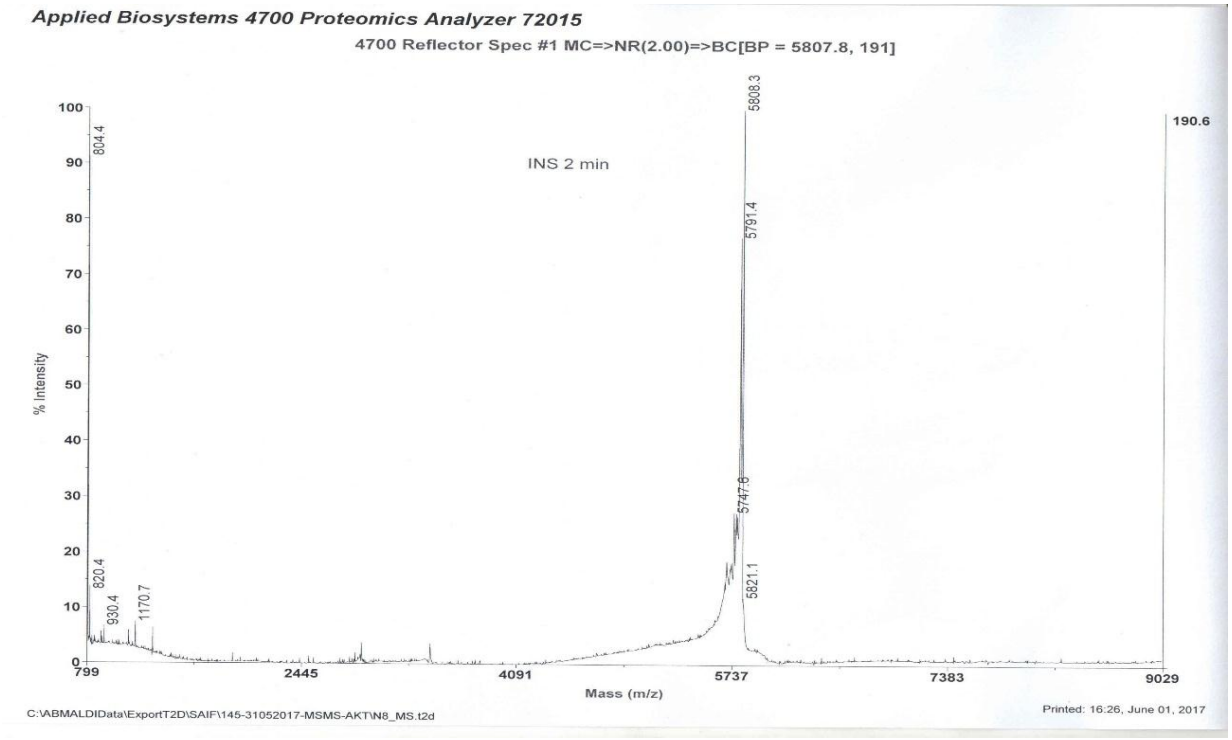

Figure 4.6 MALDI-TOF spectra of insulin released from NE made with 2 min ultra-sonication showing molecular weight 5808.3 Daltons

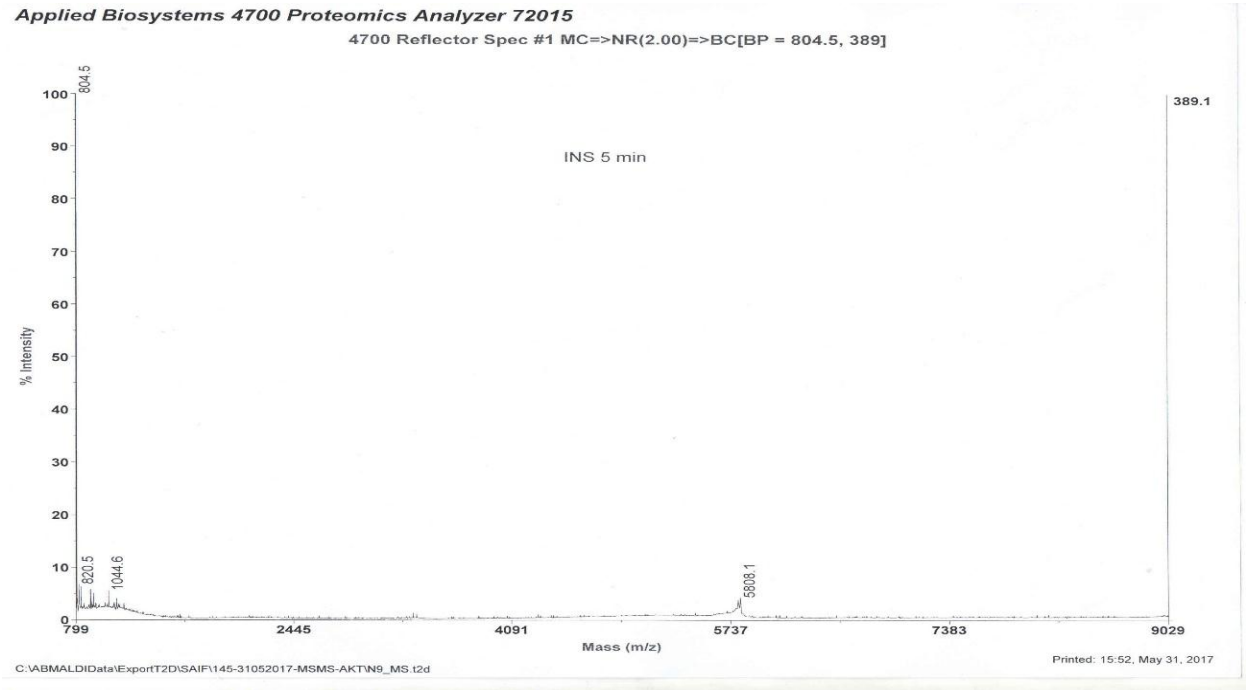

Figure 4.7 MALDI-TOF spectra of insulin released from NE made with 5 min ultra-sonication showing molecular weight 5808.1 Daltons

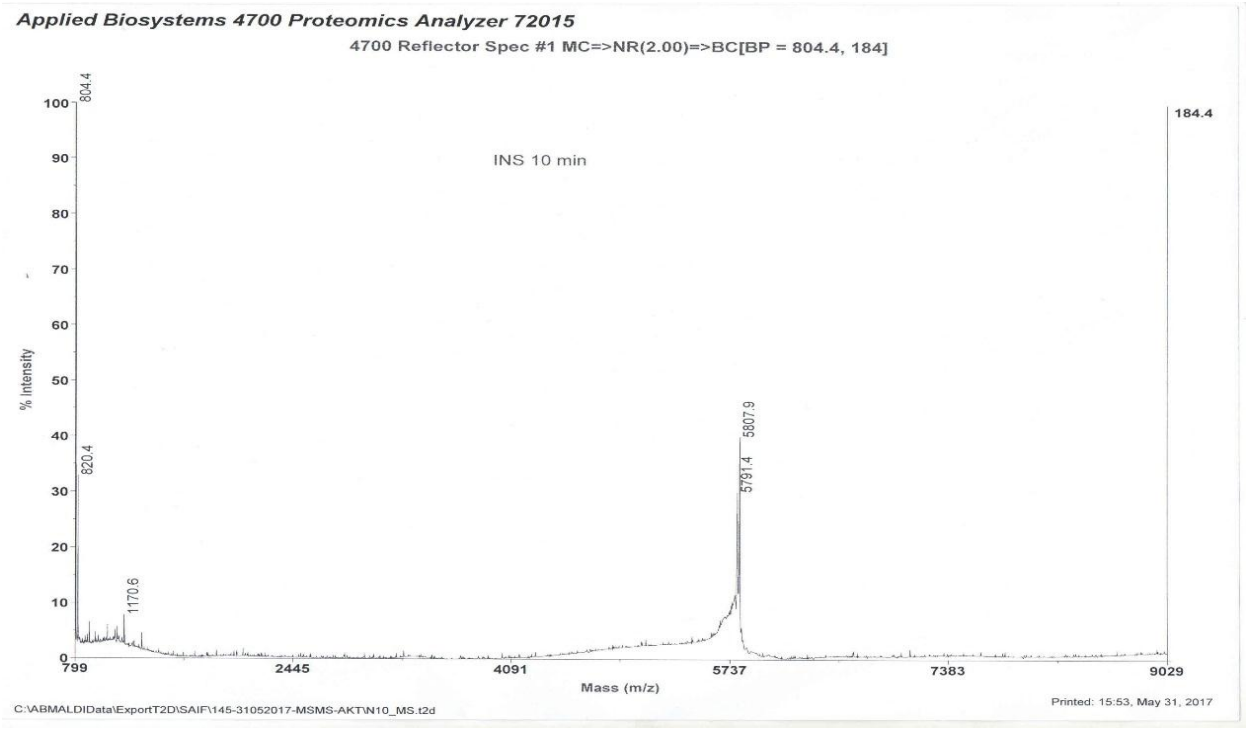

Figure 4.8 MALDI-TOF spectra of insulin released from NE made with 10 min ultra-sonication showing molecular weight 5807.9 Daltons

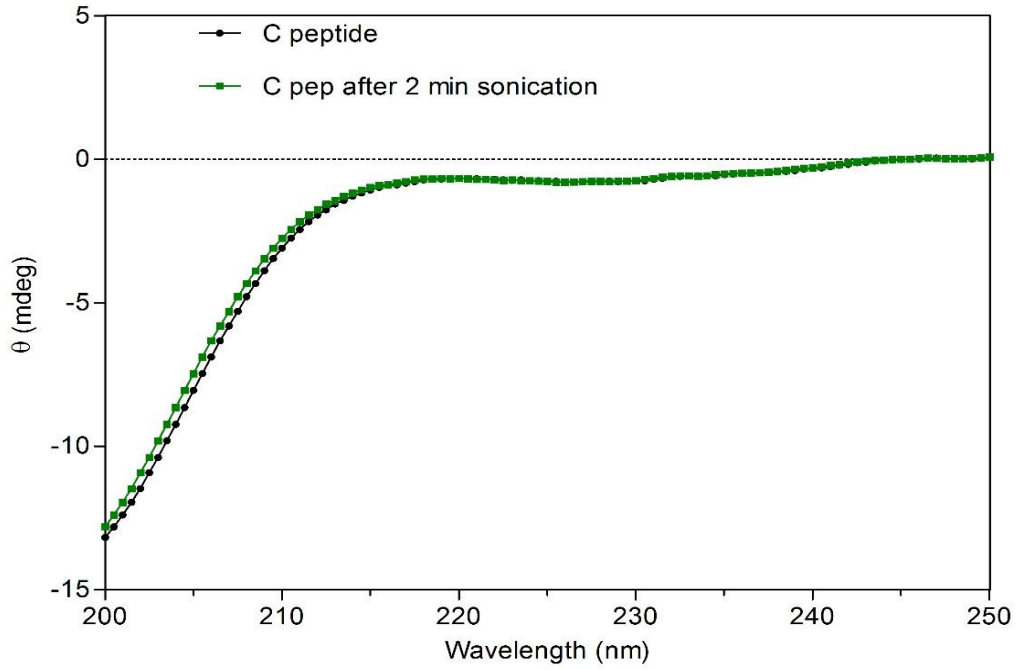

Figure 4.9 UV-CD spectra of standard c-peptide and c-peptide released from NE made with 2 min sonication.

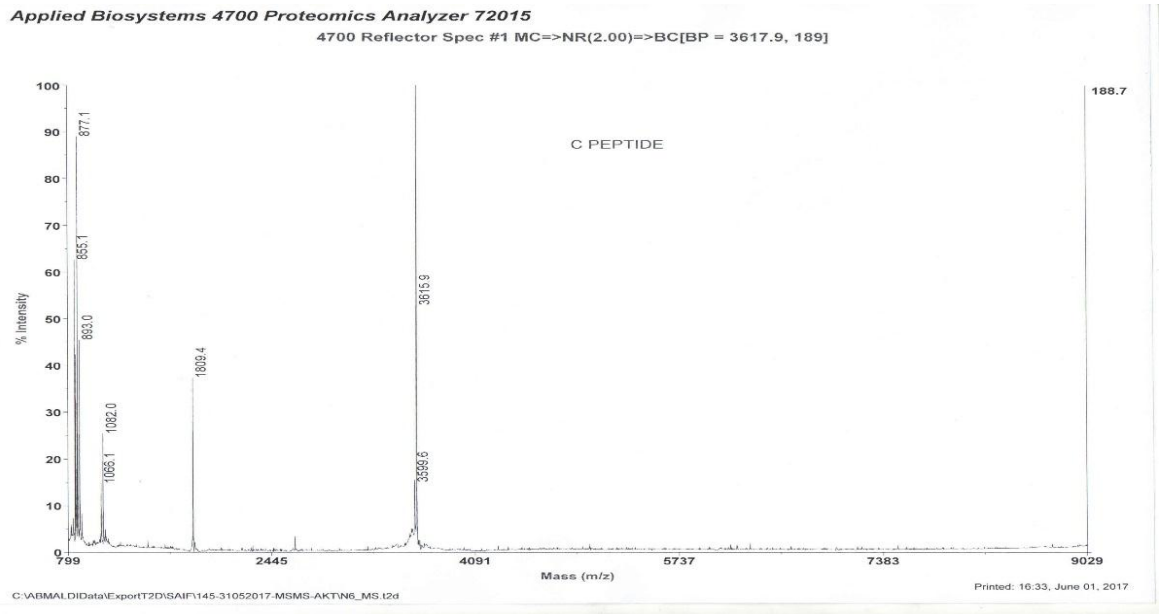

Figure 4.10 MALDI-TOF spectra of standard c-peptide showing molecular weight 3615.9 Daltons

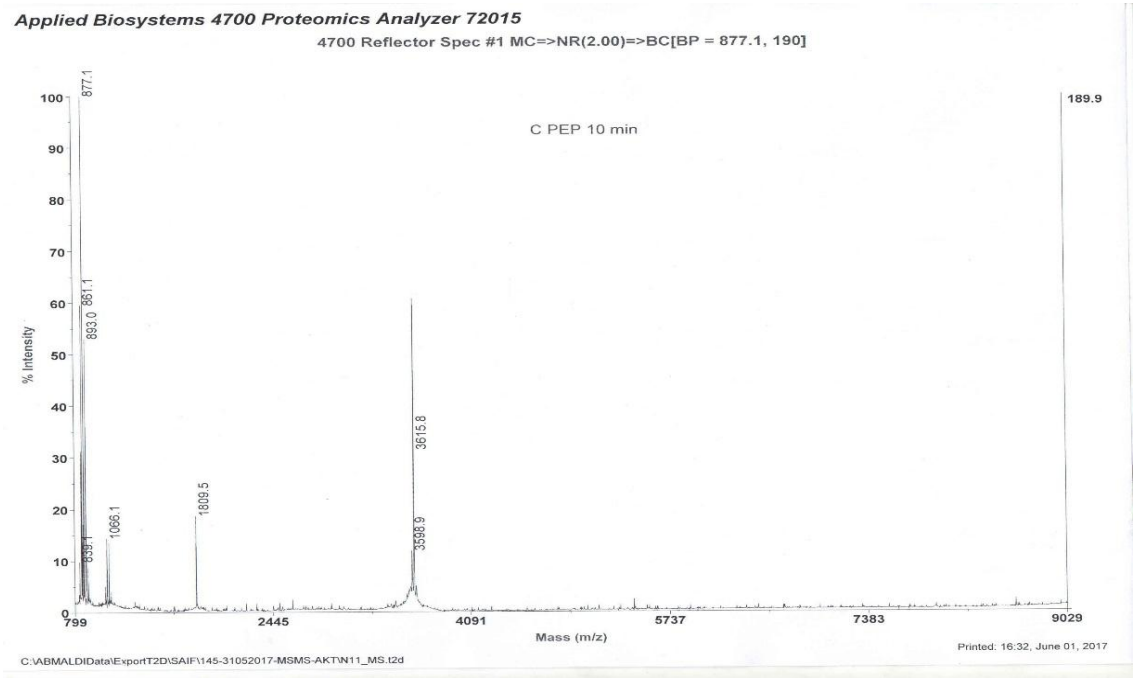

Figure 4.11 MALDI-TOF spectra of standard c-peptide released from NE made with 10 min ultra-sonication showing molecular weight 3615.8 Daltons

4.5.3 Characterization

4.5.3.1 Visual inspection

Amongst the nano-emulsions made from selected four oils, palm oil nano-emulsion showed creaming after 15 days, olive oil and sesame oil showed subtle phase separation after 30 days. Linseed oil nano-emulsion remained stable for 60 days without any phase separation or creaming phenomena. Photographic images are shown in figure 4.12.

Figure 4.12 Visual inspection of different nano-emulsion formulations.

4.5.3.2 Entrapment efficiency

Entrapment of proteins and peptide directly in oil part is difficult that is why w/o/w nano-emulsion was used wherein, hydrophilic insulin and c-peptide can reside in aqueous core. Entrapment of 64% to 87% insulin and 55% to 79% of c-peptide was attained for various batches as shown in figure 4.13. The optimized formulation LNE7 showed entrapment efficiency of 87.6 ± 7.48 % for insulin and 73.4 ± 6.44 % for c-peptide, respectively.

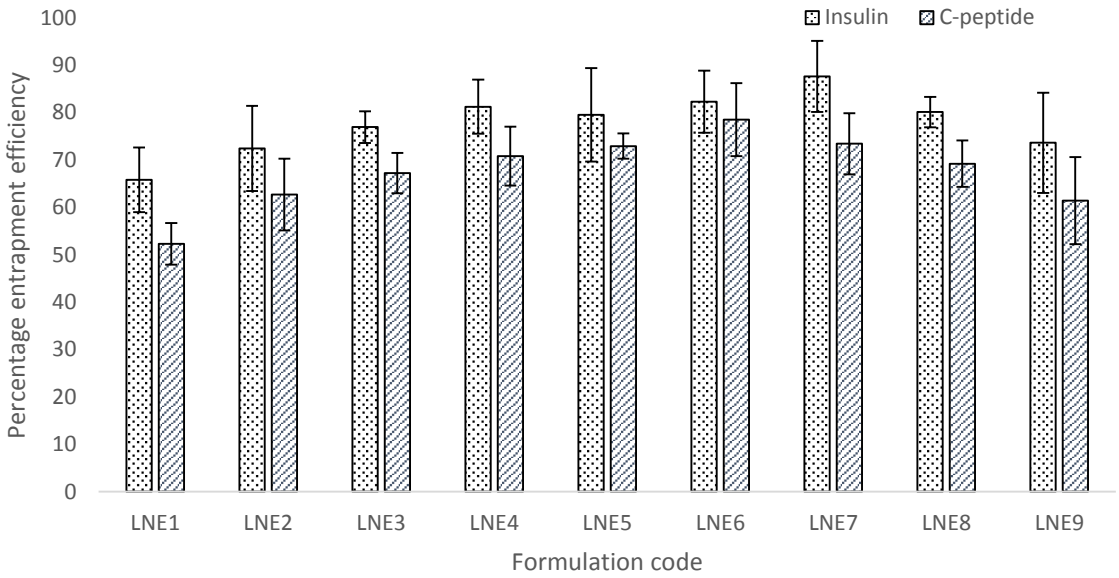

Figure 4.13 Entrapment efficiency of insulin and c-peptide in different batches of linseed oil nano-emulsion formulations.

4.5.3.3 *In vitro* drug release study

Optimized poly-l-lysine coated linseed oil nano-emulsion formulation (LNE7) was evaluated for *in vitro* drug release in SGF pH 1.2, SIF pH 6.8, and PBS pH 7.4 to mimic the physiological conditions. Formulation was filled in sac made up of dialysis membrane (MWCO 12KDa) and allowed to release the content in SGF pH 1.2 for initial 2 hours and then transferred to SIF pH 6.8; kept for 6 hours and then after kept in phosphate buffer saline pH 7.4 up to 24 hours. Samples were withdrawn at specified time points up to 24 hours. At each time point, 0.5ml sample was withdrawn and 0.5ml respective buffer was replenished to maintain the sink condition. Insulin and c-peptide were quantified by Enzyme Immuno Assay (EIA) performed by ELISA kit according to the standard protocols.

Drug release was not observed in SGF pH 1.2 for initial 2 hours which may be due to the layers made up of cationic poly-l-lysine and pluronic F 127 on oil droplets. Thereafter, initial burst of 15 to 20% release was observed in SIF pH 6.8 within 4 hour followed by controlled release up to 24 hours (Figure 4.14).

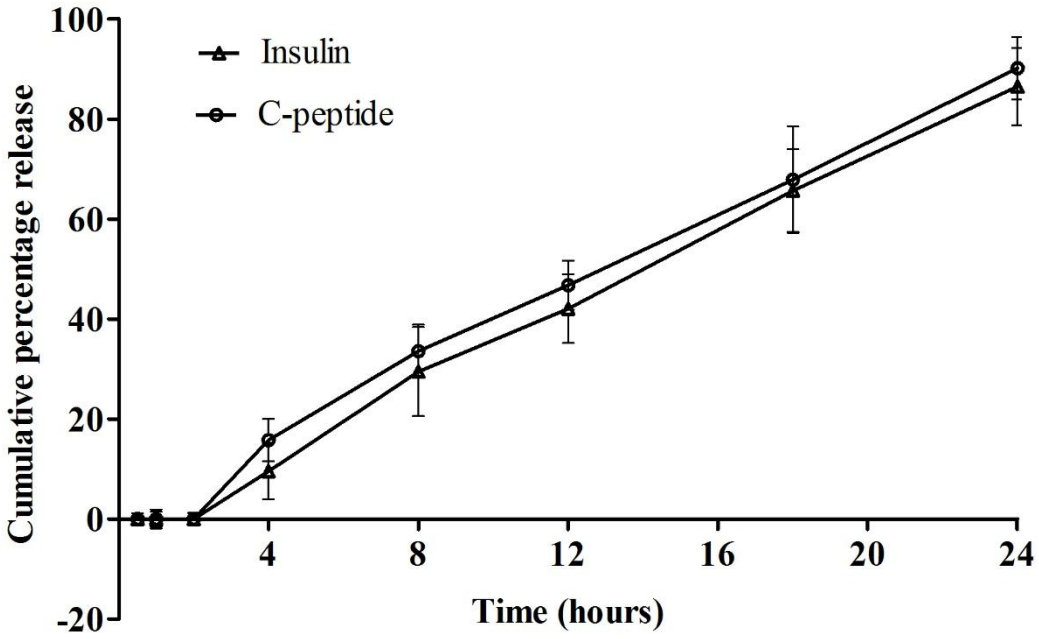

Figure 4.14 *In vitro* drug release profile of insulin and c-peptide from PLL coated LNE7 at pH 1.2 (in SGF for first 2 hours), pH 6.8 (in SIF for 6 hours) and pH 7.4 (in PBS up to 24 hours)

4.5.3.4 Transmission Electron Microscopy (TEM)

To see the morphology and structure characteristic of developed poly-l-lysine coated linseed oil nano-emulsion, high resolution TEM was used. The obtained microscopic image (figure 4.15) revealed that globules are almost spherical in shape, well dispersed with uniform distribution without coalescence, and have size of approximately 200 nm as in support with results of zetasizer. The quite visible peripheral different layer on oil globules may be due to poly-l-lysine coating.

(A) **(B)**

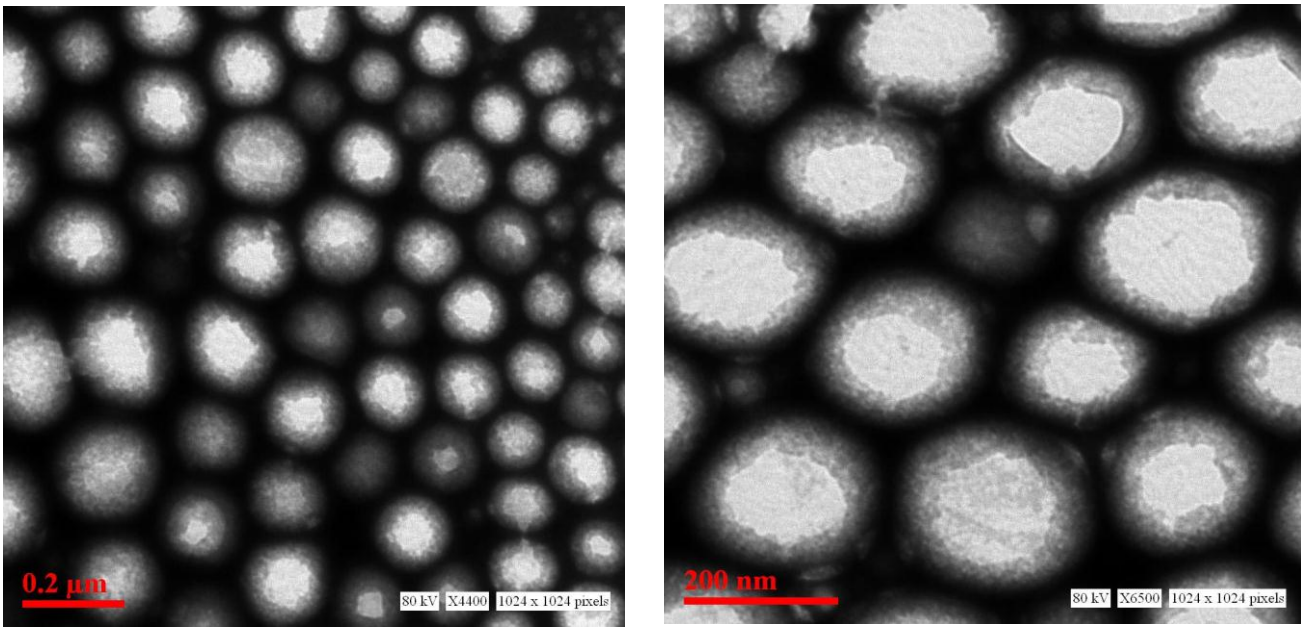

Figure 4.15 Transmission electron microscopic image of poly-l-lysine coated linseed oil nano-emulsion (A) TEM image with 4400x magnification showing uniform and poly-dispersed oil globules. (B) TEM image with 6500x magnification showing smooth surface with distinct layer of poly-l-lysine on periphery.

4.5.3.5 *In vitro* cell uptake study

To assess cell penetrating potential of formulated linseed oil nano-emulsion, quantitative cell uptake was measured by quantifying cell associated mean fluorescence intensity using flow cytometer. From the obtained results as shown in figure 4.16A, it was observed that cell uptake of uncoated FITC-LNE7 was 4.55 fold higher than FITC solution, which may be due to absorption enhancing property of labrasol and vitamin E TPGS [37]. While the poly-l-lysine coated FITC-LNE7 showed 8.28 fold higher uptake compared to FITC solution in HCT116 intestinal cell lines (figure 4.16B).

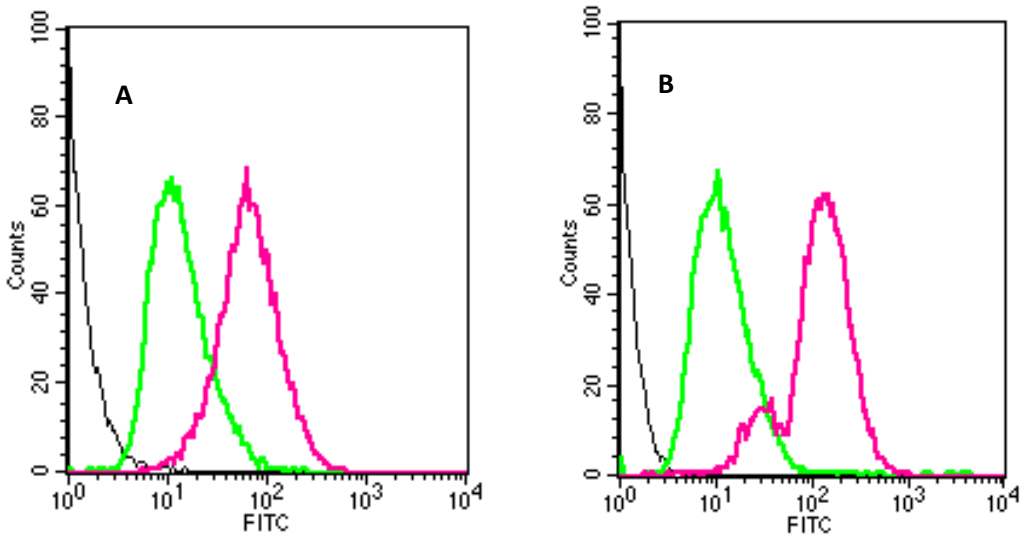

Figure 4.16 Histogram showing cell uptake of (A) uncoated FITC-LNE7 nano-emulsion and (B) ploy-l-lysine coated FITC-LNE7 nano-emulsion in HCT116 cells.

Note: [Black line denotes control untreated cells, green line denotes cells treated with FITC solution and pink line denotes cells treated with FITC loaded LNE7]

4.5.3.6 Trans Epithelial Electrical Resistance (TEER)

TEER due to tight junction restricts the para cellular transport of high molecular weight, hydrophilic bio-macromolecules like insulin and c-peptide. Therefore, this study was performed to check that if uncoated and poly-l-lysine coated linseed oil nano-emulsion have the property of opening the tight junction. Generally, caco-2 cell monolayer has a TEER value between 350-400 $\Omega*cm^2$ and when the tight junction opens up the resistance (TEER) value decreases. According to the obtained results as shown in figure 4.17, the free insulin and c-peptide solution didn't show any significant decrement in %TEER compared to zero time point but uncoated LNE7 showed sharp decrease up to 65 %TEER two hour post treatment which may be due to properties of labrasol, vitamin E TPGS and pluronic F127 surfactants. The highest decrement in % TEER was observed at 2 hours after treatment with poly-l-lysine coated LNE7 where the % TEER reached approximately 40% as shown in figure 4.17. Here, the cell adhesion properties of poly-l-lysine and positive charge formed by its layer on nano-emulsion may be responsible. Poly-l-lysine is reported also to have property of opening the tight epithelial junction [38]. Therefore, it can be concluded that the opening of tight junction will facilitate para cellular transport resulting

in enhanced bio availability of both peptide. After removal of treatment, at 6 hour time point recovery of TEER was observed up to 80 – 90 % TEER. The recovery in TEER value is important to note because it signifies the transient opening of tight junction and not the permanent damage. However, 100% recovery in TEER was not attained.

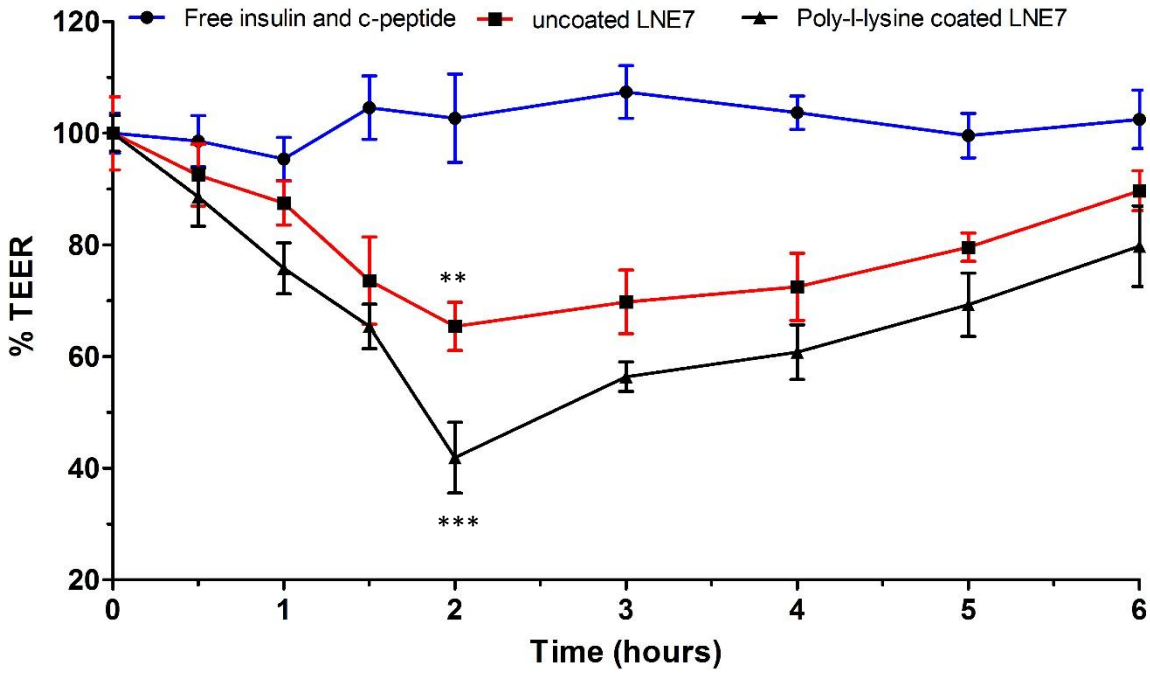

Figure 4.17 Change in percentage TEER of Caco-2 cell monolayer after treatment with free insulin and c-peptide solution, uncoated LNE7 and ploy-l-lysine coated LNE7. Results are represented as % TEER of the basal value at zero time point (t_0). (Mean ± S.D; n=6) ***p<0.0001 ; Free insulin and c-peptide vs Poly-l-lysine coated LNE7, **p<0.05 Free insulin and c-peptide vs uncoated LNE7

4.5.3.7 *In vitro* bio-activity

It can be concluded that the conformational stability and structural integrity of the insulin housed in nano-emulsion were remained intact as suggested by CD spectroscopic and MALDI-TOF results. However, the potential of formulation system regarding delivery of insulin and c-peptide like labile macromolecules in its therapeutically viable form was yet to be tested. As insulin act like growth factor physiologically, it can bind with IGF-1 receptors present on the cell membrane of MCF-7 cells and can show concentration

dependent proliferation. This created the scientific base for testing our hypothesis. Briefly, Approximately 50,000 MCF-7 cells/well were seeded in 96 well plate, supplemented with excess of RPMI 1640 culture medium. The cells were treated with different concentrations (0.5, 1, 2, 3, 4, 5 µg/ml) of pure insulin (positive control), Blank ULNE, Blank CLNE, insulin bearing INS-ULNE and INS-CLNE. Herein, control wells wherein, cells were not treated with insulin but only same volume of culture medium was added served as reference growth. The cell proliferation was measured by gold standard MTT assay. As shown in the figure 4.18 uncoated linseed oil nano-emulsion (Blank ULNE) and PLL coated LNE (Blank CLNE) without insulin didn't show any proliferative effect which is due to unavailability of the insulin as a growth factor in case of formulations while direct availability of insulin in dissolved form in case of pure solution. Moreover, pure insulin exhibited significantly high proliferation (~183% at 5 µg/ml conc.) than INS-ULNE (~153% at 5 µg/ml conc.) which may be justified based on controlled release of insulin from INS-ULNE and hence comparatively lesser availability at a time. However, PLL coated INS-CLNE (~170% at 5 µg/ml conc.) showed almost comparable proliferative action to the pure insulin and significantly higher proliferative action than uncoated INS-ULNE. Herein, PLL coating played a significant role as poly-l-lysine is well-known and in common use as cell adherent moiety, and helped nano-emulsion to reach in close proximity of the MCF-7 cells [39]. Moreover, we want to clarify that c-peptide does not have any cell proliferative activity and in our experiments also we got similar results but herein, those results are not shown to reduce the data trafficking in a single histogram. Thus, we can conclude that released insulin from both INS-ULNE and INS-CLNE formulations, is in therapeutically active form. Moreover, the data demonstrated that developed formulations are capable to protect the labile insulin molecule in its bio-active form.

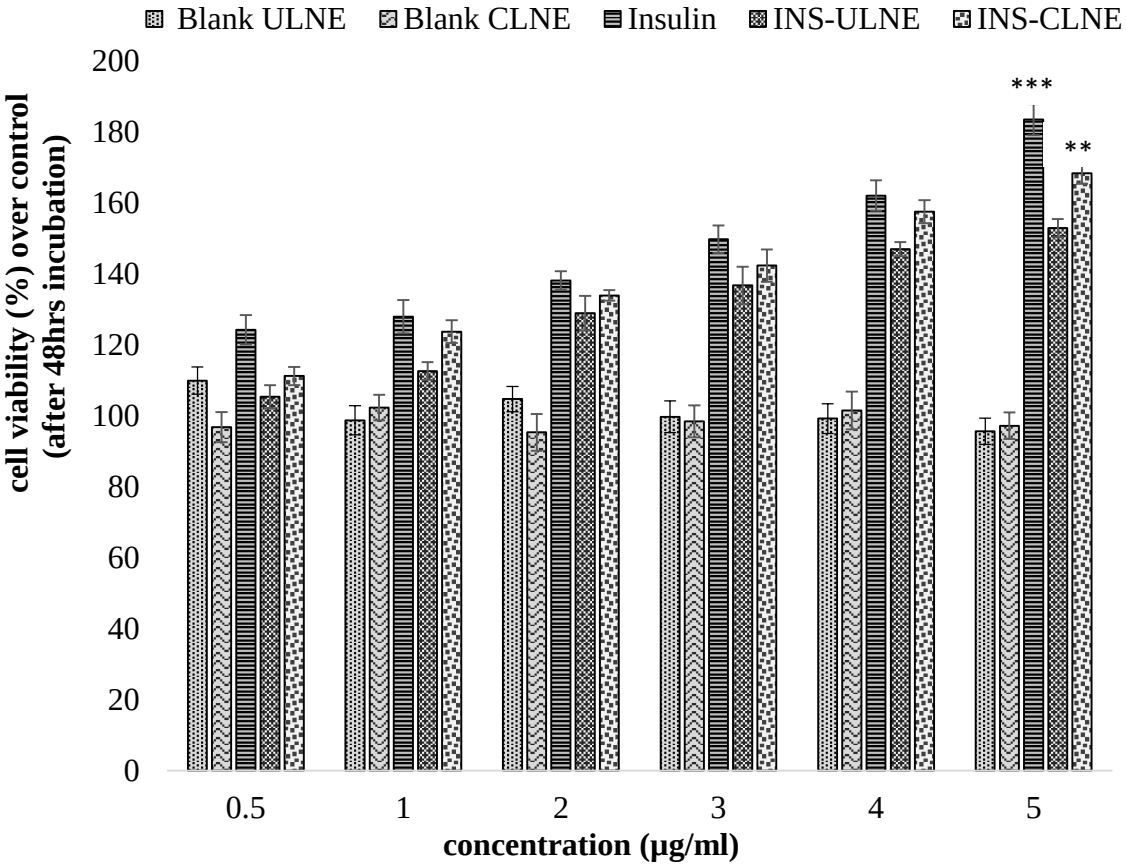

Figure 4.18 *In vitro* bio-activity of pure insulin (positive control), Blank ULNE, Blank CLNE, insulin bearing INS-ULNE and INS-CLNE was confirmed by MTT cell proliferation assay on MCF-7 cells (**Mean ± S.D; n=3**) ***p<0.0001 Blank ULNE and Blank CLNE vs pure INS, **p<0.05 Blank CLNE vs INS-CLNE

4.5.3.8 Stability study

The short term stability study at ambient temperature (25 ± 2°C) and cool temperature (4 ± 2°C) was executed to assess effect of storage at this condition on prepared optimized poly-l-lysine coated LNE7 nano-emulsion. After 90 days subtle change in mean globule size and zeta potential was observed (figure 4.19 and 4.20). The mean globule size was enlarged by 20 to 30 nm and zeta potential was decreased by 4 to 5 mV. Overall, good stability was noticed for prepared nano-emulsion.

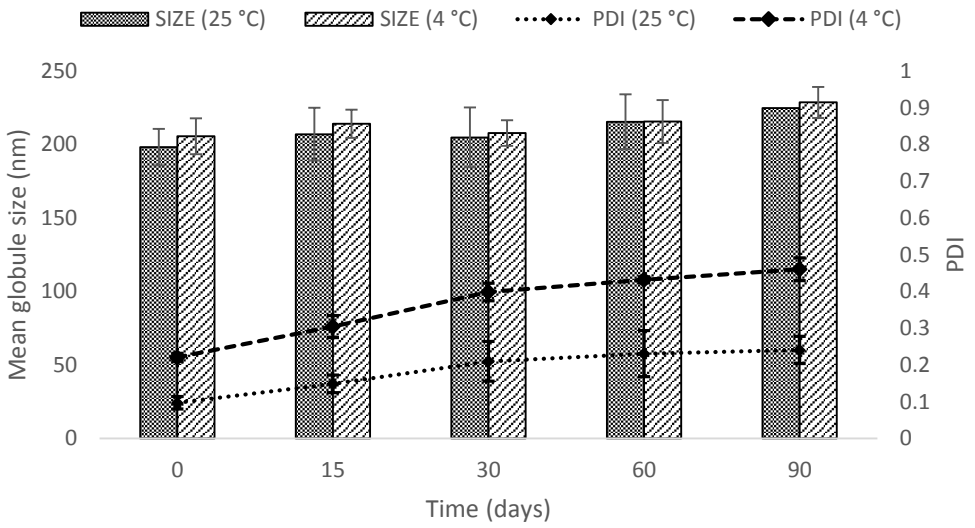

Figure 4.19 Effect of storage at 25 °C and 4 °C on mean hydrodynamic diameter (nm) and polydisersityindex (PDI) of the Polyl-lysine coated LNE7.

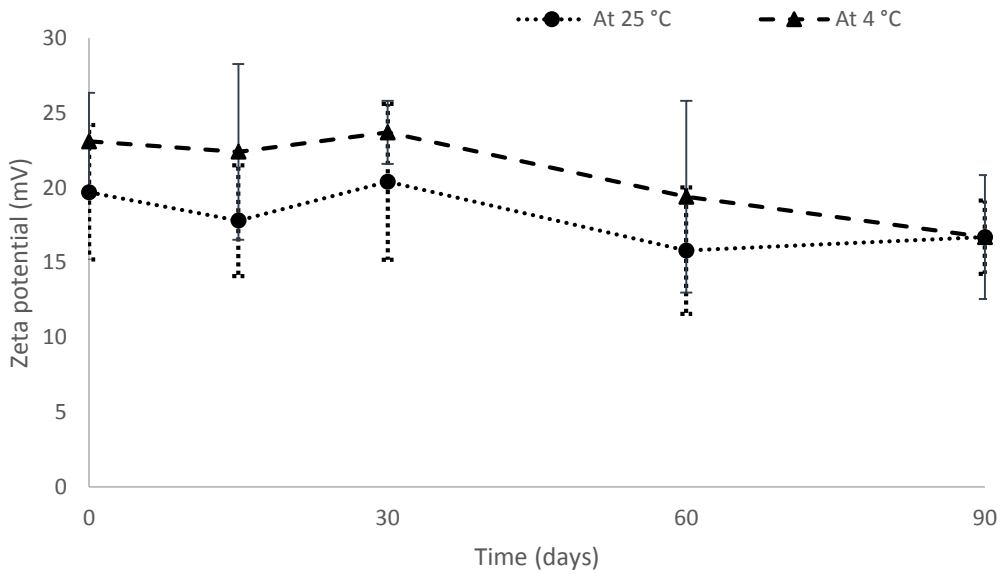

Figure 4.20 Effect of storage at 25 °C and 4 °C on zeta potential of the Poly l-lysine coated LNE7.

4.5.3.9 *In vivo* efficacy

To estimate the *in vivo* efficacy of prepared oral formulations in comparison to gold standard sub-cutaneous insulin, blood glucose levels were measured at pre-determined time points after oral ingestion of insulin and c-peptide loaded ULNE7 and Poly-l-lysine coated CLNE7 at the dose equivalent to 10 IU/Kg of insulin and compared to sub-cutaneously administered insulin in PBS 7.4 at the dose of 2 IU/Kg. Herein, diabetic control group served as baseline for the blood glucose level for comparing the blood glucose lowering effect mediated by formulations. A very quick fall in blood glucose level was observed in SC insulin treated group as compared to oral formulations, Uncoated LNE7 and PLL Coated LNE7. Though the blood glucose was lowered quickly and reached to 39.4±1.63 mg/dl after 2 hours, it could not be maintained for longer time and started rising after 4 hours and reached back to more than 300 mg/dl at 12 hours. The PLL Coated LNE7 formulation started lowering the blood glucose after 2 hours and managed to lower and kept it under 200 mg/dl for 12 hours. On the other hand, uncoated LNE7 managed to lower the blood glucose level to 195.75±6.17 mg/dl and maintained it below 300 mg/dl for 8 hours. The better glycemic control for 12 hours observed with PLL coated LNE7 is due to poly l-lysine's muco-adhesive property and capability of opening the tight junction of epithelial cells of intestine by reducing trans-epithelial electrical resistance.

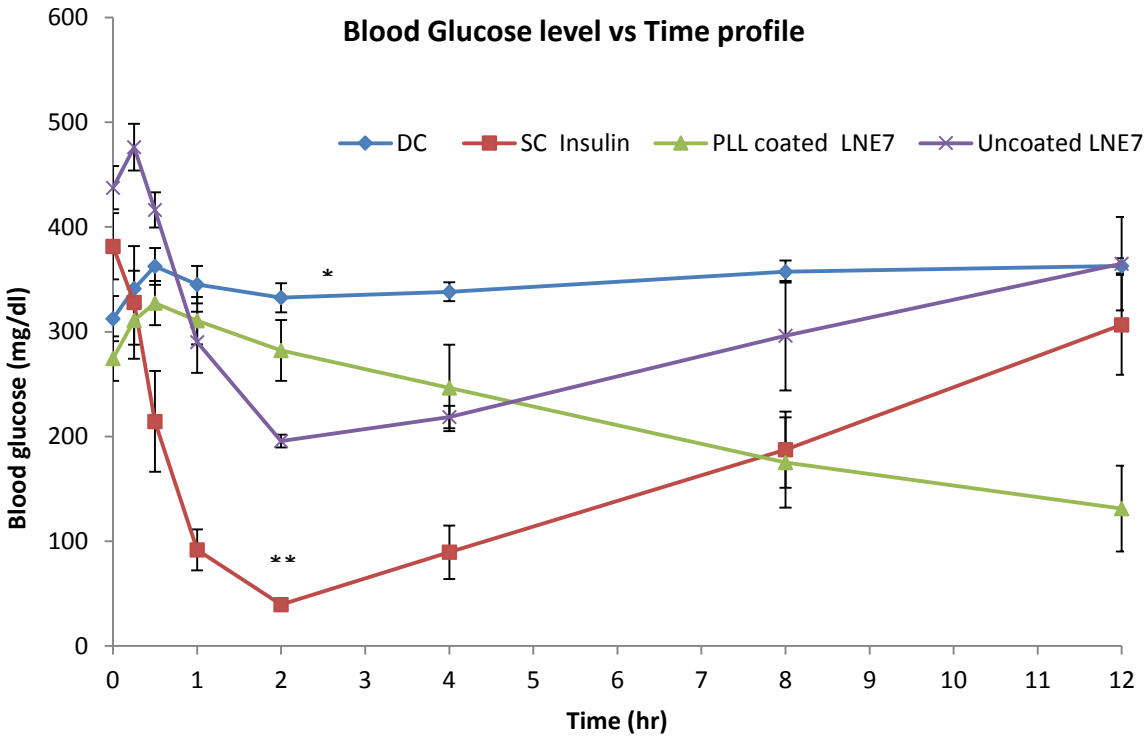

Figure 4.21 Blood glucose levels in diabetic rats after oral administration of uncoated LNE7 and PLL coated LNE7 at the dose equivalent to 10 IU/Kg of insulin and sub-cutaneous administration of insulin in PBS 7.4 at the dose of 2 IU/Kg. (n=5, Mean ± SEM)

*p<0.01 DC vs SC insulin and uncoated LNE7 and PLL coated LNE7; **p<0.05 SC insulin vs uncoated LNE7 and PLL coated LNE7

4.5.3.10 Plasma insulin and c-peptide Level

The plasma was separated from the blood samples withdrawn at different time intervals and sheltered at -80°C. The plasma insulin and c-peptide levels were measured by analyzing the plasma samples with the help of ELISA kit in accordance with the protocols provided by manufacturers. The calculation was done and plasma insulin versus time profile was generated as shown in figure 22. Similarly the data was generated for c-peptide level as shown in figure 23. A baseline plasma insulin level in diabetic control group was noted to be 80.56±5.18 µIU/ml. Plasma insulin level was suddenly started to increase and reach the level of 745.34± 105.14 µIU/ml concentration after 30 minutes in case of sub-cutaneously administered insulin solution. Thereafter, the plasma insulin level started falling and came back to 134.06±65.70 µIU/ml at 2 hours and remained below for 12 hours.

In case of Uncoated LNE7 formulation, plasma insulin gradually increased to a maximum level of 125.97±24.55 µIU/ml, 2 hours post-administration and maintained above 100.55 ± 24.07 µIU/ml up to 8 hours. PLL coated LNE7 provided maximum plasma insulin level of 205.13 ± 93.26 µIU/ml, after 2 hours of administration and maintained it above 110.55± 9.01 µIU/ml up to 12 hours. Herein, the high plasma level above 100 µIU/ml maintenance for 12 hours is due to controlled release and greater bio-availability of insulin from the PLL coated LNE7.

When the formulations were administered, 10 µg c-peptide was co-delivered with 10IU/kg of insulin. Therefore, c-peptide level was also quantified in the blood plasma samples. A normal basal c-peptide level of 29.67 ± 3.01 nmol/L was found in diabetic control group and group treated with sub-cutaneous insulin, as no external c-peptide was delivered. PLL coated LNE7 formulation bearing insulin and c-peptide gave rise to the c-peptide level up to 78.13± 3.13 nmol/L at 2 hours and it was maintained above 37.27 ± 2.66 nmol/L up to 12 hours as compared to uncoated LNE7 which provided 64.96 ± 3.22 nmol/L at 2 hours and maintained it above 35.14 ± 1.68 nmol/L up to 12 hours.

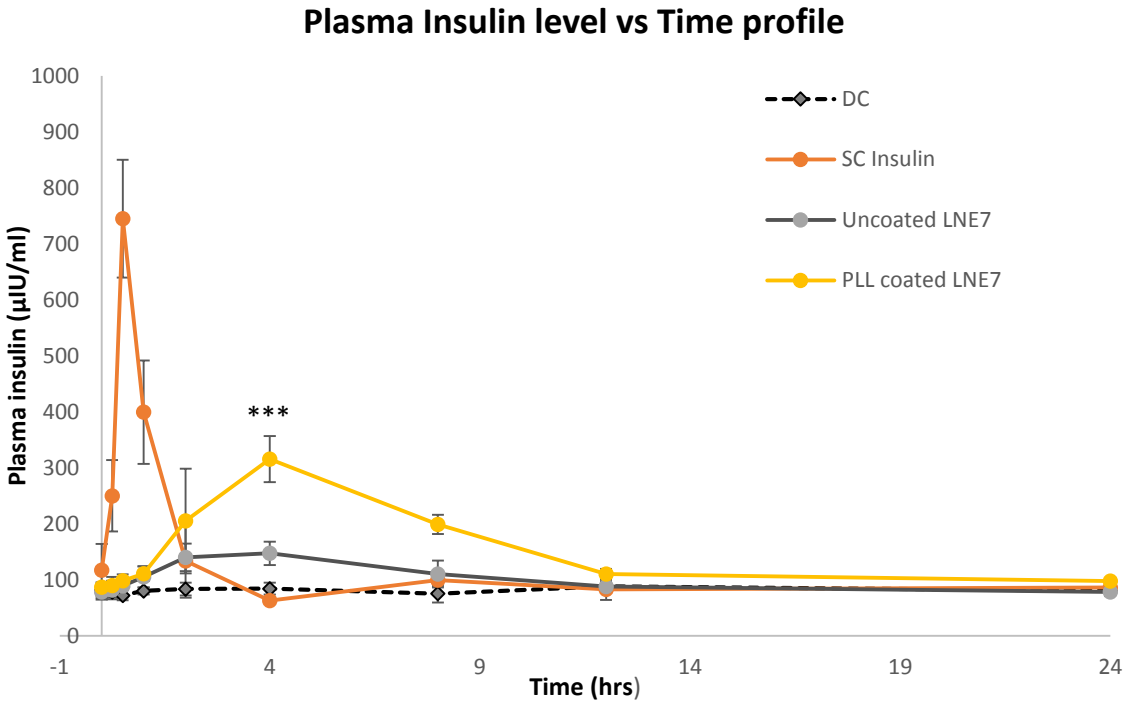

Figure 4.22 Plasma insulin levels in diabetic rats after oral administration of uncoated LNE7 and PLL coated LNE7 at the dose equivalent to 10 IU/Kg of insulin and sub-cutaneous administration of insulin solution in PBS 7.4 at the dose of 2 IU/Kg. (n=5, Mean ± SEM)

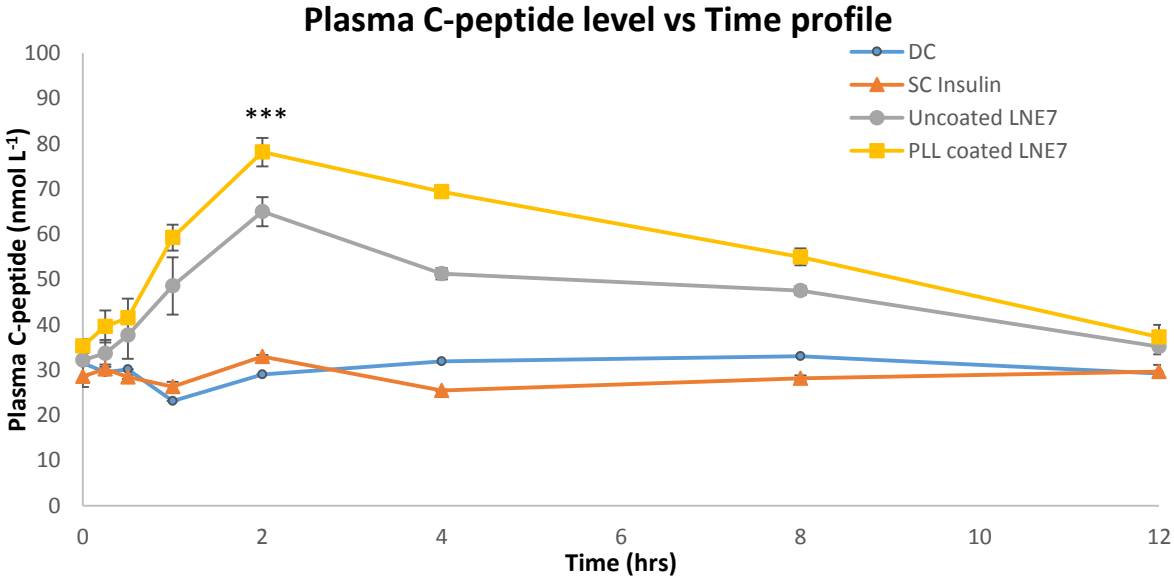

Figure 4.23 Plasma c-peptide level in diabetic rats after oral administration of uncoated LNE7 and PLL coated LNE7 at the dose equivalent to 10 µg/Kg of c-peptide (n=5, Mean ± SEM)

*** Significant difference p<0.05, PLL coated LNE7 vs uncoated LNE7, SC insulin and diabetic control

4.5.3.11 Pharmacokinetics and oral bioavailability

Non compartmental analysis was done through WinNonlin 6.0 software and pharmacokinetic parameters observed after oral administration of uncoated LNE7, PLL coated LNE7 and subcutaneous administration of pure insulin solution in PBS pH 7.4 are shown in table 4.6. It is clearly visible from the Cmax value that despite of administering uncoated LNE7 and PLL coated LNE7 via oral route at the dose five fold higher (10 IU/kg) than pure insulin via SC route, the maximum plasma concentration of insulin was attained significantly higher in case of SC insulin which is totally due to route of administration assisted advantage. Moreover, if we compare uncoated LNE7 vs PLL coated LNE7, we can conclude that due to muco-adhesive and cell penetrating properties of PLL significantly higher Cmax (i.e. almost two fold) was achieved in case of PLL coated LNE7 as compared to uncoated LNE7. Significantly higher Tmax as compared to SC insulin (0.5 hours) was observed after administering uncoated LNE7 (4 hours) as well as PLL coated LNE7 (4 hours) via oral route, which is due to controlled release offered by the formulation and time to cross the physiological barriers after oral administration. The comparison of area under the curve (AUC) value suggested that PLL coated LNE7 is more proficient in enhancing the absorption and hence bio-availability as compared to uncoated LNE7. The relative bio-availability of developed uncoated LNE7 (10 IU/kg) and PLL coated LNE7 (10 IU/kg) was calculated and observed to be 18.38% and 27.99%, respectively, with reference to sub-cutaneously administered insulin (2 IU/kg).

Table 4.6 Pharmacokinetic parameters after oral administration uncoated LNE7, PLL coated LNE7 at the dose equivalent to 10 IU/Kg of insulin and sub-cutaneous administration of insulin solution in PBS 7.4 at the dose of 2 IU/Kg.

Pharmacokinetic Parameter (Unit)	Sub-cutaneous insulin	Uncoated LNE7	PLL coated LNE7
Dose (IU/kg)	2	10	10
Tmax (hr)	**0.5**	**4**	**4**
Cmax (µIU/ml)	745.35	147.64	315.73
AUC (hr* µIU/ml)	2626.61	2414.90	3676.98
Relative Oral Bioavailability (%)	**100**	**18.38**	**27.99**

4.6 CONCLUSION

Poly-l-lysine coated oral w/o/w nano-emulsion for combined delivery of insulin and c-peptide was successfully developed, characterized and evaluated. The results obtained from *in vitro* and *in vivo* studies indicated that developed formulation is stable and capable enough of protecting the insulin and c-peptide from hostile GIT, helping in absorption of macromolecules from microfold cells and transcellular transport, releasing in therapeutically viable form and improving the pharmacokinetic profile of insulin after oral administration. Moreover, the unique concept of co- delivery of c-peptide along with insulin will help in better management of diabetes mellitus type I and II due to additional benefits of c-peptide as compared to conventional insulin therapy. We may enunciate that we have successfully delivered human recombinant insulin via oral route with relative oral bioavailability of 27.99%. Finally, we hope that the research carried out will significantly help to achieve the delusive yet attainable goal of developing commercially viable oral delivery system of insulin.

4.7 REFERENCES

1. Pawar, V.K., et al., *Targeting of gastrointestinal tract for amended delivery of protein/peptide therapeutics: strategies and industrial perspectives.* J Control Release, 2014. **196**: p. 168-83.
2. Bolli, G.B., *Insulin treatment in type 1 diabetes.* Endocr Pract, 2006. **12 Suppl 1**: p. 105-9.
3. Swinnen, S.G., J.B. Hoekstra, and J.H. DeVries, *Insulin therapy for type 2 diabetes.* Diabetes care, 2009. **32 Suppl 2**(Suppl 2): p. S253-S259.
4. Cefalu, W.T., *Concept, Strategies, and Feasibility of Noninvasive Insulin Delivery.* Diabetes Care, 2004. **27**(1): p. 239.
5. Fowler, M.J., *Microvascular and Macrovascular Complications of Diabetes.* Clinical Diabetes, 2008. **26**(2): p. 77.
6. Yosten, G.L.C., et al., *Physiological effects and therapeutic potential of proinsulin C-peptide.* American Journal of Physiology - Endocrinology And Metabolism, 2014. **307**(11): p. E955-E968.
7. Hills, C.E. and N.J. Brunskill, *Cellular and physiological effects of C-peptide.* Clin Sci (Lond), 2009. **116**(7): p. 565-74.
8. Janghorbani, M., M. Dehghani, and M. Salehi-Marzijarani, *Systematic Review and Meta-analysis of Insulin Therapy and Risk of Cancer.* Hormones and Cancer, 2012. **3**(4): p. 137-146.
9. Erpeldinger, S., et al., *Efficacy and safety of insulin in type 2 diabetes: meta-analysis of randomised controlled trials.* BMC Endocrine Disorders, 2016. **16**(1): p. 39.
10. Marques, R.G., M.J. Fontaine, and J. Rogers, *C-peptide: much more than a byproduct of insulin biosynthesis.* Pancreas, 2004. **29**(3): p. 231-8.
11. Wahren, J., et al., *Role of C-peptide in human physiology.* Am J Physiol Endocrinol Metab, 2000. **278**(5): p. E759-68.
12. Johansson, B.L., S. Sjoberg, and J. Wahren, *The influence of human C-peptide on renal function and glucose utilization in type 1 (insulin-dependent) diabetic patients.* Diabetologia, 1992. **35**(2): p. 121-8.
13. Johansson, B.L., et al., *Influence of combined C-peptide and insulin administration on renal function and metabolic control in diabetes type 1.* J Clin Endocrinol Metab, 1993. **77**(4): p. 976-81.
14. Ekberg, K., et al., *Amelioration of sensory nerve dysfunction by C-Peptide in patients with type 1 diabetes.* Diabetes, 2003. **52**(2): p. 536-41.
15. Hansen, A., et al., *C-Peptide Exerts Beneficial Effects on Myocardial Blood Flow and Function in Patients With Type 1 Diabetes.* Diabetes, 2002. **51**(10): p. 3077-3082.
16. des Rieux, A., et al., *Nanoparticles as potential oral delivery systems of proteins and vaccines: A mechanistic approach.* Journal of Controlled Release, 2006. **116**(1): p. 1-27.
17. Ensign, L.M., R. Cone, and J. Hanes, *Oral drug delivery with polymeric nanoparticles: The gastrointestinal mucus barriers.* Advanced Drug Delivery Reviews, 2012. **64**(6): p. 557-570.
18. Swaminathan, J. and C. Ehrhardt, *Liposomal delivery of proteins and peptides.* Expert Opin Drug Deliv, 2012. **9**(12): p. 1489-503.
19. Fan, T., et al., *Design and evaluation of solid lipid nanoparticles modified with peptide ligand for oral delivery of protein drugs.* Eur J Pharm Biopharm, 2014. **88**(2): p. 518-28.
20. Venkata Ramana Rao, S. and J. Shao, *Self-nanoemulsifying drug delivery systems (SNEDDS) for oral delivery of protein drugs: I. Formulation development.* International Journal of Pharmaceutics, 2008. **362**(1–2): p. 2-9.
21. Niu, Z., et al., *Rational design of polyarginine nanocapsules intended to help peptides overcoming intestinal barriers.* Journal of Controlled Release.

22. Nitta, S.K. and K. Numata, *Biopolymer-Based Nanoparticles for Drug/Gene Delivery and Tissue Engineering.* International Journal of Molecular Sciences, 2013. **14**(1): p. 1629-1654.
23. Nojehdehian, H., et al., *Preparation and surface characterization of poly-L-lysine-coated PLGA microsphere scaffolds containing retinoic acid for nerve tissue engineering: in vitro study.* Colloids Surf B Biointerfaces, 2009. **73**(1): p. 23-9.
24. Cournarie, F., et al., *Insulin-loaded W/O/W multiple emulsions: comparison of the performances of systems prepared with medium-chain-triglycerides and fish oil.* European Journal of Pharmaceutics and Biopharmaceutics, 2004. **58**(3): p. 477-482.
25. Choi, W.I., et al., *A Solvent-Free Thermosponge Nanoparticle Platform for Efficient Delivery of Labile Proteins.* Nano Letters, 2014. **14**(11): p. 6449-6455.
26. Samarji, R. and M. Balbaa, *Anti-diabetic activity of different oils through their effect on arylsulfatases.* Journal of Diabetes and Metabolic Disorders, 2014. **13**: p. 116.
27. Sankar, D., et al., *Sesame oil exhibits synergistic effect with anti-diabetic medication in patients with type 2 diabetes mellitus.* Clin Nutr, 2011. **30**(3): p. 351-8.
28. Kato, M., et al., *Effect of Alpha-Linolenic Acid on Blood Glucose, Insulin and GLUT4 Protein Content of Type 2 Diabetic Mice.* JOURNAL OF HEALTH SCIENCE, 2000. **46**(6): p. 489-492.
29. Ngala, R.A., et al., *Effect of dietary vegetable oil consumption on blood glucose levels, lipid profile and weight in diabetic mice: an experimental case—control study.* BMC Nutrition, 2016. **2**(1): p. 28.
30. Sharma, S., et al., *Investigating the role of Pluronic-g-Cationic polyelectrolyte as functional stabilizer for nanocrystals: Impact on Paclitaxel oral bioavailability and tumor growth.* Acta Biomater, 2015. **26**: p. 169-83.
31. Yu, S.H., et al., *Nanoparticle-induced tight-junction opening for the transport of an anti-angiogenic sulfated polysaccharide across Caco-2 cell monolayers.* Acta Biomater, 2013. **9**(7): p. 7449-59.
32. Dupont, J. and D. Le Roith, *Insulin-like growth factor 1 and oestradiol promote cell proliferation of MCF-7 breast cancer cells: new insights into their synergistic effects.* Molecular pathology : MP, 2001. **54**(3): p. 149-154.
33. Chacon, E., D. Acosta, and J.J. Lemasters, *9 - Primary Cultures of Cardiac Myocytes as In Vitro Models for Pharmacological and Toxicological Assessments*, in *In Vitro Methods in Pharmaceutical Research*, J.V. Castell and M.J. Gómez-Lechón, Editors. 1997, Academic Press: San Diego. p. 209-223.
34. Deeds, M.C., et al., *Single dose streptozotocin-induced diabetes: considerations for study design in islet transplantation models.* Lab Anim, 2011. **45**(3): p. 131-40.
35. Greenfield, N.J., *Using circular dichroism spectra to estimate protein secondary structure.* Nat Protoc, 2006. **1**(6): p. 2876-90.
36. Lee, S., et al., *Synthesis and biological properties of insulin-deoxycholic acid chemical conjugates.* Bioconjug Chem, 2005. **16**(3): p. 615-20.
37. Chen, W., et al., *Bioavailability study of berberine and the enhancing effects of TPGS on intestinal absorption in rats.* AAPS PharmSciTech, 2011. **12**(2): p. 705-11.
38. Nemoto, E., et al., *Effects of poly-L-arginine on the permeation of hydrophilic compounds through surface ocular tissues.* Biol Pharm Bull, 2006. **29**(1): p. 155-60.
39. Mazia, D., G. Schatten, and W. Sale, *Adhesion of cells to surfaces coated with polylysine. Applications to electron microscopy.* J Cell Biol, 1975. **66**(1): p. 198-200.

CHAPTER 5

Summary

&

Conclusion

Oral delivery of proteins and peptides still remains a perplexing field for formulation scientists. Though, myriad of literature is available showing promising strategies for successful oral delivery by circumventing the impeding factors on the way, not a single success has been cherished commercially. Therefore, with a view to design a comprehensive drug delivery system with all the necessary attributes, strong efforts were made. Amongst them, the efforts which got positive scientific outcomes and held a promise to fulfill the objective are summarized and possible future prospects are suggested.

5.1 Thermo-responsive size shifting polymeric nanoparticles for oral delivery of insulin

To overcome the pain shots and patient compliance related issues in the drug delivery of biologics, a novel approach has been undertaken to provide labile proteins and peptides by the most preferred route i.e. oral. A platform has been architected to incorporate positively as well as negatively charged proteins by solvent free manner which bypass the possible detriment of labile proteins by organic solvents and/or mechanical energy i.e. homogenization, ultrasonication etc. A thermo-responsive NPs comprising polymeric core (PLGA or PLA-NH_2) and thermo-responsive shell (pluronic) were prepared by nanoprecipitation method. The unique thermal property of pluronic provided swelling of shell at 4°C and de-swelling at 37°C which was utilized to incorporate protein molecules. First of all, suitable pluronic was selected from group of pluronics (pluronic F 127, pluronic F 68, pluronic P 123) by formulating thermo-responsive NPs at various ratios of PLGA to pluronic and evaluating for swelling/de-swelling phenomena. The pluronic which can impart higher degree of swelling and de-swelling to the thermo-responsive shell was preferred. After screening process, pluronic F 127 come up as best thermo-responsive polymer cum surfactant amongst all the pluronics tried. Afterwards, for delivery of negatively charged insulin as a model protein, PLA-NH_2 NPs were prepared and optimized with respect to mean hydrodynamic diameter, PDI, zeta potential and percentage entrapment efficiency. The optimized formulation was coated with cellulose acetate phthalate and the coating was confirmed by increase in size and reversal of zeta potential. *In vitro* drug release of insulin was performed. The CAP coated thermo-responsive PLA NPs demonstrated no release at pH 1.2 in initial 2 hours, but release was observed at pH 6.8 with burst release (up to 30%) in next 6 hours followed by controlled release up to 72 hours. Here, it was presumed that after CAP coating, PLA NPs would be up taken by M

cells present on Peyer's patches. MALDI-TOF mass spectra of insulin released from formulation during in vitro drug release revealed that the CAP coated thermo-responsive PLA NPs can deliver insulin orally without degradation.

The developed thermo-sensitive size shifting NPs (TNPs) were characterized for their morphology by TEM and found roughly spherical in shape with approximately 50 nm size. The stability studies at 25 °C and 4 °C suggested the formulation stable for three months. CD spectrometry demonstrated that insulin released from TNPs retained the characteristic band when compared to UV-CD spectra of standard insulin solution. In vitro uptake of FITC loaded TNPs in HCT 116 and caco-2 intestinal cell lines was observed 17 fold and 15 fold higher, respectively. Caco-2 cell monolayer study revealed that uncoated PLA TNPs and CAP coated PLA TNPs both have property to, transiently, open up the epithelial tight junctions of intestinal membrane. Successful attempts have been made to enhance the encapsulation efficiency. Because the main driving force for encapsulation of insulin inside TNPs is the electrostatic interaction, charge difference between TNPs and insulin plays a pivotal role. Therefore, charge of insulin was shifted towards more negative by change in pH of solution and maximum encapsulation was attained up to 91% at pH 10. Here, it was also assured that insulin remains stable during the encapsulation process as well as after release. The in vitro bio-activity of the released insulin from INS@TNPs and INS@CAP-TNPs was confirmed by cell viability (MTT) assay on MCF-7 cell lines which express IGF-1 receptor responsible for insulin dependent proliferation. Moreover, INS@CAP-TNPs successfully handled blood glucose level below ~200 mg/dl for 12 hours with 50% decrement of starting blood glucose level. It provided 16.49% relative bioavailability with comparison to SC insulin which was considered as 100% bio-available. Comprehensively, we can conclude that the architected cellulose acetate phthalate coated thermo-responsive size shifting nanoparticles with positive core made up of PLA-NH2 serve as the promising platform for oral delivery of negatively charged protein/peptide molecules like insulin. The developed nanoparticle with negative core made up of PLGA can also be exploited for delivery of positively charged proteins such as erythropoietin and interleukin-10.

5.2 Poly-l-lysine coated Linseed oil nano-emulsion for combined delivery of insulin and c-peptide

Various natural oils having effects that can help in diabetes type I, II and diabetic complications were screened from array of natural oils and four oils (olive oil, palm oil, sesame oil and linseed oil) were found suitable to formulate oral poly-l-lysine coated w/o/w nano-emulsion containing insulin and c-peptide. Nano-emulsions were made by using minimum ultra-sonication for 2 min and stirring at 800 rpm for 30 minutes to avoid any damage to the labile insulin and c-peptide. The structural stability, confirmation and integrity was evaluated by CD spectrophotometry and MALDI-TOF. The nano-emulsion components were selected by performing preliminary studies and further optimized. Poly-l-lysine coating was confirmed by charge reversal of uncoated nano-emulsion from negative (-21.7 mV) to positive (18.3 mV). The prepared formulations were characterized for mean globule size, polydispersity index and zeta potential. Entrapment efficiency of insulin and c-peptide was measured by enzyme immune assay (EIA) with the help of ELISA kit. The optimized formulation LNE7 showed 87.6 ± 7.48 % entrapment efficiency for insulin and 73.4 ± 6.44 % for c-peptide, respectively. In vitro drug release from LNE7 was performed in simulated gastric fluid pH 1.2, simulated intestinal fluid pH 6.8 and phosphate buffer saline pH 7.4 to mimic the physiological conditions. No release was found in simulated gastric fluid pH 1.2. Biphasic drug release with initial burst of 20 - 30 % in initial 2 hours and then controlled release up to 24 hours was noticed. TEM image revealed that globules are almost spherical in shape, well dispersed with uniform distribution without coalescence, and have size of approximately 200 nm as in support with results of zetasizer. In vitro cell uptake was performed in HCT116 cell lines and found that cell uptake of uncoated FITC-LNE7 and poly-l-lysine coated FITC-LNE7 was 4.55 fold and 8.28 fold higher than FITC solution, respectively. Trans-epithelial electrical resistance study revealed tight junction opening potential of uncoated as well as coated linseed oil nano-emulsion. % TEER was decreased to 65 % and 40 % after two hours of treatment with uncoated LNE7 and poly-l-lysine coated LNE7, respectively. This shows promising absorption enhancing capability of the formulation to help penetrate insulin and c-peptide in intestinal lumen. Three months stability study indicated good stability of the prepared optimized poly-l-lysine coated linseed oil nano-emulsion without any significant change in physico-chemical characteristics. Animal Experiments suggested that the uncoated LNE7 and PLL coated LNE7 formulation provided better glycemic control by keeping the blood glucose level below 200 mg/dl upto 8 hours and 12 hours, respectively, as compared to SC insulin which showed its hypoglycemic effect only for very short time course of 4 hours.

From plasma insulin and c-peptide level data it is quite visible that the oral nano-emulsions have promisingly delivered the labile insulin and c-peptide to the absorption site in its bio-active form with structural integrity.

The architected nano-sized formulations for oral delivery of insulin and c-petide holds a great potential to serve as a backbone for development of further improved formulations. As future prospects, these formulations can be coated by l-penetratin for enhanced absorption of insulin. Moreover, absorption of insulin can be augmented by targeting microfold cells. An interesting suggestion would be to rethink the way conventional insulin therapy is. The physiological role and benefits of c-peptide in management of diabetes mellitus should be offered by combined delivery of insulin and c-peptide.

List of Publications

LIST OF PUBLICATION

1. Singh Y, Tomar S, Khan S, Meher JG, Pawar VK, **Raval K**, et al. Bridging small interfering RNA with giant therapeutic outcomes using nanometric liposomes. **Journal of Controlled Release**. 2015;220, Part A:368-87.
2. Singh PK, Sah P, Meher JG, Joshi S, Pawar VK, **Raval K**, et al. Macrophage-targeted chitosan anchored PLGA nanoparticles bearing doxorubicin and amphotericin B against visceral leishmaniasis. **RSC Advances**. 2016;6(75):71705-18.
3. Y. Singh, A. Chandrashekhar, V K. Pawar ,V.Saravanakumar, JG.Meher , **K. Raval** , P. K. Singh and M.K. Chourasia. Novel validated RP-HPLC method for Bendamustine hydrochloride based on ion-pair chromatography: Application in determining infusion stability and pharmacokinetics. **Journal of Chromatographic Science**. 2016.
4. Pawar V.K., Singh Y, Sharma K, Shrivastav A, Sharma A, Singh A, Meher J. G., Singh P, **Raval K**, Bora H. K., Datta D, Lal J, Chourasia M. K. Doxorubicin Hydrochloride Loaded Zymosan-Polyethylenimine Biopolymeric Nanoparticles for Dual 'Chemoimmunotherapeutic' Intervention in Breast Cancer. **Pharmaceutical Research**, 2017.
5. Singh Y, Pawar V.K., Meher JG, **Raval K**, Kumar A, Shrivastava, R, Bhadauria, S, Chourasia M K, Targeting tumor associated macrophages (TAMs) via nanocarriers. **Journal of Controlled Release**, 2017. **254**: p. 92-106.
6. Singh Y, Meher JG, **Raval K**, Khan F. A, Chaurasia M, Jain N. K, Chourasia M K, Nanoemulsion: Concepts, development and applications in drug delivery. **Journal of Controlled Release**, 2017. 252: p. 28-49.
7. Singh, Y.,Chandrashekhar, A., Meher, J. G., Durga Rao Viswanadham, K. K., Pawar, V. K., **Raval, K.**, Sharma, K., Singh, P. K., Kumar, A., Chourasia, M. K. Nanosized complexation assemblies housed inside reverse micelles churn out monocytic delivery cores for bendamustine hydrochloride. **European Journal of Pharmaceutics and Biopharmaceutics**, 2017. 113: p. 198-210.
8. Singh, Y., Durga Rao Viswanadham, K. K., Kumar Jajoriya, A., Meher, J. G., **Raval, K.**, Jaiswal, S., Dewangan, J., Bora, H. K., Rath, S. K., Lal, J., Mishra, D. P., Chourasia, M. K. Click Biotinylation of PLGA Template for Biotin Receptor

Oriented Delivery of Doxorubicin Hydrochloride in 4T1 Cell-Induced Breast Cancer. Molecular Pharmaceutics, 2017.

9. Singh, Pankaj K., Pawar, Vivek K., Jaiswal, Anil K., Singh, Yuvraj, Srikanth, Cheruvu Hanumanth, Chaurasia, Mohini, Bora, Himangsu K., **Raval, Kavit,** Meher, Jaya Gopal, Gayen, Jiaur R., Dube, Anuradha, Chourasia,, Manish K. Chitosan coated PluronicF127 micelles for effective delivery of Amphotericin B in experimental visceral leishmaniasis. **International Journal of Biological Macromolecules**, 2017. 105: p. 1220-1231.

10. Singh, P.K., Jaiswal, A. K., Pawar, V. K., **Raval, K.**, Kumar, A., Bora, H. K., Dube, A., Chourasia, M. K. Fabrication of 3-O-sn-Phosphatidyl-L-serine Anchored PLGA Nanoparticle Bearing Amphotericin B for Macrophage Targeting. **Pharmaceutical Research**, 2018. 35(3): p. 60.

11. Pawar, V.K., Singh, Y., Sharma, K., Shrivastava, A., Sharma, A., Singh, A., Meher, J.G., Singh, P., **Raval, K.**, Kumar, A., Bora, H. K., Datta, D., Lal, J., Chourasia, M. K. Improved chemotherapy against breast cancer through immunotherapeutic activity of fucoidan decorated electrostatically assembled nanoparticles bearing doxorubicin. **International Journal of Biological Macromolecules**, 2018.

LIST OF PATENT

1. Chourasia Manish K. Singh Pankaj K., **Raval Kavit**, Pawar Vivek K., Cheruvu H. Srikanth, Gayen Jiaur R., Dwivedi Anil Kumar, A controlled release formulation for enhanced oral bioavailability of hydrophobic drugs. **Application No.201611002387 A**, the Patent Office Journal No. 30/2017: p. 25200.